



מכון ויצמן למדע

WEIZMANN INSTITUTE OF SCIENCE

Thesis for the degree

Doctor of Philosophy

Submitted to the Scientific Council of the

Weizmann Institute of Science

Rehovot, Israel

עבודת גמר (תזה) לתואר

דוקטור לפילוסופיה

מוגשת למועצה המדעית של

מכון ויצמן למדע

רחובות, ישראל

By

**Anat Shemer**

מאת

**ענת שמר**

בחינת תפקידי המיקרוגליה במודלים  
עכבריים של תגובות דלקתיות

Studying microglia functions in  
inflammatory responses in vivo

Advisor:

Prof. Steffen Jung

מנחה:

פרופ' סטפן יונג

December 2019

טבת תש"פ

### *Acknowledgments*

I would like to express my sincere gratitude to my advisor, Prof. Steffen Jung for his help, guidance and support during the past 6.5 years I spent in his lab. Steffen for me is an example for the ideal scientist, driven by curiosity, passion and love for science, and always requires the highest of standards.

I would also like to thank my MSc co-advisor, Prof. Avi Ben-Nun, who passed away earlier this year. Avi was a world-class scientist, one of the founding fathers of the EAE model, and was an inspiration for both young and experienced scientists. I will be always grateful for the warm welcoming I received from Avi as the first professor I encounter at the Weizmann Institute, starting my MSc training.

To my parents, my biggest supporters, who always encourage me to achieve and to do what I love. Thank you for helping and making efforts to remove all obstacles along the way.

I would also like to thank my amazing husband, Eliran, for his great support and encouragement in the past 13 years. And finally, to my boy Alon, for giving a new meaning to my life in the past two years.

*Declaration*

I hereby declare this thesis is a summary of my own independent research.

Collaborations included in this thesis are as follows:

In *project I*, The RNAseq and ATACseq analyses were performed by Jonathan Grozovsky.

*Project II* is a collaboration with Dr. Yochai Wolf.

In *project IV*, the electrophysiological measurements were performed by Dr. Nicola Maggio.

*Table of Contents*

List of abbreviations.....	1
Abstract.....	3
Abstract in Hebrew.....	4
Introduction.....	5
Project I.....	10
Introduction.....	10
Results.....	12
Discussion.....	19
Figure legends.....	23
Figures.....	28
Project II.....	41
Introduction.....	41
Results.....	43
Discussion.....	46
Figure legends.....	48
Figures.....	50
Project III.....	54
Introduction.....	54
Results.....	56
Discussion.....	59
Figure legends.....	61
Figures.....	63
Project IV.....	67
Introduction.....	67
Results.....	69
Discussion.....	76
Figure legends.....	79
Figures.....	86

Final discussion.....	93
Materials and methods.....	96
References.....	103

*List of abbreviations*

CNS - Central nervous system

BBB - Blood-brain barrier

EMP - Erythro-myeloid precursors

YS - Yolk sac

TREM2 - Triggering receptor expressed on myeloid cells 2

AD - Alzheimer's Disease

WT - Wild type

BM - Bone marrow

ALD - Adrenoleukodystrophy

ALS - Amyotrophic lateral sclerosis

HSC - Hematopoietic stem cell

MLD - Metachromatic leukodystrophy

WAS – Wiskott-Aldrich syndrome

MS - Multiple sclerosis

EAE - Experimental autoimmune encephalomyelitis

MOG - Myelin oligodendrocyte glycoprotein

IL23 - Interleukin-23

MHCII - Major histocompatibility complex class II

LN - Lymph nodes

DAM - Disease-associated microglia

IFN - Interferon

LPS - Lipopolysaccharide

IL10 - Interleukin-10

IL10R - IL10 receptor

TF - Transcription factor

AGM - Aorto-gonado-mesonephros

TBI - Total body irradiation

BMT - Bone marrow transfer

DEG - Differentially expressed genes

GSEA - Gene Set Enrichment Analysis  
IGV - Integrative Genomics Viewer  
PCA - Principle component analysis  
TSS - Transcription start site  
SPF - Specific-pathogen-free  
KC - Kupffer cells  
AM - alveolar macrophages  
APC - Antigen presenting cell  
DC - Dendritic cell  
TAK1 - Transforming growth factor  $\beta$  activating kinase 1  
CC - Corpus callosum  
NO - Nitric oxide  
SC - Spinal cord  
KO - Knockout  
TNF $\alpha$  - Tumor necrosis factor alpha  
GM-CSF - Granulocyte macrophage colony-stimulating factor  
TZM - T zone macrophages  
JAK - Janus kinase  
STAT - Signal transducer and activator of transcription  
i.p. - Intra-peritoneal  
LTP - Long-term potentiation  
HSCT - Hematopoietic stem cell transplantation  
BAM - Barrier-associated macrophages

## *Abstract*

Microglia are macrophages that seed the embryonic neuro-epithelium, expand and eventually reside in the adult brain and spinal cord, where they intimately interact with neurons and other glial cells. Microglia are thought to prune excess synapses and thus critically contribute to the fitness of neuronal circuitries. Moreover, as central nervous system (CNS)-resident immune cells, microglia are poised to respond to peripheral challenges of the organism and likely involved in orchestrating ensuing CNS immune responses. Microglia research has bloomed in recent years, with increased attention to ‘microgliopathies’, in which mutant microglia are suggested to be the underlying cause. However, the discrimination of resident microglia from cell infiltrates entering from the periphery especially under pathology, is still a major challenge in the field. My thesis focused on dissecting the heterogeneity of microglia and bone marrow (BM)-derived brain macrophages, and studying the contribution of microglial activation in different pathological settings. In *Project I*, we demonstrated that although BM-derived brain macrophages acquire microglial characteristics, such as radio-resistance, longevity and morphology, they remain distinct from host microglia in their transcriptome and epigenome. The two populations remain also functionally distinct as they respond differently to challenge. These findings are of clinical relevance for patients undergoing BM transplantation, that results in a partial microglia replacement by engrafted macrophages.

In *Projects II and III*, we probed the role of microglia as antigen presenting cells or producers of the cytokine IL23 in a murine model of multiple sclerosis. Using a CX3CR1<sup>CreER</sup>-based *in vivo* gene manipulation system, we ablated MHCII or IL23 from microglia while sparing peripheral cells. We established that in the respective mutant animals, clinical symptoms were unaltered, suggesting that microglia are dispensable for the two functions. However, when we ablated IL23 in all tissue macrophages, mice were resistant to disease induction, suggesting a novel role for lymph node macrophages in autoimmunity. Finally, in *Project IV*, we revealed a novel role for IL10 in curbing detrimental hyperactivation of microglia following peripheral endotoxin challenge, driven by uncontrolled production of TNF by microglia. Our data provide evidence that microglia are critical regulators of sickness behavior, as these mutants succumb to fatal sickness and impaired neuronal function, and are of relevance for severe settings, as sepsis and bacteremia.

מיקרוגליה הם מקרופגים המיישבים את רקמת הנוירו-אפיתיליום העוברית, מתחלקים, ובסופו של תהליך מיישבים את המח וחוט השדרה באורגניזם הבוגר, שם הם עוברים אינטראקציה עם נוירונים ותאי גליה אחרים. מיקרוגליה גוזמים סינפסות עודפות ולכן תרומתם לחיווט נוירונים תקין היא קריטית. בנוסף, כתאים חיסוניים של מערכת העצבים במרכזית, מיקרוגליה מגיבים לאתגרים פריפראליים באורגניזם, וכנראה מעורבים ברגולציה ותיאום תגובות חיסוניות מתאימות. חקר המיקרוגליה פורח בשנים האחרונות, עם מודעות הולכת וגוברת לקבוצת מחלות בהן מיקרוגליה הוצעו להיות הגורמים למחלה. ואולם, האבחנה בין מיקרוגליה לבין תאים פריפראליים שעלולים לחדור למח, כאלה שמקורם ממח העצמם או ממונוציטים, אינה ברורה, בייחוד בתהליכים פתולוגיים, ולכן מהווה אתגר משמעותי בתחום מחקר זה. תזה זו מתמקדת בניסיון להבחין בין אוכלוסיית המיקרוגליה לבין מקרופגים שמאכלסים את רקמת המח ומקורם ממח העצם, ובחקר תרומת אקטיביציית המיקרוגליה במודלים פתולוגיים שונים. בפרויקט מספר 1, אנו מדגימים שלמרות שמקרופגים ברקמת המח שמקורם ממח העצם מסגלים לעצמם תכונות דומות לאלו של מיקרוגליה, כמו עמידות להקרנה, אורך חיים ארוך, ומציגים מורפולגיה זהה לזו של מיקרוגליה, ישנם הבדליים מהותיים בביטוי הדנ"א והרנ"א של שתי האוכלוסיות. שתי האוכלוסיות גם מגיבות באופן שונה למודל של זיהום חיידקי, ולכן הן שונות מבחינה פונקציונלית. ממצאים אלה רלוונטיים לחולים אשר עברו השתלת מח עצם, בהם ישנה החלפה חלקית של אוכלוסיית המיקרוגליה ע"י מקרופגים שמקורם במח העצם. בפרויקט מספר 2 ו-3, אנו חוקרים את היכולת של תאי המיקרוגליה בהצגת אנטיגן ובייצור של הציטוקין אינטרלוקין-23. בעזרת מודל עכברי לעריכת גנים ספציפית בתאי המיקרוגליה, הצלחנו למחוק את שני הגנים שאחראים לפעולות אלו, במודל עכברי לטרשת נפוצה. לא הבחנו בשינוי בתסמינים הקליניים בחיות אלו, ממצא המצביע על כך שמיקרוגליה אינם משחקים תפקיד בכיצוע שתי פעולות אלו. ואולם, כאשר מחקנו את הגן המקודד לאינטרלוקין-23 מכל אוכלוסיות המקרופגים בפריפריה, חיות אלו היו עמידות לפיתוח תסמינים קליניים. ממצא זה מצביע על תפקיד חדשני של מקרופגים בבלוטות הלימפה בביסוס התגובה הפתולוגית ההולמת במודל העכברי לטרשת נפוצה. בפרויקט 4, אנו מגלים תפקיד חדש לאינטרלוקין-10 בויסות אקטיביציית יתר של מיקרוגליה במודל עכברי של זיהום חיידקי. הממצאים שלנו מציעים שמיקרוגליה הם רגולטורים קריטיים של תסמיני המחלה, בעקבות מוות של העכברים המוטנטיים במודל זה. תוצאות אלה רלוונטיות למודלים שונים של זיהומים חיידקיים.

## *Introduction*

### Microglia: Resident macrophages of the central nervous system (CNS)

Microglia are mononuclear phagocytes residing in the central nervous system (CNS), sequestered behind the blood-brain barrier (BBB). As the resident macrophages of the brain parenchyma, microglia have been recognized as critical players in CNS development, pathology and homeostasis.<sup>1</sup> Specifically, microglia contribute to synaptic remodeling, neurogenesis, and the routine clearance of debris and dead cells.<sup>2,3,4,5</sup> Microglia furthermore act as immune sensors and take part in the CNS immune defense. When sensing injury, microglia cells undergo activation and respond by increased phagocytosis and secretion of cytokines.<sup>6</sup> The microglia population is established during embryonic development, from myb-independent erythro-myeloid precursors (EMP) that arise in the yolk sac (YS).<sup>7,8</sup> Unlike other macrophage populations, such as cells residing in skin, lung and heart, which can be partially replenished by recruited monocytes, the microglia pool relies exclusively on longevity and limited self-renewal.<sup>9</sup> Moreover, although monocyte infiltration is observed during CNS injury, monocyte-derived brain macrophages do not permanently contribute to the resident microglia pool and are cleared once homeostasis is restored.<sup>10</sup>

Microglia research has bloomed in recent years with emerging evidence for their clinical relevance. For instance, longevity of microglia renders these cells especially vulnerable to aging.<sup>11</sup> In line with the recent notion that microglia seem critical for proper brain development and neuronal connectivity, specific deficiencies in these cells have been associated with many CNS pathologies, including both psychiatric and neurological disorders.<sup>12</sup> These ‘microgliopathies’, in which microglia are suggested to be the underlying cause and drivers of the pathology, include colony stimulating factor 1 receptor (CSFR1) mutations in hereditary diffuse leukoencephalopathy with spheroids (HDLS),<sup>13</sup> and neurodegenerative diseases such as triggering receptor expressed on myeloid cells 2 (TREM2)-associated frontotemporal dementia<sup>14</sup> and CD33-associated Alzheimer’s disease (AD).<sup>15,16</sup>

In this thesis, I focused on the following current challenges in the field.

**(1) Dissecting the heterogeneity of microglia and BM-derived brain macrophages**

Therapeutic approaches to ‘microgliopathies’ could include microglia replacement by wild type (WT) cells. Moreover, microglia replacement by bone marrow (BM)-derived cells has also been proposed as treatment for metabolic disorders, such as adrenoleukodystrophy (ALD) and Hurler syndrome, as well as neuroinflammatory disorders (e.g. amyotrophic lateral sclerosis (ALS), Alzheimer disease (AD) in order to slow down disease progression or improve clinical symptoms.<sup>17</sup> Hematopoietic stem cell (HSC) gene therapy was shown to arrest the neuro-inflammatory demyelinating process in a gene therapy approach to treat metachromatic leukodystrophy (MLD) albeit with delay.<sup>17</sup> Of note, replacement of YS-derived microglia by HSC-derived cells is also a byproduct of therapeutic stem cell transplantations that are routinely used to treat monogenic immune disorders, such as Wiskott–Aldrich syndrome (WAS) and IL10 receptor deficiencies.<sup>17</sup> To what extent HSC-derived cells can replace the host microglia (especially after conditioning) and if these restore functions by cross-correction remains unclear.

Understanding how engrafted cells perform in the host, in particular following challenge, is therefore of considerable clinical importance, not only in HSC transplantation but also in HSC gene therapy approaches of disorders with a neurological phenotype. In *Project I*, we performed a comparative analysis of YS-derived microglia and BM graft-derived parenchymal brain macrophages, in both steady state and upon challenge. The results of this study were published in *Shemer et al., 2018*.<sup>18</sup> Collectively, we established that BM-derived brain macrophages that persistently seed the CNS of recipient organisms following irradiation remain distinct from host microglia with respect to their transcriptomes, chromatin accessibility landscapes and response to challenge.<sup>18</sup>

## **(2) Examining the unique contributions of microglia, monocyte-derived brain macrophages, and peripheral macrophages in CNS autoimmunity**

Microglia were suggested to play an active role in multiple sclerosis (MS), an inflammatory and demyelinating autoimmune disease of the CNS, characterized by axonal damage, inflammation, and BBB disruption.<sup>19</sup> Genetic make up has been shown to predispose to MS, and correlations were also found with viral infections and environmental factors.<sup>20</sup> Although its etiology is not entirely clear, MS is known to be associated with a massive infiltration of peripheral immune cells, including both myeloid cells and T lymphocytes.<sup>20</sup> Interestingly, microglia activation well precedes this infiltration and demyelination,<sup>21</sup> implying that microglia may play a role in the earliest stages of disease development.

Experimental autoimmune encephalomyelitis (EAE) is the most common animal model for MS, and induced by immunization of rodents with myelin antigens, such as myelin oligodendrocyte glycoprotein (MOG).<sup>22</sup> Among the MS symptoms that are recapitulated by EAE are CNS inflammation, paralysis, weight loss, and demyelination. Pioneering studies suggested an involvement of microglia in EAE pathogenesis, as inhibition of microglia activation resulted in the attenuation of disease severity, inflammation, and demyelination.<sup>23,24</sup> However, these early studies suffered from a lack of specificity.

Our group has established a novel mouse model that enables us to genetically manipulate microglia in their physiological context,<sup>25</sup> distinguish them from monocyte-derived cells and most peripheral macrophage populations – a major challenge in microglia research. Microglia express unique high and stable levels of the CX<sub>3</sub>CR1 chemokine receptor.<sup>26</sup> In CX<sub>3</sub>CR1<sup>Cre</sup> mice, microglia hence undergo spontaneous rearrangements of loxP-flanked alleles. In contrast, in CX<sub>3</sub>CR1<sup>CreER</sup> mice, the Cre recombinase is kept latent in the cytoplasm and requires Tamoxifen (TAM) administration for its nuclear translocation and activation.<sup>25</sup> Rearrangements in TAM-treated CX<sub>3</sub>CR1<sup>CreER</sup> mice occur in microglia but also other, peripheral CX<sub>3</sub>CR1 expressing myeloid cells, including monocytes.<sup>25</sup> However, since the latter are continuously replaced by BM-derived cells<sup>25</sup> gene manipulations in these cellular compartments are only temporary. Therefore, CX<sub>3</sub>CR1<sup>CreER</sup> mice allow a rather specific manipulation of microglia in otherwise intact animals.

We took advantage of this model system to specifically target microglia and dissect their functions during EAE pathophysiology, specifically those of antigen presentation (*project II*) and IL23 production (*project III*). Since microglia elevate major histocompatibility complex

class II (MHCII) expression during the induction of EAE, they were presumed to act as antigen presenting cells (APC).<sup>27</sup> In order to investigate whether microglial MHCII has a direct role in EAE progression, or is a mere activation marker on these cells, we generated mice with a specific microglial MHCII deletion by using the  $CX_3CR1^{CreER}$  mouse. The results of this study were published in *Wolf, Shemer, Levy-Efrati et al., 2018*.<sup>28</sup> We have established that as opposed to the general assumption in the field, microglia do not contribute to antigen presentation to initiate CNS autoimmunity, and are not crucial for the priming of encephalitogenic T cells during the course of EAE.<sup>28</sup>

IL23, an inflammatory cytokine from the IL12 family, has emerged as the major pathogenic agent in EAE,<sup>29</sup> as IL23-deficient mice were shown to be protected from disease induction.<sup>30</sup> Microglia and other myeloid cells were suggested to be the source of IL23,<sup>31</sup> although the critical source for EAE induction is yet to be defined. Also, whether IL23 is needed in the CNS or in the periphery for EAE induction is not clear.<sup>32</sup> Our results suggest that in fact microglial IL23 is dispensable for the disease induction and progression, whereas peripheral macrophages, that most likely reside in the lymph nodes (LN) T cell zone, are crucial for Th17 expansion and EAE induction (*unpublished observation*).

### **(3) Defining the circuits controlling microglial activation**

Recent studies have suggested that distinct brain pathologies are associated with discrete microglia activation modules.<sup>33</sup> Specifically, this includes a Disease-associated microglia (DAM) or MgND signature of microglia,<sup>34,35</sup> that was revealed to be associated with neurodegenerative diseases, such as AD and ALS. In EAE, involving inflammatory immune cell infiltrates and interferon (IFN) exposure,<sup>28</sup> microglia have been shown to adopt different expression pattern associated.<sup>36,37</sup> Systemic endotoxin challenge by injection of lipopolysaccharide (LPS), was reported to lead to an overall different microglia response.<sup>38</sup> The existence of such distinct response patterns could bear potential for targeted therapy.<sup>33</sup>

Although arguably of equal importance to understand CNS pathology, modules that curb microglia activation or are critical for microglia to restore homeostasis, have remained less well explored. Microglia quiescence has been shown to require expression of *Sall1*, a member of the Spalt (“Spalt-like” (*Sall*)) family of transcriptional regulators,<sup>39</sup> one of the microglia signature genes. Likewise, and supported by the characteristic microglial  $Tgf\beta$  receptor expression,  $Tgf\beta$  prevents spontaneous microglia hyperactivation.<sup>40</sup> Finally,

microglia activation has been shown to be controlled by CD200 Ligand–Receptor Interactions.<sup>41</sup>

The anti-inflammatory cytokine IL10 has been extensively studied in relation to controlling activation of lymphoid and myeloid immune cells.<sup>42</sup> Our group has recently revealed that macrophage-restricted ablation of the IL10 receptor (IL10R) results in spontaneous colitis, as intestinal macrophages require constant IL10 signal in order to maintain gut homeostasis.<sup>43,44</sup> To date, no definitive role was demonstrated for IL10 in maintenance of CNS homeostasis, although numerous studies have suggested that microglia produce and require IL10 signaling. However, this assumption was largely based on the analysis of cultured microglia, which were demonstrated to be distinct from the respective cells in the *in vivo* context.<sup>45</sup> In this thesis we reveal a novel role for IL10 in curbing deleterious microglia hyperactivation upon LPS challenge, using the CX<sub>3</sub>CR1<sup>CreER</sup> model system (*project IV*).

Project I: Comparison of host microglia and engrafted brain macrophages –  
Analysis of transcriptome, chromatin landscape and response to LPS challenge

*Introduction*

Macrophages were shown in the mouse to arise from three distinct developmental pathways that differentially contribute to the respective tissue compartments in the embryo and adult. Like other embryonic tissue macrophages, microglia first develop from primitive macrophage progenitors that originate in the mouse around E7.25 in the YS, are thought to be independent of the transcription factor (TF) Myb and infiltrate the brain without monocytic intermediate.<sup>46,7,8</sup> YS macrophage-derived microglia persist throughout adulthood. Most other tissue macrophages are however replaced shortly after by fetal monocytes that derive from myb-dependent multipotent EMP that also arise in the YS, but are currently thought to be consumed before birth. Starting from E10.5, definitive hematopoiesis commences with the generation of HSC in the aorto-gonado-mesonephros (AGM) region. HSC first locate to the fetal liver but eventually seed the BM to maintain adult lymphoid and myeloid hematopoiesis. Most EMP-derived tissue macrophage compartments persevere throughout adulthood without significant input from HSC-derived cells. In barrier tissues, such as the gut and skin, as well as other selected organs, such as the heart, HSC-derived cells can however progressively replace embryonic macrophages involving a blood monocyte intermediate.<sup>9</sup>

Differential contributions of the three developmental pathways to specific tissue macrophage compartments seem determined by the availability of limited niches at the time of precursor appearance.<sup>47</sup> In support of this notion, following experimentally induced niche liberation by genetic deficiencies, such as a *Csf1r* mutation, irradiation or macrophage ablation, tissue macrophage compartments can be seeded by progenitors other than the original ones.<sup>48,49,50,51</sup>

Tissue macrophages display distinct transcriptomes and epigenomes<sup>52,53</sup> that are gradually acquired during their development.<sup>54,55</sup> Establishment of molecular macrophage identities depends on the exposure to tissue specific environmental factors.<sup>56,9</sup> Accordingly, characteristic tissue macrophage signatures, including gene expression and epigenetic marks, are rapidly lost upon *ex vivo* culture, as best established for microglia.<sup>53,45</sup>

As discussed earlier, microglia have been recognized as critical players in CNS development and homeostasis. They contribute to synaptic pruning, neurogenesis and clearance of debris

and dead cells<sup>2,3,4,5,57</sup> and also act as immune sensors playing an important part in the CNS immune defense.<sup>58</sup> In recent years, it has been suggested that mutations affecting microglia functions result in neuropsychiatric or neurologic disorders.<sup>12</sup> Therapies to these ‘microgliopathies’ were suggested to include microglia replacement by WT cells. In fact, replacing microglia with BM-derived cells has also been proposed as treatment for various metabolic and neurodegenerative disorders.<sup>17</sup> HSC gene therapy was shown to arrest the neuro-inflammatory demyelinating process in a gene therapy approach to treat MLD albeit with delay.<sup>17</sup> Of note, a byproduct of stem cell transplantation, which is routinely used to treat monogenic immune diseases, is replacement of YS-derived microglia by HSC-derived cells. To what extent these HSC-derived cells can phenocopy the innate host microglia functions remain to be discovered. Understanding how engrafted cells perform in the host, in particular following challenge, is therefore highly, not only in HSC transplantation, but also in HSC gene therapy approaches of disorders with a neurological phenotype.

Here we report a comparative analysis of YS-derived microglia and BM graft-derived parenchymal brain macrophages. Using RNAseq and ATACseq of host and engrafted macrophages isolated from mouse BM chimeras, we show that these cells acquire microglia characteristics such as longevity, morphology and gene expression features, but still remain significantly distinct with respect to transcriptomes and chromatin accessibility landscapes. Furthermore, host and graft cells display discrete responses to challenge by peripheral endotoxin exposure. Finally, by extending our finding to clinical settings, we confirm that in human HSC transplant patients, grafted cells also remain distinct from host microglia. Collectively, these data establish that engrafted macrophages differ from host microglia even after prolonged residence in the brain parenchyma and could have considerable clinical implications for patients treated by HSC gene therapy.

## Results

### Engrafted macrophages acquire longevity and radio-resistance

Following total body irradiation (TBI), myeloid precursors enter the brain and contribute to the parenchymal macrophage compartment.<sup>59,60,61</sup> Host microglia are relatively radio-resistant and unless combined with conditioning, engraftment of the brain macrophage pool was therefore reported to be limited.<sup>60,62,63,64</sup> It furthermore remained unclear to what extent graft-derived cells acquire over time microglia characteristics, such as longevity and radio-resistance. To address this issue, we generated BM chimeras by lethally irradiating WT mice (CD45.2) (950cGy) and transplanting them with CX<sub>3</sub>CR1<sup>GFP</sup> BM (CD45.1)<sup>26</sup> (**Supplementary Fig. 1A**). Four months after irradiation and BM transfer (BMT), monocyte precursors in the BM and circulating blood monocytes of the chimeras were all CD45.1<sup>+</sup> GFP<sup>+</sup> and hence exclusively derived from the BM graft (**Supplementary Fig. 1B, C**). Analysis of the CD45<sup>int</sup> CD11b<sup>+</sup> Ly6C<sup>-</sup> Ly6G<sup>-</sup> microglia compartment of the chimeras revealed the presence of GFP<sup>+</sup> graft- and GFP<sup>-</sup> host-derived cells (**Supplementary Fig. 1D**). In line with earlier reports, grafted cells initially constituted only a small fraction of the parenchymal brain macrophage population. However, the cells progressively replaced the host microglia (**Supplementary Fig. 1D**). The expansion of the GFP<sup>+</sup> infiltrate could indicate ongoing peripheral input. Alternatively, the undamaged non-irradiated CNS-resident graft-derived cells might have an advantage over the irradiated host microglia, and gradually outcompete the latter during the reported infrequent microglial local proliferation.<sup>65,66</sup> To distinguish between these options, we performed a tandem engraftment. Recipient mice (CD45.1/2) were irradiated twice, 15 weeks apart, followed by engraftment with CX<sub>3</sub>CR1<sup>GFP</sup> BM (CD45.1) and CX<sub>3</sub>CR1<sup>Cre</sup>:R26-RFP<sup>fl/fl</sup> BM (CD45.2), respectively (**Fig. 1A**). Blood analysis of the chimeras 7 weeks after the second BMT, showed that monocytes were exclusive derivatives of the second graft (**Fig. 1B**), as were myeloid BM precursors (**Supplementary Fig. 1E**). In contrast, analysis of the CNS compartment of the chimeras revealed the presence of three distinct macrophage populations: Host microglia (CD45.1/2<sup>+</sup>), cells derived from the first graft (CD45.1<sup>+</sup> GFP<sup>+</sup>), and cells derived from the second BM graft (CD45.2<sup>+</sup> RFP<sup>+</sup>) (**Fig. 1C, D, Supplementary Fig. 1F**). Presence of cells derived from the first graft establishes that these (1) acquired radio-resistance and (2) persisted in the chimeras for more than 2 months without contribution from the periphery. Corroborating the above results, cells derived from both grafts expanded on the expense of the host microglia (**Figure 1D**). CX<sub>3</sub>CR1<sup>GFP</sup> (CD45.1) and CX<sub>3</sub>CR1<sup>Cre</sup>:R26-RFP<sup>fl/fl</sup> (CD45.2) cells with ramified microglia morphology were detected in the brain parenchyma (**Fig. 1E**). Collectively, these

data establish that engrafted cells adopt microglia characteristics, such as relative radio-resistance, longevity and morphology.

### **Macrophages engrafting conditioned brains display expansion**

To further characterize the engraftment process, including clonal dynamics of the BM-derived cells, we collaborated with Dr. Tuan Leng Tay and Dr. Kerstin Cornils to use two complementary approaches, comprising (1) transplantation of BM isolated from *Cx3cr1<sup>CreER</sup>:R26<sup>Confetti</sup>* ('Microfetti') mice<sup>66</sup> and (2) transplantation of lineage negative BM cells marked by a genetic barcode prior to transplantation.<sup>67</sup> The detailed experimental setup and findings can be found in *Shemer et al., 2018*.<sup>18</sup> To summarize, clusters of same color in close proximity in brains of 'Microfetti' mice provided evidence of local proliferation, rather than ongoing peripheral contribution of BM-derived cells. In addition, the genetic barcoding experiment shows that a major fraction of the grafted cells originates from transduced precursors that seed the host CNS early after engraftment and is maintained by local proliferation independent from ongoing hematopoiesis. Taken together, these results establish that efficiently engrafted donor cells adopt the phenotype and distribution of resident microglia within this cellular network, and expand locally with kinetics specific to brain regions and conditioning paradigms.

### **Engrafted cells exhibit transcriptomes distinct from microglia**

BM graft-derived parenchymal brain macrophages acquire characteristics such as ramified morphology, longevity and radio-resistance and can hence be considered engrafted microglia-like cells that could potentially be employed for therapeutic purposes. Recent studies have highlighted the impact of the tissue environment on macrophage identities, including epigenomes and expression profiles.<sup>52,53</sup> To test whether graft-derived microglia acquire in the CNS such a global molecular imprint, we transplanted lethally irradiated 6 week old WT mice with congenic WT BM harboring CD45.1 alleles. Nine months post transplantation, chimeras were sacrificed and brain macrophages were isolated for transcriptome and epigenome analysis by RNAseq<sup>68</sup> and ATACseq,<sup>69</sup> respectively. At this time point, half of the CNS macrophages of the chimeras were of graft origin (**Fig. 2A, Supplementary Fig. 2A**).

Global RNAseq analysis of parenchymal host and graft brain macrophages isolated from individual BM chimeras revealed that engrafted cells and host microglia showed significant transcriptome overlap, clearly distinguishing them from monocytes that served as reference

for HSC-derived cell population (**Fig. 2B, C**).<sup>70</sup> Of the total 11,614 detected transcripts, 10,635 (91%) displayed a lower than 2 fold-difference between the engrafted cells and host microglia. On the other hand, 979 transcripts were differentially expressed between these two populations (absolute value of log<sub>2</sub>-fold change > 1, p-value < 0.05) (**Supplementary Fig. 3A**). Expression of 469 genes was restricted to host microglia, while 510 genes were uniquely expressed by the engrafted cells (**Supplementary Fig. 3A, B**). Engrafted macrophages, but not host microglia displayed for instance mRNA encoding CCR2, Lysozyme, CD38, CD74, Mrc1, ApoE and Ms4a7 (**Fig. 2E, Supplementary Fig. 3B**). Differentially expressed genes (DEG) included TFs such as the basic helix-loop-helix TF Hes1, the Krueppel-like zinc finger TF Klf12, the retinoic acid receptor RxRg and the TGFβ-associated signal transducer Smad3, that were preferentially transcribed in host cells. Conversely, engrafted macrophages displayed increased expression of the estrogen receptor Esr1, the runt-domain TF Runx3 and the macrophage survival factor Nr4a1, as compared to host cells (**Fig. 2D**). Of note, the host microglia in this case were irradiated and differences observed between the two populations could hence arise from radiation damage; transcriptomes of engrafted cells however also differed significantly from age-matched non-irradiated microglia (**Supplementary Fig. 3C**).

Supporting the notion of their microglia-like identity, engrafted cells expressed similar levels of the DNA-RNA binding protein TDP-43 encoded by the *Tardbp* gene recently implied as regulator of microglial phagocytosis,<sup>71</sup> the Two-Pore Domain Potassium Channel THIK-1, encoded by the *Kcnk13* gene and shown to be critical for microglial ramification, surveillance, and IL1β release<sup>72</sup> and the TF Mef2c, reported to restrain microglia responses (**Fig. 2F**).<sup>73</sup> Likewise, the graft also displayed expression of ‘microglia signature’ genes that have been proposed to distinguish these cells from other tissue macrophages and acute monocyte infiltrates associated with inflammation,<sup>40,74</sup> including Fc receptor-like molecule (*Fcrls*) and TGFβ receptor (*Tgfbr*), which is critical to establish microglia identity (**Fig. 2F**).<sup>40</sup> Other proposed ‘microglia signature genes’, such as *P2ry12*, *Tmem119*, *SiglecH* and *HexB* displayed either significantly reduced expression in the grafted cells or were exclusively expressed by host microglia, like the ones encoding the Sodium/glucose cotransporter 1 (*Slc2a5*), the phosphoglycoprotein protein CD34 (*Cd34*) and the transcriptional repressors Sall1 (*Sall1*) and Sall3 (*Sall3*) (**Fig. 2G, Supplementary Fig. 3D**). Of note, lack of some microglia markers had been reported before for cells retrieved from acutely engrafted brains.<sup>50,75,39,40</sup>

The expression signature of the engrafted macrophages showed a considerable overlap with the transcriptome of perivascular macrophages,<sup>76,34,77</sup> including present and absent transcripts, such as *ApoE*, *Msn4a7*, *Slc2a5* and *Sall1*, respectively. Gene Set Enrichment Analysis (GSEA)<sup>34</sup> revealed that engrafted macrophages displayed an activation signature as compared to host microglia (**Supplementary Fig. 4A**). Finally, and corroborating our data, the list of genes we report as differentially expressed by engrafted and host cells also displayed a considerable overlap with results recently reported by two other groups (**Supplementary Fig. 4B**).<sup>78,79</sup>

*Sall1*, a member of the *Spalt* ('Spalt-like' (Sall)) family of evolutionarily conserved transcriptional regulators critical for organogenesis, acts as repressor by recruitment of the Nucleosome Remodeling and Deacetylase Corepressor Complex (NurD). Binding motifs of *Sall1* and hence its direct genomic targets remain undefined precluding a direct assessment of the impact of the lack of the repressor on the expression signature of the grafted macrophages. Interestingly though, comparison of the recently reported list of genes differentially expressed by WT and *Sall1*-deficient microglia<sup>39</sup> and that of host and graft brain macrophages revealed in this study, showed significant overlap (**Fig. 2H**). This included expression of genes otherwise restricted to macrophages residing in non-CNS tissues, such as *Msr1*, encoding a scavenger receptor, and *Cyp4f18* encoding cytochrome P450 (**Fig. 2I**). Furthermore, like *Sall1*-deficient microglia,<sup>39</sup> grafted CNS macrophages displayed an activation signature, as reflected by expression of *Cybb* encoding the Cytochrome b-245 heavy chain and *Axl* encoding a member of a tyrosine kinase receptor family critical for debris clearance (**Fig. 2I, Supplementary Fig. 4B**).<sup>57</sup> This suggests that a major fraction of the differential expression of host microglia and engrafted cells could be explained by the specific absence of the transcriptional repressor *Sall1* from the former cells. Overall, these findings establish that engrafted macrophages that persist in the brain and acquire microglia characteristics such as morphology and radio-resistance, also show significant transcriptome overlap with host microglia, but remain a molecularly distinct population.

### **Engrafted macrophages and microglia exhibit distinct chromatin accessibility landscapes**

To further define engrafted cells and host microglia we performed an epigenome analysis using ATACseq that identifies open chromatin regions by virtue of their accessibility for

'tagmentation' by transposases.<sup>69</sup> Correlated ATACseq replicates (**Supplementary Fig. 5A**) performed on graft and host microglia isolated from BM chimeras detected 58,947 total accessible regions (corresponding to 16,156 genes). Corroborating the observed differential gene expression (**Fig. 2**), host microglia but not engrafted cells, displayed ATAC signals in the *Sall1* and *Klf2* loci as indicated in Integrative Genomics Viewer (IGV) tracks (**Fig. 3A**). ATAC peaks in other genomic locations, such as *ApoE* and *Ms4a7*, were restricted to genomes of engrafted cells, in line with mRNA detection in these cells, but not host microglia (**Fig. 3B**). As ATACseq does not discriminate between bound transcriptional activators and repressors, some differentially expressed loci did not show epigenetic differences. This included for instance the MHCII locus (*H2-ab1*), which displayed similar ATACseq peaks in host microglia and the graft that lack and display *H2-ab1* transcripts, respectively (**Fig. 3C**). These loci might be transcriptionally silenced, but activated upon cell stimulation. Similar 'poised' states, that might be revealed following challenge, can be assumed for gene loci, that displayed differential ATAC peaks, but were transcriptionally active in neither the host nor the engrafted cells. Finally, rare genes, such as the *Dbi* locus showed equal expression, but differential ATAC profiles suggest that their transcription is driven by distinct TFs (**Fig. 3C**). Global quantification of differential ATAC peaks between the two brain macrophage populations revealed that 6% of the total accessible regions (or 8.7% of the associated genes) were distinct. Specifically, 1,506 peaks (corresponding to 941 genes) displayed a >4 fold significant (p-value<0.01) enrichment in host microglia and 2,176 peaks (corresponding to 1,465 genes) were increased in BM graft-derived cells (**Fig. 3D**).

### **Engrafted macrophages respond unlike microglia to challenge**

Given the significant transcriptome and chromatin landscapes differences between the host and BM-graft derived macrophages that persists for extended periods of time post-transplantation, we next examined whether the two populations are functionally distinct. To that end, chimeras were challenged nine months post-transplantation by a peripheral injection of the bacterial endotoxin LPS, an established paradigm for inflammation associated with robust microglia responses to systemic cytokine secretion. Host and engrafted cells were isolated from the brains of the chimeras 12 hours post LPS challenge, global RNA and ATAC sequencing were performed, and results were compared to the samples obtained from non-challenged mice presented earlier (**Fig. 2, 3**). Principle component analysis (PCA) revealed a high degree of similarity within each group, but segregation of the host and graft samples (**Fig. 4A**). Host and grafted cells responded with altered expression of 745 shared genes. 940

genes were changed in grafted cells only, and 602 genes were changed in host microglia upon LPS challenge (**Fig. 4B**). Examples for these three categories are shown in **Fig. 4C, D** and **Supplementary Fig. 6A**. Genes commonly induced by engrafted cells and host microglia in response to the LPS challenge comprised *Tnf*, *Ccl5* and *Tnfaip3*, encoding the A20 deubiquitinase that negatively regulates NFκB–dependent gene expression. Commonly downregulated genes comprised *Trem2*, *Cx3cr1* and *Aif1*. The graft specific response included upregulation of *Clec4e*, *Pirb*, *Isg15*, *Irf7* and downmodulation of *Mgl2*, *Cmah* and *CD36*. Genes specifically induced in host microglia encoded the scavenger receptor Marco, Gpr65, Tlr2 and Il12b. Moreover, host microglia silenced expression of *Sall1* and *Upk1b* (**Fig. 4D**). Ingenuity analysis of transcriptomes of engrafted and host brain macrophages isolated from chimeras with and without peripheral LPS challenge revealed potential distinct upstream regulators acting on these populations, as well as a differential representation of activated functional pathways (**Supplementary Table 1**). Engrafted macrophages displayed for instance activation of pathways controlled by IL1β and IFNγ and suppressed by IL10.

ATACseq analysis revealed differential epigenome alterations between engrafted and host cells in response to the LPS challenge. Specifically, correlated ATACseq replicates (**Supplementary Fig. 7A**) performed on engrafted and host cells isolated from BM chimeras after LPS challenge detected 46,485 total accessible regions (corresponding to 15,390 genes). Global quantification of differential ATAC peaks between the two brain macrophage populations revealed a total of 552 peaks (corresponding to 391 genes) that displayed a >4 fold significant (p-value<0.01) enrichment in host microglia and 841 peaks (corresponding to 618 genes) that were increased to the same extent in BM graft-derived cells (**Fig. 5A**).

Overall, differences between host and graft cells were less pronounced after LPS challenge (**Fig. 3D, 5A**). Appearance of ATACseq peaks was correlated with differential gene expression between the two macrophage populations (**Fig. 5B**). Transcripts encoding the scavenger receptor Marco were absent from host microglia, but specifically induced in these cells but not engrafted cells following the LPS challenge (**Fig. 5B**). Likewise, the *Marco* locus (92kb) in microglia of unchallenged animals displayed 5 ATACseq peaks that were all restricted to the host cells (I-V; **Fig. 5B**). LPS challenge resulted in loss of one peak (IV) and the induction of 3 additional peaks (VI- VIII), again restricted to host microglia (**Fig. 5B**). An induced peak located 53,411 bp downstream of the Transcription start site (TSS) displayed a host-specific Nfkb1 motif, whereas a second peak located 19,210 bp upstream of the Marco

TSS displayed a host-specific AP-1 (Fos-related) motif (**Fig. 5B**). Engrafted macrophages on the other hand, displayed as compared to host microglia prominent induction of Secreted Phosphoprotein 1 (SPP1) / Osteopontin (**Fig. 5C**), a factor that got recent attention as part of a microglia signature that could be associated with certain CNS pathologies.<sup>33</sup> In accordance with the expression results, *Spp1* loci (74kb) of engrafted macrophages displayed following LPS challenge 3 ATACseq peaks (V- VII), that were significantly enhanced over host microglia (**Fig. 5C**). An induced peak located 54,402 bp upstream of the TSS displayed a TBX5 motif, whereas a second peak located 38,600 bp upstream of the *Spp1* TSS displayed an AP-1 (Jun-related) motif (**Fig. 5C**). Collectively, these data establish that engrafted microglia respond differently from host microglia to a challenge and are hence functionally distinct.

### **Engrafted macrophages in human brain differ from microglia**

Engrafted brain macrophages differ from host microglia by their gene expression (**Fig. 2B**). To confirm this finding for protein expression, a histological analysis of brains of the BM chimeras generated by TBI and Busulfan conditioning, was performed in collaboration with the lab of Prof. Marco Prinz. The detailed experiment can be reviewed in *Shemer et al., 2018*.<sup>18</sup> In summary, in concordance with our transcriptome data (**Fig. 2G**), analysis for *Tmem119* and *P2ry12* expression revealed absence of these markers from the graft, while labeled engrafted cells displayed ApoE and MHCII.

To finally extrapolate our finding to a human setting, the Prinz lab also analyzed *post mortem* brains of patients that had underwent HSC transplantation. Specifically, they took advantage of gender-mismatched grafts that allowed identification of the transplant by virtue of its Y-chromosomes through chromogenic *in situ* hybridization (CISH). To summarize, Ramified Iba1<sup>+</sup> microglia-like cells harboring the Y chromosome could be readily identified juxtaposed to Y chromosome-negative host microglia in cortex, cerebellum and hippocampus sections of the subject brains. As observed in the murine chimeras, also human P2Y<sub>12</sub> receptor expression, which was proposed to be a human microglia marker,<sup>80,81</sup> was found to be restricted to host cells, but absent from Y chromosome-positive brain macrophages cells. Collectively, these data establish that in the CNS of patients that underwent HSC transplantation, graft-derived cells remained functionally distinct from host microglia and strengthen the conclusion that HSC-derived engrafted cells differ from host microglia.

## *Discussion*

Here we established that BM-derived brain macrophages that persistently seed the CNS of recipient organisms following irradiation or myelo-ablation remain distinct from host microglia with respect to their transcriptomes, chromatin accessibility landscapes and response to challenge.

Following the engraftment of conditioned recipient mice, transplanted cells establish under the influence of the CNS microenvironment a characteristic microglia transcriptome that distinguishes these cells from other tissue macrophages.<sup>40</sup> Thus, nine tenth of their transcriptome is shared with host microglia, including expression of Fc receptor-like molecules (Fcrls) and Tgfb receptor (Tgfbr), as well as the MADS box transcription enhancer factor 2 (Mef2c). Moreover, residence in the CNS endowed engrafted cells with microglia characteristics, such as longevity, radio-resistance and ramified morphology. Engrafted cells however failed to adopt complete host microglia identity even after prolonged CNS residence. Corroborating and extending earlier reports,<sup>75,39,40</sup> this included significantly reduced mRNA expression of the microglia markers Tmem119, SiglecH and P2yr12 and complete lack of the transcriptional repressors Sall1 and Sall3. Conversely, engrafted macrophages expressed genes absent from host microglia, including Ccr2, Ifnar1, Msa4a7 and ApoE, and displayed Msr1 and Axl mRNAs, potentially related to the absence of Sall1.<sup>39</sup> Transcriptomes of engrafted macrophages showed considerable overlap with perivascular macrophages and indication of cell activation, such as an underrepresentation of a regulatory pathway driven by IL10, as compared to host microglia. Comparative transcriptome analysis showed that our data are well in line with recent studies<sup>78,79</sup> that reported that also macrophages that engraft the brain of mice conditionally depleted of microglia due to a Csf1r deficiency retain a transcriptional identity distinct from host cells.

Analysis of open chromatin revealed that graft cells acquire a transposase-accessible profile that is similar to that of host cells and is enriched for a common set of motifs that are recognized by TFs known to be important for microglia development, such as PU.1 and MEF2c. However, host and graft cells also exhibit significant differences in open chromatin that are associated with distinct motif enrichment patterns and the observed differences in gene expression. These findings imply that the distinct developmental origins of host and graft cells determine the ability of the brain environment to fully activate the complement of transcription factors required for microglia identity, most notably exemplified by lack of

induction of *Sall1* in graft cells. The differences in chromatin landscapes under resting conditions are likely to contribute to the host and graft-specific responses to LPS challenge. This possibility is supported by the observation that alternative motifs for NFκB and AP-1 factors are enriched in open chromatin of host and graft cells. We interpret this finding to reflect the binding of NFκB and AP-1 dimers and heterodimers to different locations in the genome that are specified by the specified by host or graft-specific combinations of transcription factors, respectively.

The exact origin of the BM-derived engrafted cells in the chimeric organisms remains to be defined. In a classic study, Ajami and colleagues established that non-parenchymal brain macrophages that can persistently seed the host brain originate from non-monocytic BM-resident myeloid progenitors characterized by the absence of CX3CR1 expression.<sup>59</sup> Likewise, other studies suggested that a transient wave of early hematopoietic progenitors infiltrates the host CNS during transplantation and following local proliferation, establishing the graft.<sup>64</sup> This notion is supported by the results of our ‘Microfetti’ and barcoding approaches that establish that engrafted macrophages undergo clonal proliferation and thereby likely progressively outcompete irradiation or busulfan-damaged host microglia. Moreover, the conclusion that engrafted cells arose from cells that do not contribute to long-term hematopoiesis in the chimeras is also in line with the prominent detection of private clones in this population, which are not shared with the other hematopoietic compartments.

Future studies could aim to identify cells that upon engraftment will give rise to closer mimics of host microglia, including for instance expression of *Sall1*. This could include cells linked with the unique developmental YS origin of microglia,<sup>78</sup> or otherwise manipulated cells such as microglia-like cells derived from induced-pluripotent-stem-cell (iPS)-derived primitive macrophages.<sup>82</sup> Furthermore, in the context of gene therapy, viral vectors could be used to express transgenes to engineer the engrafted cells to boost engraftment and modulate their function. Of note however, under certain pathological conditions, the distinct engrafted BM-derived macrophages we report might also be advantageous as compared to host microglia. BM-derived cells could for instance be superior to YS-derived microglia in the handling of the debris burden associated with senescence<sup>83</sup> or amyloid plaques that arise during AD.<sup>84</sup> Elucidation of such scenarios should profit from the molecular definition of the engrafted cells and host microglia like the one provided in this study. However, *in vivo* functions of microglia remain poorly understood and future dedicated experimentation will

be required to compare the performance of engrafted macrophages and host microglia in different disease models during aging and specific challenges.

Recent studies revealed a signature of disease associated microglia, termed ‘DAM’<sup>34</sup> or ‘MGnD’,<sup>35</sup> that is induced by various brain-intrinsic changes in the absence of massive peripheral infiltrates, though not following peripheral LPS challenge<sup>38,33</sup> and can occur on acute to chronic time scales.<sup>33</sup> Of note, engrafted brain macrophages displayed robust constitutive expression of some of these DAM genes, such as ApoE and Axl. Likewise, as opposed to microglia,<sup>33</sup> engrafted BM-derived brain macrophages responded to the LPS challenge with the induction of DAM/MGnD hallmarks, such as the CD44 ligand Spp1/Osteopontin. The latter might have implications when considering brain macrophage contributions to CNS pathologies. Moreover, our data support the notion that expression of genes included in the DAM/MGnD signature are in microglia under stringent control, potentially including repression by Sall1.

Results obtained from fate mapping models currently suggest that at least in the brain of unchallenged C57BL/6 mice kept in specific-pathogen-free (SPF) facilities, parenchymal macrophages are exclusively comprised of YS-derived microglia. Further experimentation will however be required to assess how absolute this exclusion of HSC-derived macrophages is, in particular following challenges. Moreover, it remains currently unclear to what extent HSC-derived macrophages might be able to seed the human brain, f.i. during extended aging, and could hence impact brain pathologies.

Tissue macrophages, such as Kupffer cells (KC) and alveolar macrophages (AM), have been reported to be faithfully replaced by BM-derived cells in irradiation chimeras and other small animal models involving deficiencies of the resident compartment.<sup>48,49,50,51</sup> While these studies were restricted to transcriptome comparison and hence might have missed epigenetic differences between graft and host cells, the inability of HSC-derived cells to achieve full host cell identity might be unique to microglia and related to features particular to these cells. Specifically, among adult tissue macrophages, only microglia derive from primitive YS macrophages and this origin could define cell identity. In contrast, generation of both KC and AM involves a monocytic intermediate, and their re-generation might hence be attainable by the closer related HSC-derived cells that can also give rise to monocytes. Alternatively, establishment of the ‘bona fide’ microglia signature might require ‘physiological’ microglia

development in the developing CNS that is associated with profound transient activation of this brain macrophage compartment.<sup>54,85,86,55</sup>

Collectively, the demonstration that engrafted cells and host microglia remain distinct sheds light on the molecular and functional heterogeneity of parenchymal brain macrophages. Moreover, when extrapolated to the human setting, our findings could have major implications for patients treated by HSC gene therapy to ameliorate lysosomal storage disorders, microgliopathies or general monogenic immuno-deficiencies.

## Figure legends

### Figure 1. Engrafted brain macrophages accumulate over time and self-maintain

- (A) Schematic of tandem BM transfer protocol.
- (B) Flow cytometric blood monocyte analysis of chimeras 16 weeks post transplantation.
- (C) Flow cytometric analysis of myeloid brain cells 16 weeks post second BMT revealing host microglia (CD45.1/2<sup>+</sup> GFP<sup>+</sup>, blue), cells derived from the first graft (CD45.1<sup>+</sup>, red) and cells derived from the second graft (CD45.2<sup>+</sup> RFP<sup>+</sup>, orange).
- (D) Distribution of host and graft-derived cells out of the total L6C/G (GR1)<sup>-</sup> CD45<sup>lo</sup> CD11b<sup>+</sup> cells in brain and spinal cord at two time points. Data are a summary of six mice.
- (E) Histological analysis 7 weeks post second BMT revealing ramified GFP<sup>+</sup> and RFP<sup>+</sup> cells with microglia morphology (scale bar 20  $\mu$ m). Representative picture

### Figure 2. Comparative transcriptome analysis of grafted cells and host microglia

- (A) Gating strategy for isolation of CNS macrophages. Host microglia were defined as Ly6C/G<sup>-</sup>CD11b<sup>+</sup>CD45.2<sup>lo</sup> cells; graft-derived cells were defined as Ly6C/G<sup>-</sup>CD11b<sup>+</sup>CD45.1<sup>lo</sup> cells.
- (B) PCA of transcriptomes of engrafted cells and host microglia and transcriptomes of monocytes subsets.<sup>70</sup>
- (C) Heatmap of RNAseq data of engrafted cells and host microglia compared to transcriptomes of Ly6C<sup>-</sup> and Ly6C<sup>+</sup> monocyte subsets.<sup>70</sup> Analysis was restricted to genes, which showed a two-fold difference and yielded p-value < 0.05 between at least two populations.
- (D) Heatmap showing differential TF expression profiles of engrafted cells and host microglia.
- (E) Examples of significantly differential (log<sub>2</sub>FC > 1 and p-value < 0.05) gene expression enriched in engrafted cells. Graphs show normalized reads from RNAseq data of samples acquired in (A), n = 4.
- (F) Examples of genes expressed in similar levels in host and engrafted cells. Graphs show normalized reads from RNAseq data of samples acquired in (A), n = 4. None of the genes were differentially expressed (log<sub>2</sub>FC < 1). Tgfb1 and Kcnk13 were of low significance (p-value < 0.05) but did not meet our FC threshold.
- (G) Examples of significantly differential (log<sub>2</sub>FC > -1, p-value < 0.05) gene expression enriched in host microglia. Graphs show normalized reads from RNAseq data of samples

acquired in (A),  $n = 4$ .

(H) Venn diagram showing overlap of genes differentially expressed by WT and *Sall1*-deficient microglia,<sup>39</sup> and genes differentially expressed by host and engrafted brain macrophages.

(I) Examples of gene expression of engrafted and host cells of genes expressed in non-CNS macrophages or *Sall1*-deficient microglia.

### **Figure 3. Comparative epigenome analysis of grafted cells and host microglia**

(A) IGV tracks of *Sall1* and *Klf2* loci showing ATAC signals in host (red) but not engrafted (blue) cells.  $N = 3$ .

(B) IGV tracks of *ApoE* and *Ms4a7* loci showing ATAC signals in engrafted cells (blue) but not host (red) microglia.  $N = 3$ .

(C) ATACseq IGV tracks (left,  $n = 3$ ) and normalized RNAseq reads (right,  $n = 4$ ) of *H2-ab1* and *Dbi* in host microglia (red) and engrafted cells (blue). +— $p$ -value  $< 10^{-5}$ , n.s.— $p$ -value  $> 0.05$ .

(D) Analysis of all 58,947 detected ATAC peaks, from which 1,506 peaks and 2,176 peaks displayed  $>4$ -fold significant ( $p$ -value  $< 0.01$ ) enrichment in host microglia and engrafted cells, respectively.

### **Figure 4. Distinct LPS responses of engrafted macrophages and host microglia**

(A) PCA of RNAseq data of graft and host microglia in steady state and 12hrs post LPS.

(B) Expression analysis of grafted cells and host microglia in steady state and 12hrs post LPS by RNAseq.

(C) Examples of genes expression of graft and host microglia in steady state and 12hrs post LPS. Significance is indicated by the symbols ( $p$ -value  $< 0.05$ ), or lack thereof ( $p$ -value  $> 0.05$ ). See *Ccl6* plot (top right) for symbol to condition conversion.

(D) Fold expression change of selected genes significantly different (absolute value of  $\log_2FC > 1$ ,  $p$ -value  $< 0.05$ ) following challenge in grafted cells (middle) or host microglia (right), as well as genes displaying comparable up- and downregulation in both engrafted cells and host microglia (left).

### **Figure 5. Comparative epigenome analysis of graft and host microglia post LPS challenge**

(A) Analysis of all 46,485 detected ATAC peaks, from which 552 peaks and 841 peaks displayed >4-fold significant (p-value < 0.01) enrichment in host microglia and engrafted cells isolated from challenged mice, respectively.

(B) Challenge induced alterations in Marco locus. Normalized sequence reads of Marco mRNA in engrafted cells and host microglia isolated from LPS challenged and unchallenged BM chimeras (top); normalized ATACseq profiles of Marco locus (bottom), with enlarged areas highlighting induced ATACseq peaks and predicted motifs.

(C) Challenge induced alterations in Spp1 locus. Normalized sequence reads of Spp1 mRNA in engrafted cells and host microglia isolated from LPS challenged and unchallenged BM chimeras (top); normalized ATACseq profiles of Spp1 locus (bottom), with enlarged areas highlighting induced ATACseq peaks and predicted motifs.

### **Supplementary Figure 1. BM-derived parenchymal brain macrophages accumulate over time post-irradiation**

(A) Schematic of BM transfer protocol.

(B) Flow cytometry analysis of myeloid BM progenitor compartment of chimeras 13 weeks post-BMT.

(C) Flow cytometry analysis of blood monocytes of chimeras 13 weeks post-BMT.

(D) Flow cytometry analysis of brain cells of chimeras 13 weeks post-BMT. Of note, Ly6C<sup>-</sup> CD11b<sup>+</sup> cells comprise host microglia (CD45.2) and BM-derived cells (GFP<sup>+</sup> CD45.1).

(E) Analysis of myeloid BM progenitor compartment of chimeras 7 weeks post second BMT. Note that none of the myeloid progenitors expressed GFP, while MDP, cMOP and monocytes do show RFP signal.

(F) Flow cytometric analysis of brain cells 16 weeks post second BMT for distribution of first and second graft-derived myeloid cells (CD11b<sup>+</sup>Ly6C/G<sup>+</sup> and CD11b<sup>+</sup>Ly6C/G<sup>-</sup>). Bar graph shows distribution of cells derived from first and second graft out of the total CD45<sup>+</sup> cells in brains at two time points. Data are a summary of 3 mice per time point.

### **Supplementary Figure 2. Flow cytometry analysis of chimeras used for isolation of cells for transcriptome and epigenome analysis**

(A) Representative flow cytometry analysis of brain of [CD45.1 > CD45.2] chimera, 9 months after engraftment. Note presence of graft derived-parenchymal macrophages (CD45.1<sup>int</sup>) and perivascular macrophages (CD45.1<sup>hi</sup>), but absence of the latter from the CD45.1<sup>+</sup> host compartment. Dot blot on the right indicates respective population in the sort gate (Fig. 3a)

(B) Representative flow cytometry analysis of brain of [CD45.1 > CD45.2] chimera, 9 months after engraftment and 12hrs after intra-peritoneal LPS treatment. Dot blot on the right indicates respective population in the sort gate (Fig. 2A).

### **Supplementary Figure 3. Comparison of transcriptomes of engrafted cells and host microglia**

(A) Volcano plot of RNAseq data of samples acquired in Fig. 2A, showing up-and down regulated genes in the graft-derived cells relative to host microglia. Analysis was restricted to expressed genes. Dark dots indicate genes showing a 2-fold difference and yielding p-values <0.05 between the two populations, N=4.

(B) Examples of gene expression enriched in engrafted cells. Graphs show normalized reads from RNAseq data of samples acquired in Fig. 2A, N=4.

(C) Correlation matrix of transcriptomes of engrafted cells and host microglia with transcriptome of microglia isolated from brains of age-matched non-irradiated C57BL/6 WT mice.

(D) Examples of gene expression enriched in host microglia. Graphs show normalized reads from RNA seq data of samples acquired in Fig. 2A, N=4.

### **Supplementary Figure 4. Pathway analysis and transcriptome comparisons**

(A) GSEA analysis of transcriptomes of HSC-derived engrafted brain macrophages and microglia.

(B) Comparative analysis of lists of genes differentially expressed by graft-derived brain macrophages and host microglia in this study to the data retrieved from the study by Kipnis and colleagues<sup>79</sup> and Bennett et al.<sup>78</sup> Blue area represents DEG of engrafted macrophages and host microglia of this study.

**Supplementary Figure 5. ATACseq data of engrafted cells and host microglia isolated from brains of unchallenged BM chimeras**

(A) Correlation analysis of ATACseq samples prepared from sorted grafted cells and host microglia.

(B) List of highly abundant motifs identified in sequences coinciding with ATACseq peaks ( $-\log_{10}(\text{p-value}) > 66.37$ ).

**Supplementary Figure 6. Comparison of engrafted cells and host microglia isolated from brains of BM chimeras subjected to peripheral LPS challenge**

(A) Examples of genes expressed by grafted cells and host microglia in steady state and 12hrs post-LPS.

(B) Heatmap showing differential TF expression profiles of grafted cells and host microglia isolated from LPS challenged chimeras.

**Supplementary Figure 7. ATACseq data of engrafted cells and microglia isolated from mice challenged with LPS**

(A) Correlation analysis of ATACseq samples prepared from sorted grafted cells and host microglia isolated from LPS challenged BM chimeras.

(B) List of highly abundant motifs identified in sequences coinciding with ATACseq peaks ( $-\log_{10}(\text{p-value}) > 50.86$ ) in grafted cells and microglia isolated from LPS challenged BM chimeras.

**Supplementary Table 1. Ingenuity Pathway analyses (IPA)**

(A) IPA analysis of genes differentially expressed by engrafted macrophages and host microglia isolated from untreated BM chimeras.

(B) IPA of transcriptomes of HSC-derived engrafted parenchymal brain macrophages and host microglia isolated from animals 12hrs after peripheral LPS challenge.

(C) IPA of genes differentially expressed by engrafted macrophages isolated from untreated BM chimeras or animals 12hrs after peripheral LPS challenge.

(D) IPA of genes differentially expressed by host microglia isolated from untreated BM chimeras or animals 12hrs after peripheral LPS challenge.

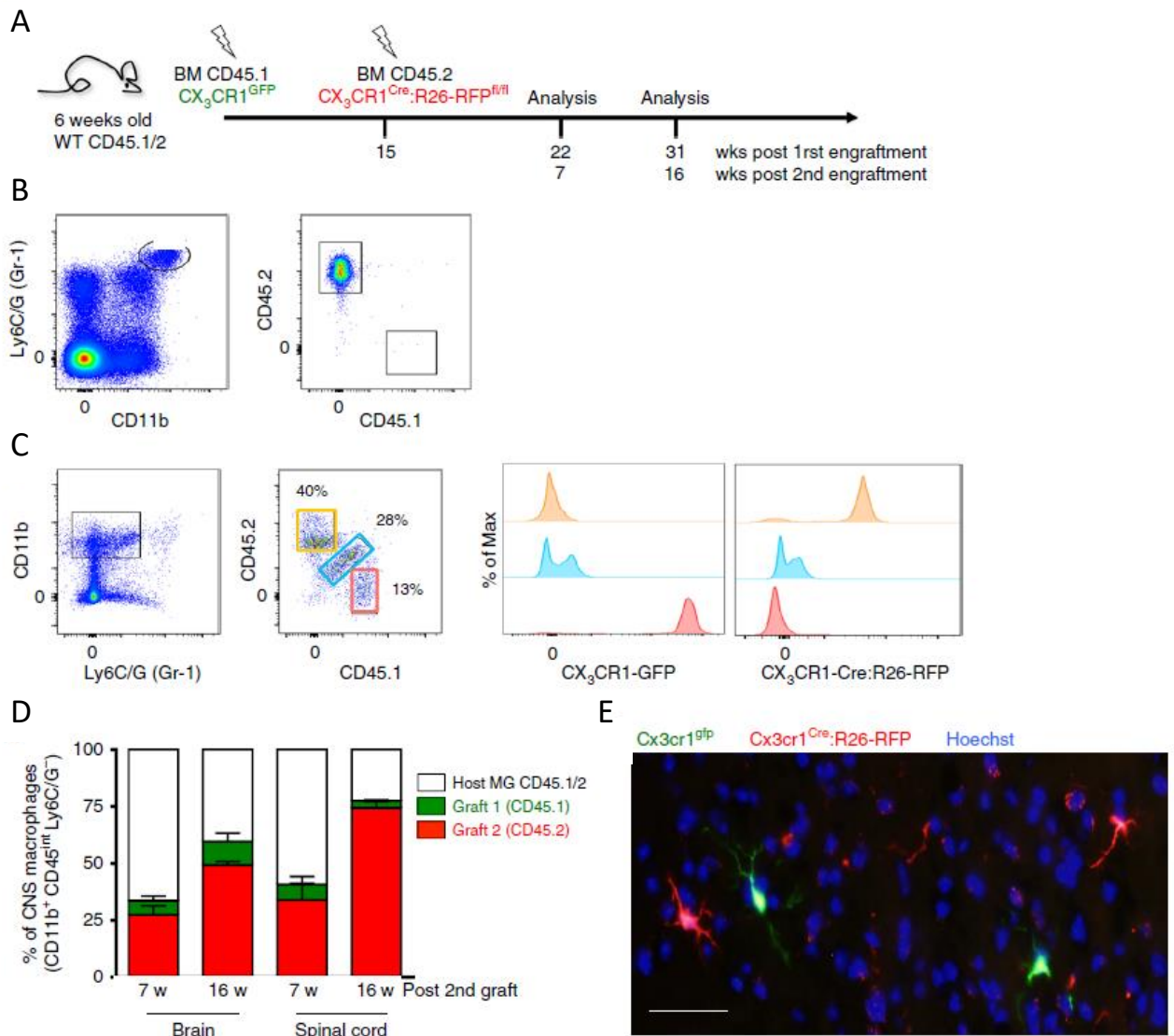


Figure 1. Engrafted brain macrophages accumulate over time and self-maintain

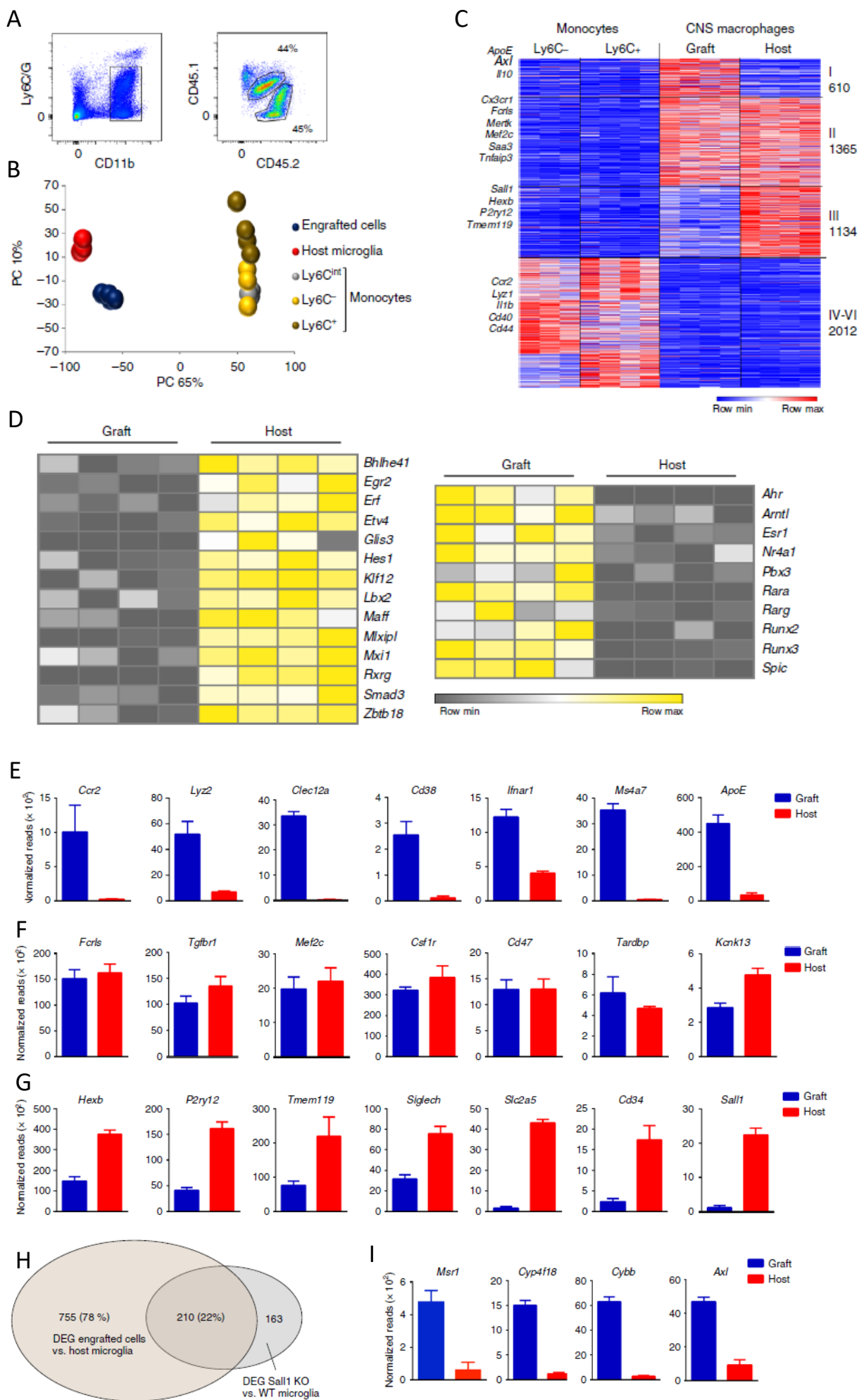


Figure 2. Comparative transcriptome analysis of grafted cells and host microglia

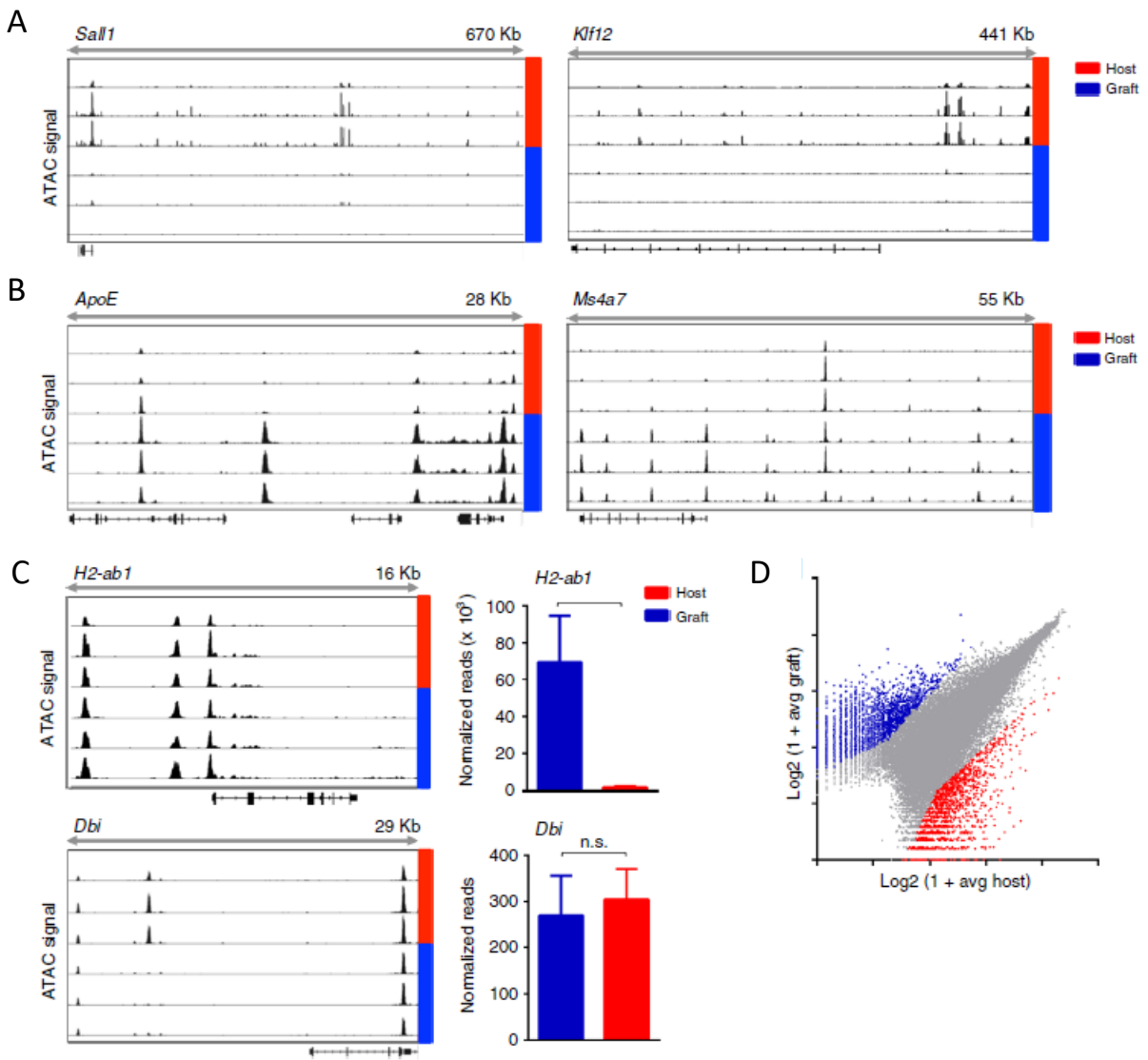


Figure 3. Comparative epigenome analysis of grafted cells and host microglia

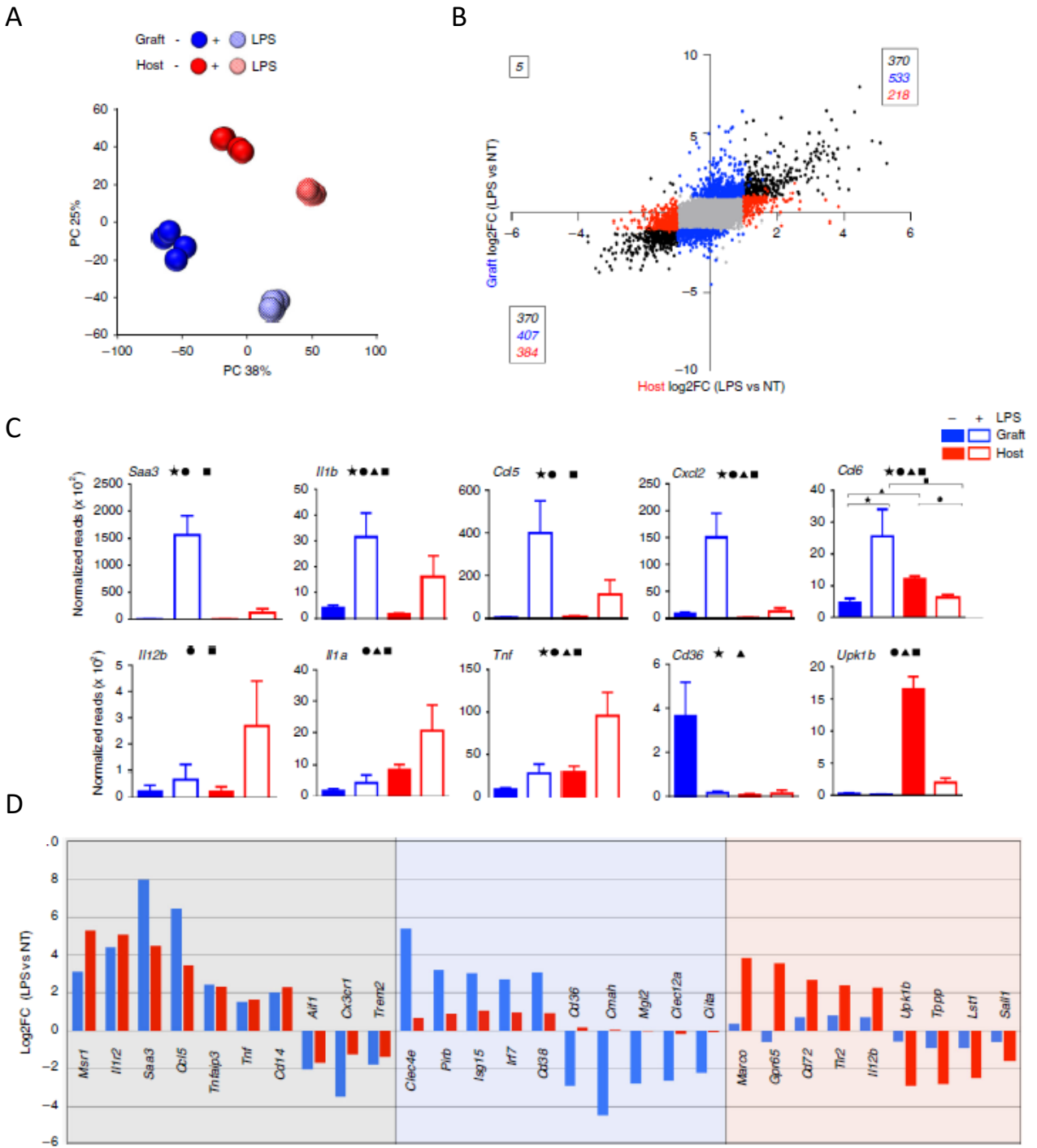


Figure 4. Distinct LPS responses of engrafted cells and host microglia

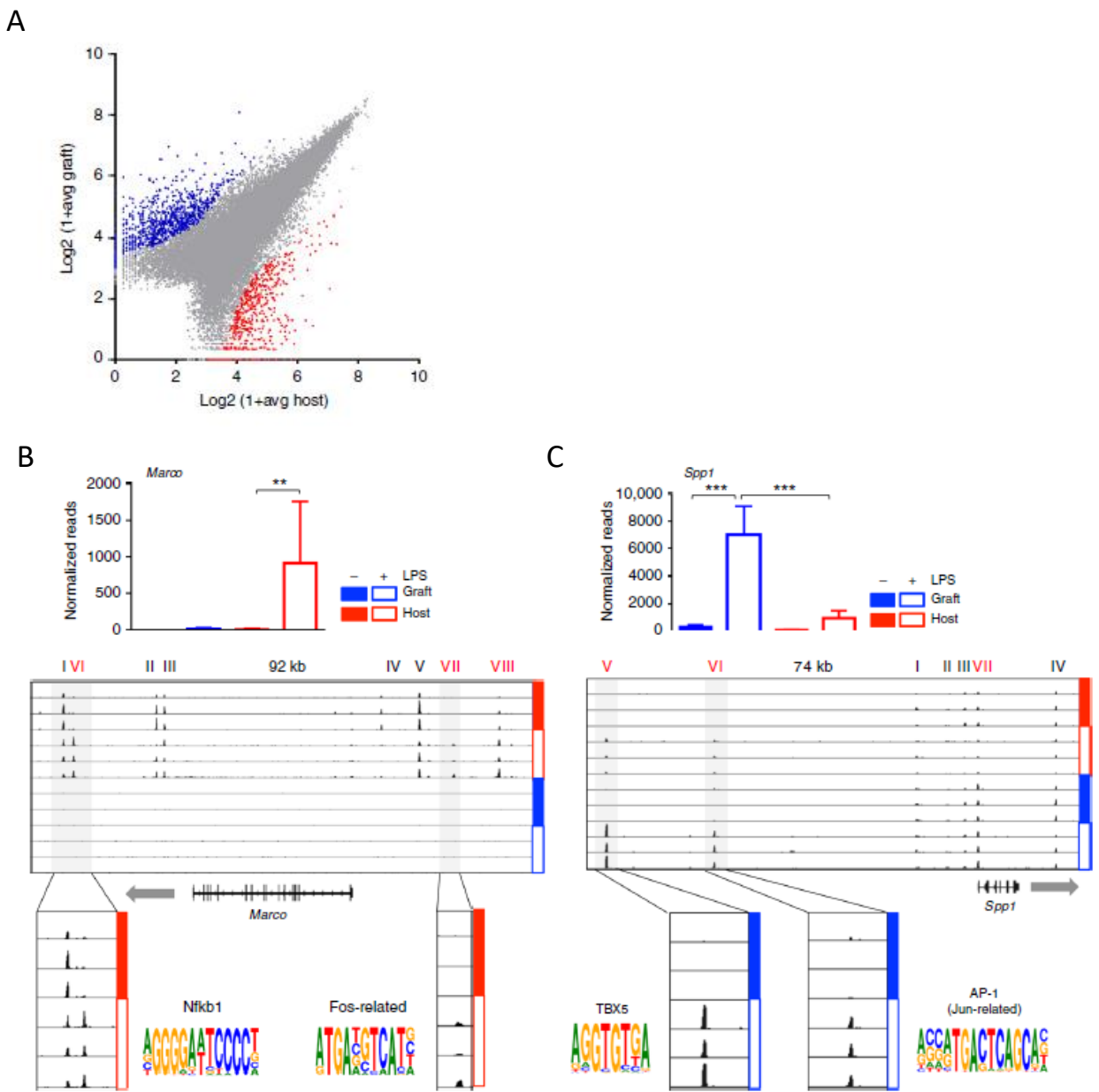
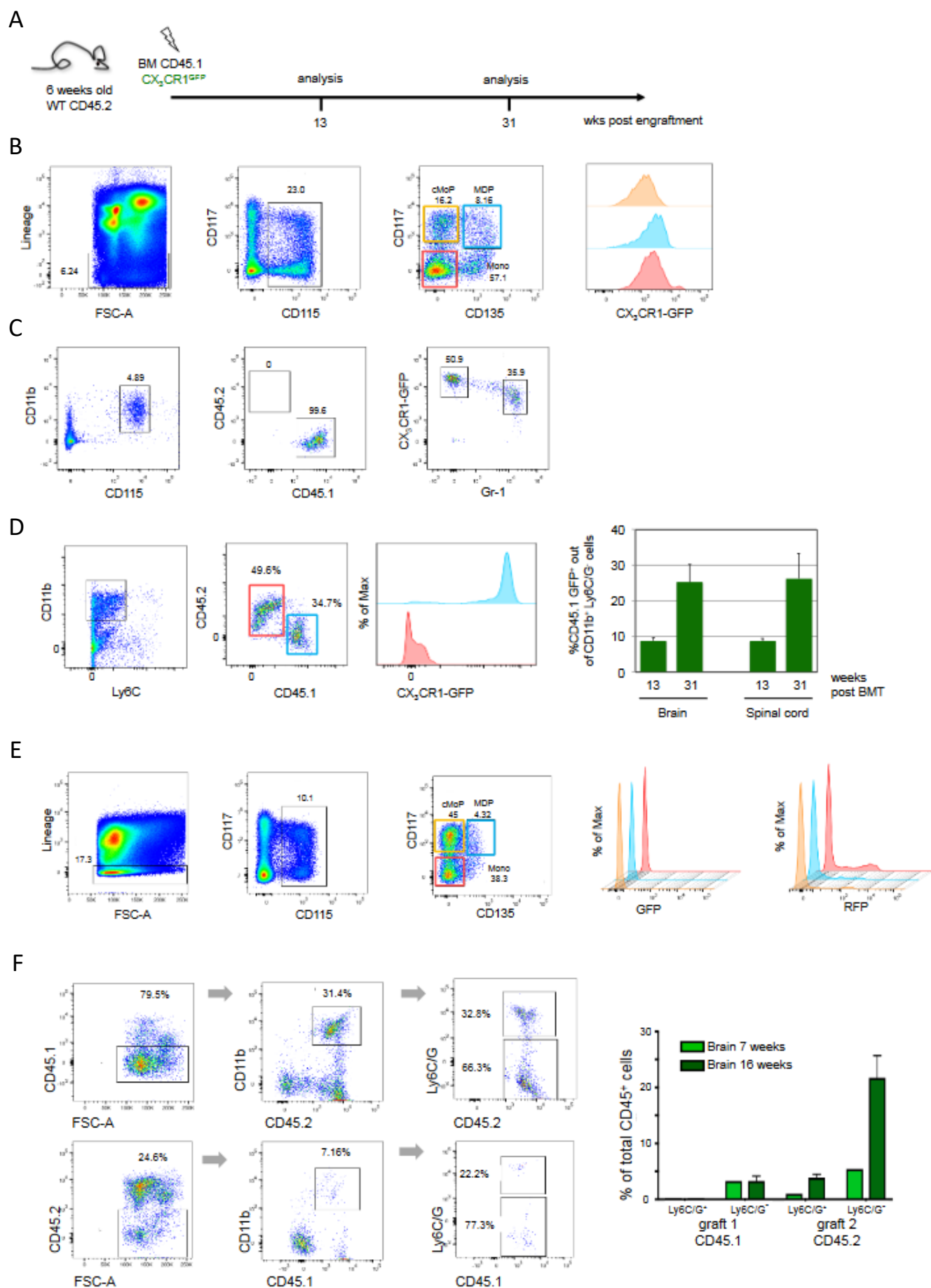
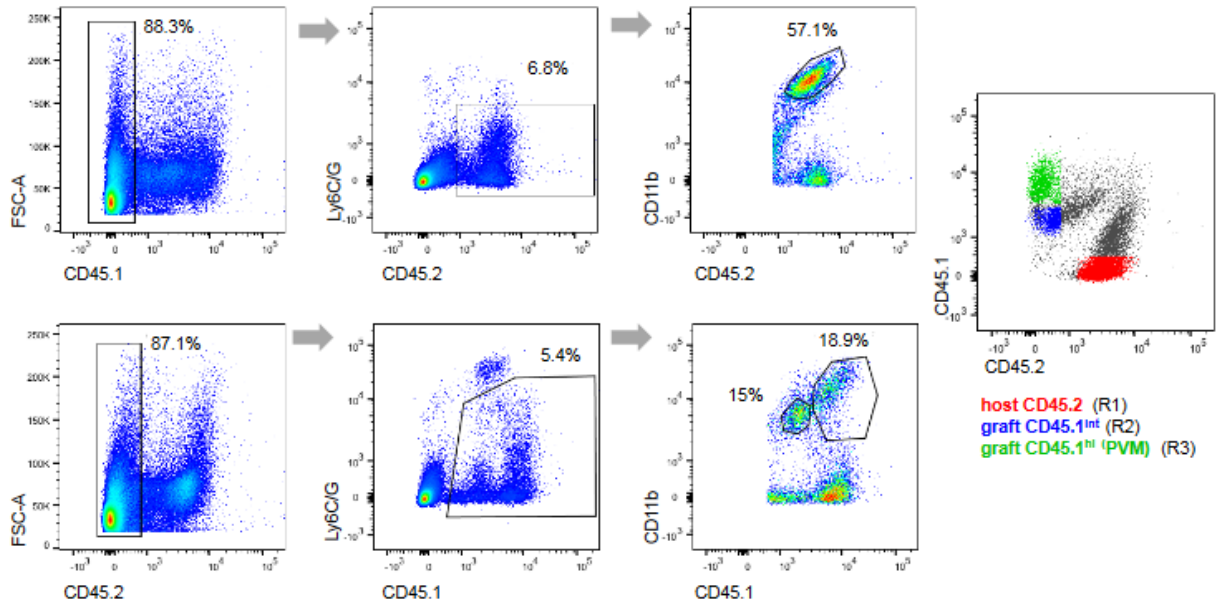


Figure 5. Comparative epigenome analysis of graft and host microglia post LPS challenge

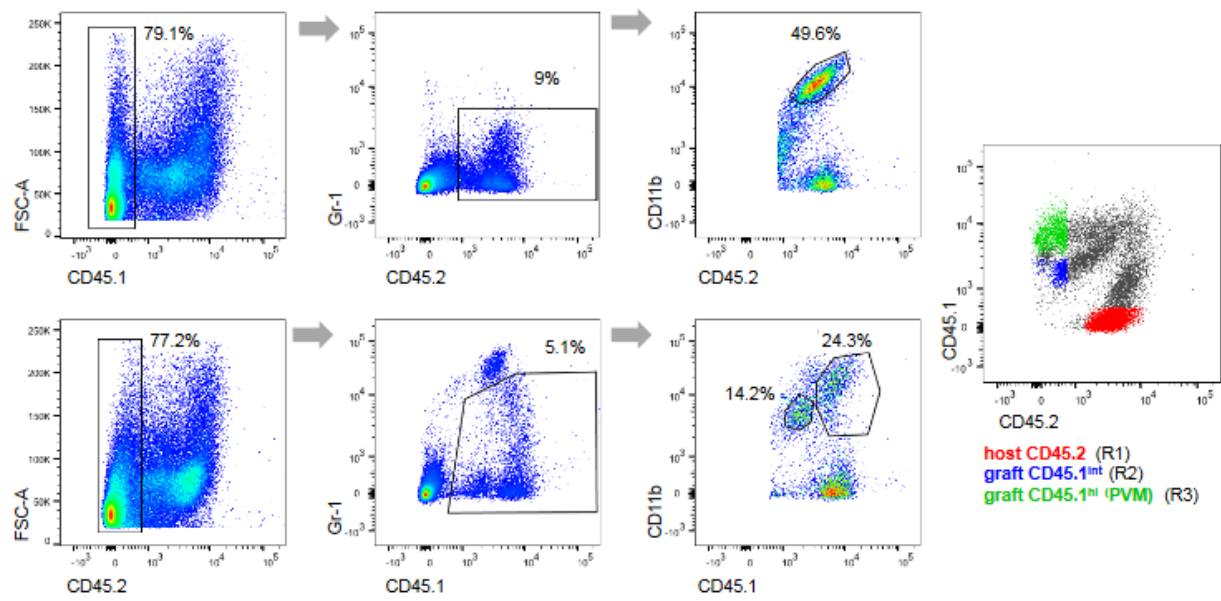


Supplementary Figure 1. BM-derived parenchymal brain macrophages accumulate over time post-irradiation.

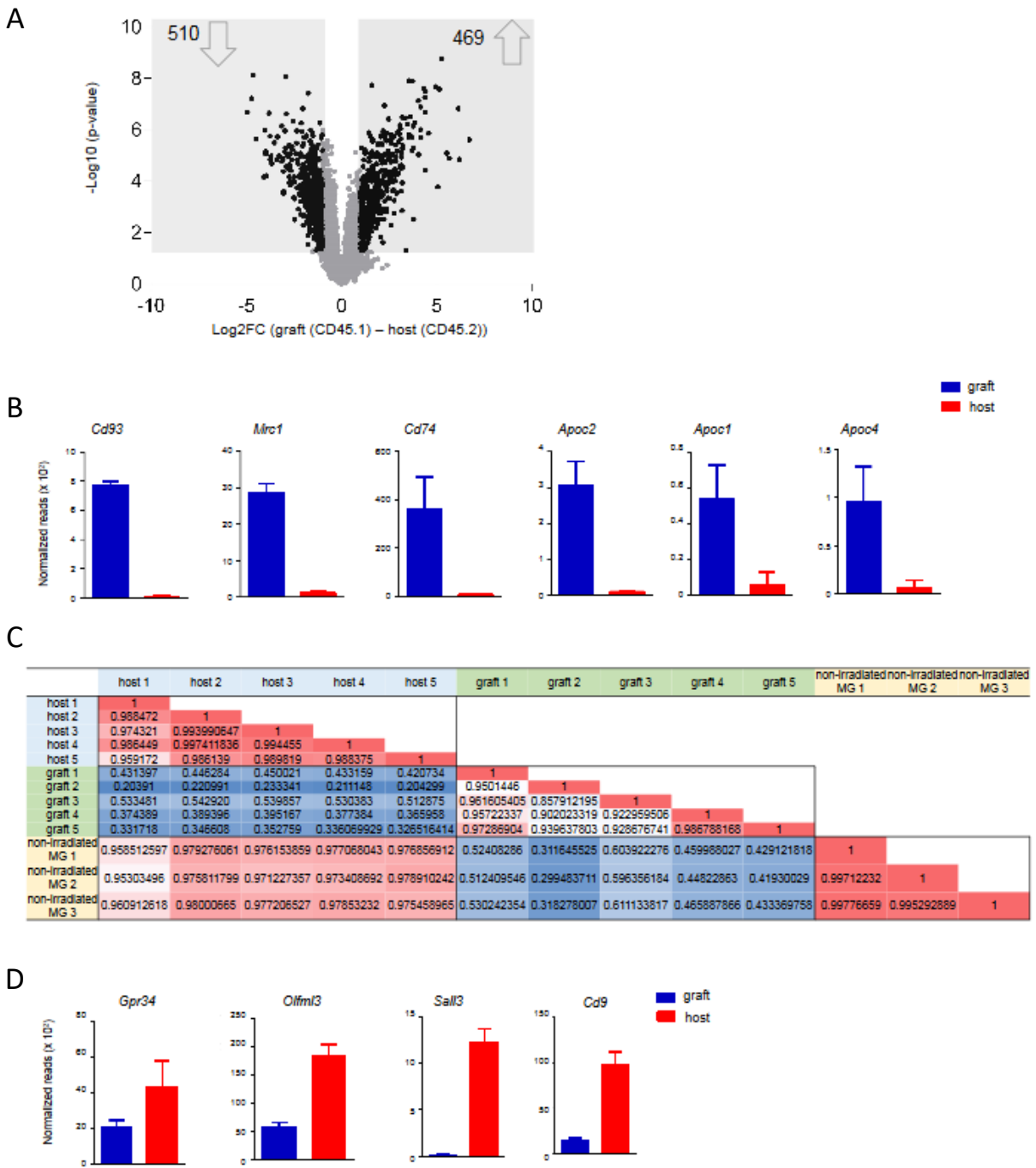
**A** untreated animals



**B** 12hrs after i.p. LPS treatment

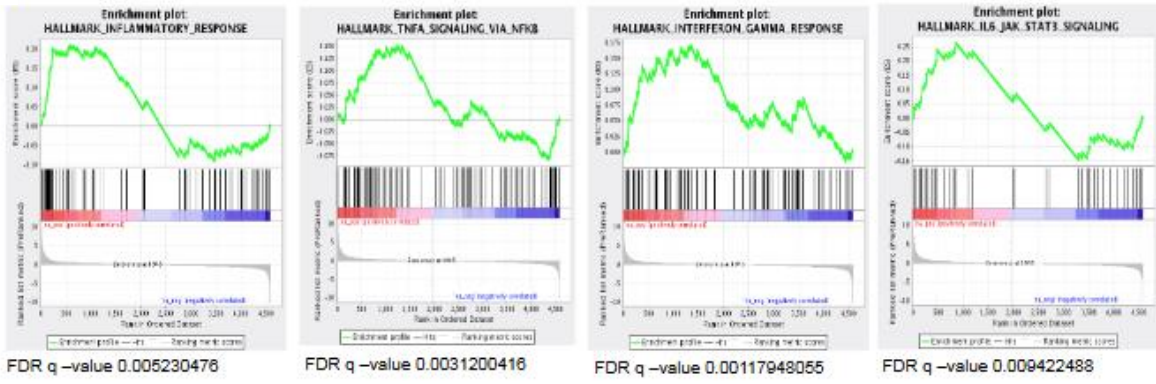


Supplementary Figure 2. Flow cytometry analysis of chimeras used for isolation of cells for transcriptome and epigenome analysis

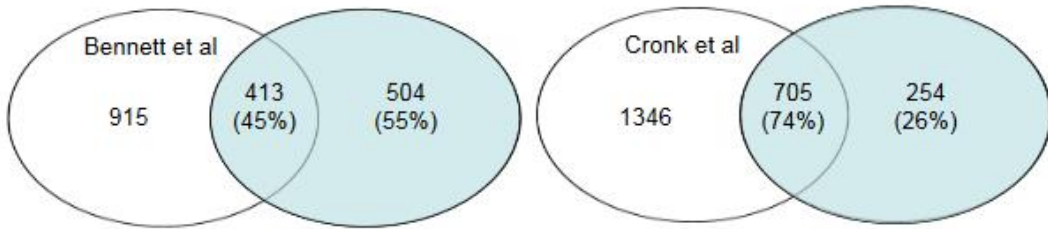


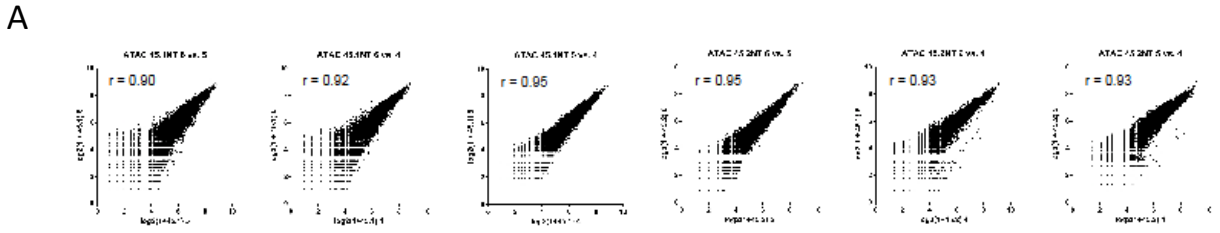
Supplementary Figure 3. Comparison of transcriptomes of engrafted cells and host microglia

A



B



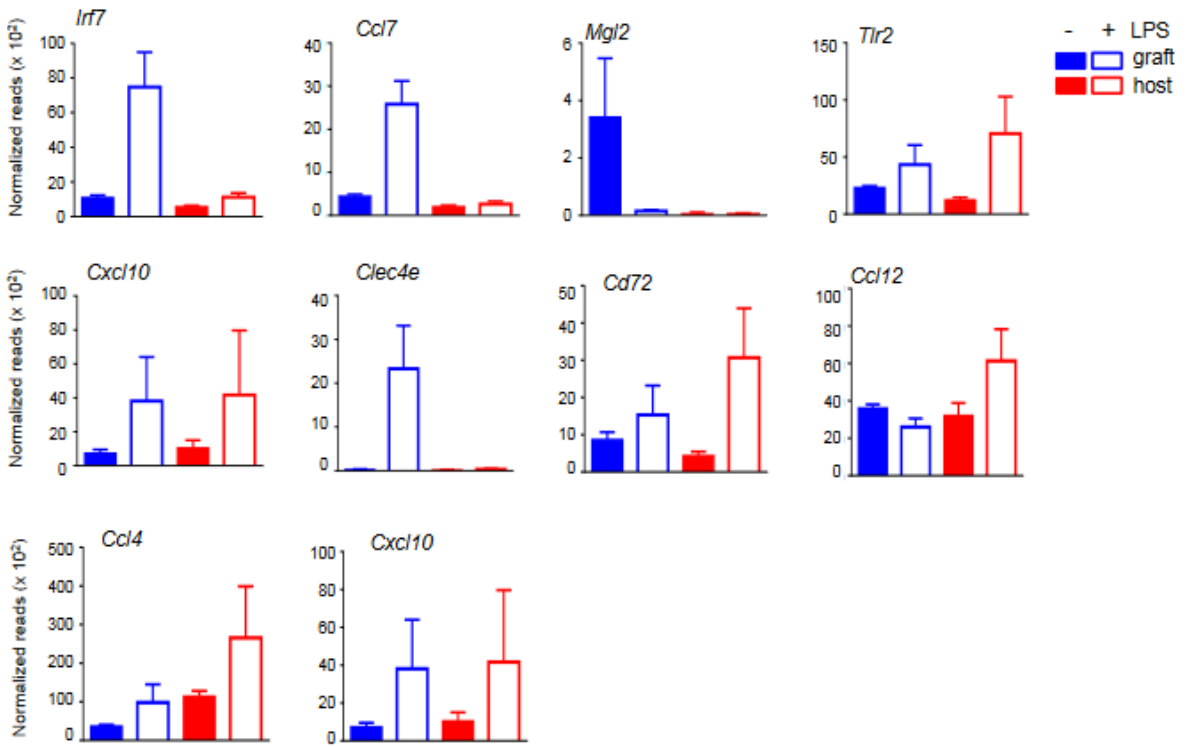


B

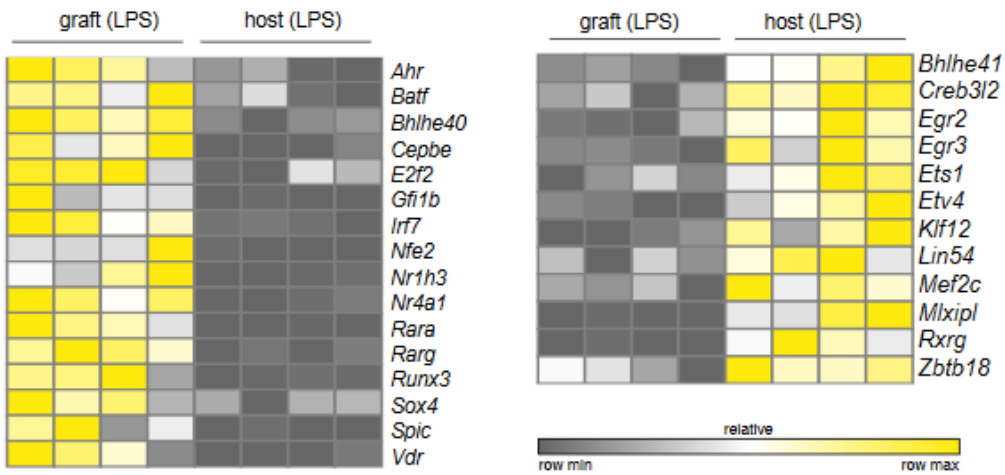
motif	-log <sub>10</sub> (p-value)	
	graft	host
BCL11A	40.04648	23.06527
CEBPA	32.43423	21.85961
CTCF	50	50
CTCF_L	50	41.91764
ETV6	50	50
Ets-related_factors_1_merged	43.98128	33.19889
Ets-related_factors_3_merged	50	50
Regulators_of_differentiation_1_merged	50	50
Runt-related_factors_2_merged	38.75022	24.48596
ZEB1	50	49.99995

Supplementary Figure 5. ATACseq data of engrafted cells and host microglia isolated from brains of unchallenged BM chimeras

A

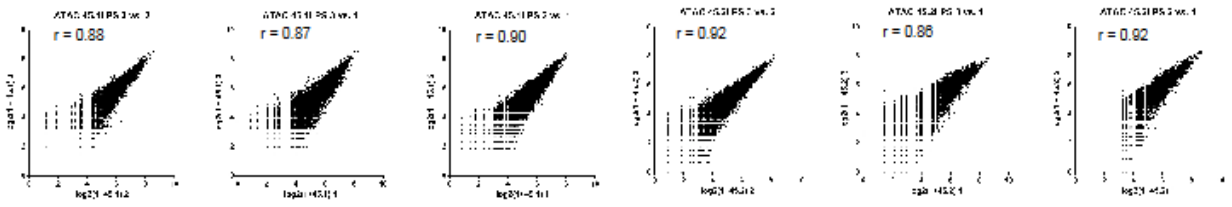


B



Supplementary Figure 6. Comparison of engrafted cells and host microglia isolated from brains of BM chimeras subjected to peripheral LPS challenge

A



B

-log<sub>10</sub> (p-value)

motif	graft	host
CEBPA	49.329186	49.9673163
CTCF	50	50
ETV6	23.1960544	35.2170259
Ets-related_factors_3_merged	50	50
ZEB1	41.0636486	39.8957154

**A**

Upstream Regulator	Expr Log Ratio (graft / host)	Predicted Activation State	Activation z-score	p-value of overlap	Mechanistic Network
TGFB1	-0.464		-0.029	1.58E-28	276 (18)
LPs			1.936	2.40E-28	299 (17)
IL4			0.083	4.74E-24	254 (15)
IFNG			1.713	1.08E-22	241 (19)
IL10RA	-0.334		-1.72	7.44E-22	193 (19)
TNF	-1.59		0.107	5.19E-21	264 (16)
dexamethasone			0.274	4.86E-20	285 (19)
IL6	-2.33		1.384	2.36E-19	261 (17)
APP	0.337		0.192	2.51E-19	244 (17)
CsF3	0		0.791	3.61E-17	234 (22)
CsF2			1.015	4.18E-17	283 (19)
IL10	5.02		-1.358	6.89E-17	237 (19)
poly rI:rc-RNA		Activated	2.711	9.02E-17	235 (18)
IL1B	1.37		1.803	1.15E-16	247 (16)
IL2		Activated	2.071	3.18E-16	251 (18)

**B**

Upstream Regulator	Expr Log Ratio (graft / host)	Predicted Activation State	Activation z-score	p-value of overlap	Mechanistic Network
LPs		Activated	6.292	2.38E-64	324 (15)
IFNG		Activated	5.652	4.75E-53	289 (14)
TNF	-1.71	Activated	5.042	2.62E-43	277 (14)
IL1B	1.03	Activated	4.395	1.70E-41	322 (14)
TGFB1	0.332		0.544	3.00E-37	311 (19)
IL4		Activated	2.937	6.06E-33	309 (15)
dexamethasone			1.166	1.06E-32	321 (16)
IL10RA	-0.159	Inhibited	-4.971	8.40E-31	217 (13)
TNFSF11		Activated	2.416	1.43E-29	259 (14)
IL13			1.037	1.87E-29	267 (15)
STAT1	0.536	Activated	4.556	5.92E-29	262 (16)
STAT3	0.14		1.69	9.19E-29	275 (18)
IL6	-0.955	Activated	3.462	2.84E-28	296 (16)
IRF3	-0.219	Activated	4.755	1.28E-27	206 (13)
E. coli B4 LPs		Activated	3.406	4.25E-27	243 (17)

**C**

Upstream Regulator	Expr Log Ratio (graft NT / LPs)	Predicted Activation State	Activation z-score	p-value of overlap	Mechanistic Network
LPs		Activated	10.409	2.79E-76	515 (13)
IFNG		Activated	7.137	5.98E-63	447 (13)
IL1B	2.85	Activated	7.232	1.47E-55	455 (13)
TNF	1.54	Activated	8.266	3.94E-51	461 (13)
IL4		Activated	3.135	5.43E-43	527 (17)
TGFB1	-0.71	Activated	3.15	1.20E-42	510 (18)
dexamethasone			0.194	1.84E-38	602 (17)
TNFSF11		Activated	4.885	1.67E-34	462 (13)
IL10RA	-0.585	Inhibited	-6.758	1.64E-30	344 (16)
poly rI:rc-RNA		Activated	6.779	2.74E-29	461 (16)
beta-estradiol		Activated	2.073	2.10E-28	649 (20)
TP53	-0.9		1.761	3.08E-28	489 (19)
CD40LG			1.886	7.21E-28	409 (15)
IL6	2.54	Activated	3.755	1.02E-27	458 (13)
PDs8059		Inhibited	-3.87	2.02E-27	550 (19)

**D**

Upstream Regulator	Expr Log Ratio (host NT / LPs)	Predicted Activation State	Activation z-score	p-value of overlap	Mechanistic Network
LPs		Activated	7.457	5.68E-33	367 (14)
IL1B	3.19	Activated	5.235	1.20E-26	315 (13)
IFNG		Activated	5.276	2.05E-25	317 (14)
TNFSF11		Activated	3.984	2.88E-23	290 (11)
poly rI:rc-RNA		Activated	5.368	1.04E-22	323 (15)
TNF	1.66	Activated	5.972	1.65E-21	310 (13)
TLR4	-1.21	Activated	4.144	1.29E-19	283 (14)
TGFB1	-1.51	Activated	2.604	3.02E-19	374 (16)
dexamethasone			0.666	5.94E-19	385 (17)
E. coli B5 LPs		Activated	4.473	1.72E-18	308 (13)
IL4			-0.634	6.98E-18	325 (17)
S. Minnesota R595 LPs		Activated	4.95	7.57E-18	285 (14)
TICAM1	-0.095	Activated	5.04	1.02E-16	227 (16)
methylprednisolone		Activated	2.942	1.54E-16	368 (19)
APP	1.26	Activated	4.786	2.25E-16	371 (16)

## Project II: The role of microglial MHCII expression in EAE induction and progression

### *Introduction*

MHCII molecules are constitutively expressed on professional APC, including dendritic cells (DC) and B cells, as well as medullary thymic epithelial cells; on other hematopoietic and even nonhematopoietic cells, MHCII surface expression can be induced under conditions of inflammation.<sup>87</sup> Microglia, the resident macrophage population of the brain and spinal cord parenchyma, express in steady state low, if any level of MHCII proteins. Induction of MHCII expression is a common feature of microglia activation in inflammatory or pathological context,<sup>88</sup> but the functional significance of microglial MHCII and its role in pathophysiology remain unclear.

MS is the most common non-traumatic disabling neurological disease of adults in the northern hemisphere.<sup>89</sup> Pathological MS features include CNS infiltration of myeloid cells and autoreactive T cells, culminating in demyelination and axonal degeneration.<sup>90</sup> These conditions also present in the common MS animal model, EAE.<sup>22</sup> Microglia were proposed to be critical for EAE development, contributing detrimental activities, either direct or through their interaction with other cells.<sup>88</sup> Specifically, interference with microglial expansion using the CD11b-TK system,<sup>24</sup> or prevention of microglia activation by deletion the transforming growth factor  $\beta$  activating kinase 1 (TAK1),<sup>91</sup> were reported to reduce disease severity. Supporting a central role in EAE development, microglia proliferate during the early stages of the EAE, even prior to monocyte infiltration.<sup>10</sup> However, other studies suggested a limited “bystander” contribution of microglia in EAE, assigning most activities to monocyte-infiltrates and their descendants.<sup>10,92</sup>

Presentation of antigen in MHCII context is critical for EAE pathophysiology, as it drives the expansion of myelin-specific CD4<sup>+</sup> T cells.<sup>93</sup> Following their 'priming' in lymph nodes, pathogenic T lymphocytes invade the CNS, where they require local reactivation by resident or infiltrating APC.<sup>93</sup> DC were reported to be insufficient for EAE induction elicited with recombinant MOG protein, suggesting contributions of other CNS-resident APC.<sup>94</sup> Moreover, EAE can also be induced following DC ablation, suggesting that lack of DC-mediated antigen presentation can be compensated by other cells.<sup>95</sup> However, whether microglia critically present myelin antigens to re-stimulate myelin-specific T cells in the CNS remains unknown.

The copper-chelator cuprizone disrupts mitochondrial enzymes and impairs oligodendrocyte function and survival, resulting in neuro-toxic demyelination.<sup>96</sup> Exposure to cuprizone diet causes demyelination of the corpus callosum (CC), the main white matter commissure and the cerebellar cortex<sup>97</sup> followed by re-myelination upon return to normal chow. Interestingly, microglia also elevate MHCII expression in this model, however it does not involve T cell infiltrates and even proceeds in total T cell absence.<sup>98,99,100</sup> Moreover, MHCII seems to play a functional role, as MHCII-deficient animals reportedly display impaired de- and re-myelination.<sup>100,101</sup> Finally, the defect also persisted in I-Ab<sup>-/-</sup> animals reconstituted with truncated I-Ab molecules (I-Ab $\beta$ tr) lacking cytoplasmic domains, leading to the conclusion, that MHCII might exert signaling activity, as also suggested by others.<sup>102,103,104</sup> Specifically, I-Ab<sup>-/-</sup> and I-Ab<sup>-/-</sup>:I-Ab $\beta$ tr mice displayed fewer proliferating microglia/macrophages and reduced amounts of brain TNF $\alpha$ , IL-1 $\beta$ , and nitric oxide (NO) compared to WT mice, suggesting a role for MHCII in microglia activation.<sup>100</sup>

Here, we used the CX3CR1<sup>CreER</sup> system<sup>25</sup> to genetically ablate MHCII in microglia, while sparing MHCII expression in peripheral and CNS-infiltrating cells, and probe for functional contributions of microglial MHCII in two demyelinating disorders, i.e. EAE and cuprizone-induced pathology. Collectively, we did not find evidence in support of a critical contribution of microglial MHCII expression for disease establishment and resolution in these experimental paradigms.

## Results

### Microglia do not express MHC II in steady state but acquire MHCII expression during EAE development

Resting microglia lack expression of MHC class II, as indicated by the absence of transcripts encoding the master regulator CT2A (*Ciita*) and MHC components (*Cd74*, *H2-Aa*, *H2-Ab1*, *H2-Eb1*) (**Fig. 6A, C**). Notably though, microglia prominently express interferon-gamma receptor subunits (*Ifngr1*, *Ifngr2*) and seem thus prepared to induce MHCII following interferon-gamma exposure (**Fig. 6A**). This poised configuration is also reflected in the activity state of *cis*-acting genomic regulatory elements in the *H2-Ab1* loci of microglia. Specifically, *H2-Ab1* enhancer regions, defined by their distance from the transcription start site, displayed an H3K4me1 signal, like MHC II-expressing colonic macrophages, but lacked the H3K27ac mark indicative of active transcription (**Fig. 6B**).<sup>105</sup> Spinal cord (SC) microglia isolated from animals suffering from EAE display alongside of the stimulation of interferon response genes (*Ifi47*, *Ifi1*, *Iigp1*, *Ifi204*, *Igtp*), a prominent induction of the MHCII module (**Fig. 6C**). Other challenges, such as a peripheral LPS injection, did however not induce microglial MHCII expression. In order to validate microglial MHCII expression on the protein level, TAM-treated *Cx3cr1<sup>CreER</sup>*:R26-YFP mice, that allow exclusive labeling of microglia<sup>25</sup> were immunized with MOG<sub>35-55</sub> peptide, and microglia were gated as the sole YFP<sup>+</sup> cells (**Supplementary Fig. 8A**). Corroborating the transcriptome data, microglia elevated CD11c, MHCII, Flt3 and the co-stimulatory molecules CD80 and CD86, while CD40 expression was unaltered (**Supplementary Fig. 8A**). Notably, MHCII induction on microglial cells was linked to the emergence of pathogenic T cell directed against oligodendrocyte antigen (MOG) and absent in animals immunized with control peptide or *Cd80/86<sup>-/-</sup>* animals<sup>106</sup>, which show impaired peripheral T cell priming (**Fig. 6D**).<sup>107</sup>

### Ablation of microglial MHCII does not alter EAE pathophysiology and microglia expression profiles

To investigate whether microglial MHCII plays a role in the establishment of EAE, we generated mice which harbor a microglial MHCII deletion by combining a *CX<sub>3</sub>CR1<sup>CreER</sup>* transgene<sup>25</sup> with *I-A<sup>b</sup>* null<sup>108</sup> and 'floxed' *I-A<sup>b</sup>* alleles.<sup>109</sup> Unlike *I-A<sup>b</sup><sup>-/-</sup>* knockout (KO) mice, TAM-treated *Cx3cr1<sup>CreER</sup>*:*I-A<sup>b</sup><sup>fl/-</sup>* animals displayed normal MHCII<sup>+</sup> B cells and an unimpaired T cell compartment (**Supplementary Fig. 8B, C**). One week after TAM treatment, splenic DC of *Cx3cr1<sup>CreER</sup>*:*I-A<sup>b</sup><sup>fl/-</sup>* mice displayed a reduction in surface MHCII, but in line with the characteristics of the *CX<sub>3</sub>CR1<sup>CreER</sup>* system,<sup>91</sup> MHCII expression of this

short-lived cellular compartment was restored by 6 weeks after TAM (**Supplementary Fig. 8D**). To examine microglial MHCII expression, we subjected TAM-treated  $CX3CR1^{CreER};I-A^b^{fl/-}$  mice to the EAE protocol. Monocyte-derived  $CD45^{hi}$  cell infiltrates of these animals displayed MHCII levels similar to controls; in contrast, microglia of the challenged animals lacked MHCII, as compared to  $I-A^b^{fl/-}$  littermate controls (**Fig. 7A**).

When immunized with MOG<sub>35-55</sub> peptide, MHCII haplo-sufficient  $I-A^b^{fl/-}$  and  $Cx3cr1^{CreER};I-A^b^{fl/-}$  mice developed EAE with a delay of approximately 4 days, compared to WT mice. However,  $Cx3cr1^{CreER};I-A^b^{fl/-}$  mice displayed an EAE onset comparable to control littermates, as well as a similar severity and disease course (**Fig. 7B-D**). Two-way analysis for the EAE disease course of  $I-A^b^{fl/-}$  and  $Cx3cr1^{CreER};I-A^b^{fl/-}$  mice revealed only a significant effect for time ( $p < 0.0001$ ) with no effect for genotype ( $p = 0.2464$ ) or interaction ( $p = 0.9993$ ). To substantiate our analysis, we also calculated the area under the disease course curves.<sup>110</sup> This analysis again yielded no significant difference ( $p = 0.6676$ , two-tailed T test; **Supplementary Fig. 8E**). Finally, we used linear regression analysis to linearize the disease course,<sup>111</sup> and used r-to-z Fisher transformation to compare the slopes of the linear regression of the disease course. Also this analysis found the difference between disease course of the two genotypes to be statistically non-significant ( $p = 0.865$ , two-tailed Fisher transformation; **Supplementary Fig. 8F**).

SC analysis revealed no differences in percentages of microglia and infiltrating monocytes/monocyte-derived macrophages (**Fig. 7E**). To test if absence of microglial MHCII affects the composition of  $CD4^+$  effector T cell infiltrates, we analyzed brains at EAE score 3, the disease peak. Total brain  $CD4^+$  T cell numbers were unaltered (**Fig. 7F**), and MOG<sub>35-55</sub> specific or non-specific re-stimulation with PMA/ionomycin *ex vivo* revealed similar proportions of Th1 ( $CD44^+ CD40L^+ IFN-\gamma^+ IL-17A^-$ ), Th17 ( $CD44^+ CD40L^+ IFN-\gamma^- IL-17A^+$ ) and double positive T cells ( $CD44^+ CD40L^+ IFN-\gamma^+ IL-17A^+$ ) (**Fig. 7G, Supplementary Fig. 8G**).  $CD45^{hi}$  MHCII<sup>+</sup> macrophages, which derive from monocytic infiltrates and are not targeted by our system, might contribute to antigen presentation. To probe for such a scenario, we depleted monocytes at day 9 and 12 following MOG challenge using the anti-CCR2 antibody MC21. Blood analysis of MC21-treated animals at day 13 confirmed absence of  $CD115^+ Ly6C^{hi}$  monocytes (**Supplementary Fig. 8H**). Moreover, monocyte ablation also strongly attenuated the disease course, as half of the MOG/ MC21-treated mice (4/9) did not

develop EAE, even up to 60 days, while the remaining animals showed less severe symptoms with no morbidity, as compared to controls (Two way analysis revealed both an highly significant effect for treatment and interaction between treatment and time,  $p < 0.001$ ; **Supplementary Fig. 8I-J**). Corroborating an earlier report,<sup>112</sup> this raises the possibility that these cells might have a role in antigen presentation in the CNS, although this requires further experimentation. The cytoplasmic domain of MHCII was reported to promote signaling<sup>102,103,104</sup> and absence of MHCII could hence have a direct intrinsic impact on microglial cells. However, global transcriptome analysis of  $CX_3CR1^{CreER};I-A^{b fl/-}$  and  $I-A^{b fl/-}$  SC microglia isolated at EAE clinical score 1 (**Supplementary Fig. 9A**), the disease onset, revealed minimal differences between mutant and WT microglia (**Supplementary Fig. 9B**). Specifically, expression of inflammatory factors, such as TNF, IL1 $\beta$  and CCL2 was unaltered between  $I-A^b$  deficient and proficient microglia (**Supplementary Fig. 9C**). Collectively, with respect to EAE disease course, myeloid cell infiltrates and the T cell compartment, as well as microglia expression profiles, we did not observe changes in the absence of microglial MHCII.

### **Microglial MHCII is dispensable in the cuprizone induced de-and re-myelination reaction**

In contrast to EAE, cuprizone-induced demyelination is not accompanied by major T cell infiltration,<sup>98</sup> although some T cell infiltrates have been reported,<sup>113</sup> as well as transient monocytic infiltrates have been reported for irradiated and busulfan-treated animals.<sup>114</sup> Nevertheless, microglial MHCII is also upregulated in this model,<sup>99,115</sup> suggesting an antigen presentation-independent role. Indeed, MHCII deficient animals have been shown to display impaired de- and remyelination reactions in the cuprizone model.<sup>100,101</sup>

The cuprizone model experiments in this project were performed by Liron Levy-Efrati and can be viewed in detail in *Wolf, Shemer, Levi-Efrati, et al. 2018*.<sup>28</sup> To summarize, we found no differences between  $CX_3CR1^{CreER};I-A^{b fl/-}$  and their controls also by using this sterile, non-autoimmune demyelination model.<sup>28</sup>

## *Discussion*

Antigen presentation within the CNS has been speculated to be performed by CNS DC,<sup>116,117</sup> infiltrating monocyte-derived macrophages,<sup>118</sup> meningeal and perivascular macrophages,<sup>119</sup> and the CNS resident microglia.<sup>88,91</sup> Here we took advantage of CX<sub>3</sub>CR1<sup>CreER</sup> mice to investigate the contribution of microglial MHCII to EAE development.

We establish that microglia do not contribute substantially to myelin antigen presentation, and are not crucial for the adequate priming of encephalitogenic T cells during the course of active EAE. Therefore, other APC in the CNS can compensate for the loss of T cell stimulation by microglia. Interestingly, a recent study has demonstrated that both CNS meningeal and perivascular macrophages, similarly to microglia, are CX<sub>3</sub>CR1-expressing long-lived cells,<sup>76</sup> and therefore expected to be targeted in the CX<sub>3</sub>CR1<sup>CreER</sup> system. This would imply that also these macrophage populations might be redundant for myelin antigen presentation at the disease onset, and suggest a key role for infiltrating, rather than CNS resident APC. However, this requires further experimentation.

To examine possible antigen presentation-independent roles of microglial MHCII we turned to a demyelination model, which does not involve T cell infiltrates, but nevertheless displays microglial MHCII expression – the cuprizone challenge. MHCII-deficient mice were reported to have an impaired ability to remyelinate damaged axons once returned to a normal diet.<sup>101</sup> However, we did not observe significant differences in the de- or remyelination processes, or accompanied cell proliferation and gene expression, in mutant mice lacking microglial *I-ab* expression. This suggests that microglial MHCII is also dispensable for cuprizone-induced pathology. It remains unclear why MHCII deficient animals show a defect in the cuprizone model.<sup>101</sup> These animals lack CD4<sup>+</sup> T cells and therefore likely display altered immune homeostasis. Secondly, MHCII absence could affect B cell functionality, which in turn could affect microbiota, which are known for their impact on the CNS.<sup>120</sup> Notably, also MHCII deficient animals reconstituted with truncated I-A $\beta$  molecules display systemic alterations.

Only scarce literature can be found concerning the unique functions of MHCII, which are antigen presentation-independent. MHCII was shown to synergize with TLR2 and TLR4<sup>121</sup> and to modulate TLR responses via the phosphatase Btk,<sup>103</sup> thus suggesting it to be a regulator of TNF $\alpha$  production, along with other inflammatory agents. Although TNF $\alpha$  plays a key role in cuprizone-induced remyelination as it is required for the recruitment of

oligodendrocyte precursors to the CC,<sup>122</sup> we did not find any evidence for microglial MHCII participation in this process or in regulation of TNF expression.

To summarize, we found no evidence for a functional role of microglial MHCII expression in the development of EAE or the de- and re-myelination episodes induced by transient cuprizone exposure. It remains to be shown whether MHCII expression is a mere by-product of other regulatory circuits or contributes to more subtle microglia activities that remain to be defined. Of note, our study does not address potential contributions of microglia, other than MHCII antigen presentation, to EAE and cuprizone pathology. Earlier studies have reported impacts of largely microglia-restricted mutations on pathogenesis in these models,<sup>91,114</sup> although the underlying mechanism requires further investigation. Likewise, the findings of our study refer to two established de-myelinating disorders in the mouse, and it remains to be shown if they can be extrapolated to MS and human demyelinating disorders.

### Figure legends

#### **Figure 6. Microglial MHCII is elevated under specific conditions**

- (A) Heatmap of expression various antigen presentation genes in selected tissue macrophages. N = 3–4 for each macrophage subset. Data retrieved from *Lavin et al., 2014*.<sup>52</sup>
- (B) Status of histone modification in H2-Ab1 locus of microglia and MHCII-expressing colonic macrophages indicated by normalized profiles of H3K4me1 and H3K27ac signals. Data retrieved from *Lavin et al., 2014*.<sup>52</sup>
- (C) Heatmap of expression of selected genes in total brain microglia taken from mice 6 hours after treatment with LPS i.p. and spinal cord microglia of mice with EAE score 3, all compared to their respective untreated controls. N = 3–4 for each microglia subset. Data are from one experiment.
- (D) FACS analysis of MHCII, CD11c and Flt3 surface levels of spinal cord microglia isolated from untreated, SIINFEKL (control peptide) immunized, MOG<sub>35–55</sub> immunized WT mice, and MOG<sub>35–55</sub> immunized CD80/86<sup>-/-</sup> mice, at day 9 post-immunization. Data are representative of two independent experiments.

#### **Figure 7. Microglial MHCII is not required for development of EAE**

- (A) FACS analysis of MHCII expression in microglia, Ly6C<sup>hi</sup> and Ly6C<sup>lo</sup> CD45<sup>hi</sup> mononuclear phagocytes in *Cx3cr1<sup>CreER</sup>:I-ab<sup>fl/-</sup>* and *I-ab<sup>fl/-</sup>* mice at day 30 post immunization with MOG<sub>35–55</sub>. N = 4, \**p* < 0.05, Mann–Whitney's u-test. Data are representative of two independent experiments.
- (B–D) EAE course (B), individual day of onset (C), and individual maximal score (D) of TAM treated immunized *I-ab<sup>+/+</sup>*, *Cx3cr1<sup>CreER</sup>:I-ab<sup>fl/-</sup>* and *I-ab<sup>fl/-</sup>* mice. Data are a representative of three independent experiments. N = 6–9. The effect size (Cohen's D) between WT (*I-ab<sup>+/+</sup>*) and control (*I-ab<sup>fl/-</sup>*) was 1.15. Our power to detect a similar difference between control *I-ab<sup>fl/-</sup>* and mutant mice *Cx3cr1<sup>CreER</sup>:I-ab<sup>fl/-</sup>* was 0.57.
- (E) FACS analysis of CD4<sup>+</sup> percentages out of total CD45<sup>+</sup> cells in spinal cord of sick (score 3) *Cx3cr1<sup>CreER</sup>:I-ab<sup>fl/-</sup>* and *I-ab<sup>fl/-</sup>* mice. Data are a representative of three independent experiments. N = 6–9.
- (F–G) FACS analysis of total CD4<sup>+</sup> T cells (F) and Th1 vs. Th17 cells in spinal cord of sick (score 3) *Cx3cr1<sup>CreER</sup>:I-ab<sup>fl/-</sup>* and *I-ab<sup>fl/-</sup>* mice, re-stimulated with MOG<sub>35–55</sub> for 6 hours and stained intracellular for IFN- $\gamma$  and IL-17A (G). Data are representative of one experiment. N = 5–6.

### **Supplementary Figure 8. EAE experiments with mice lacking microglial MHCII expression**

- (A) FACS analysis of Cx3cr1<sup>CreER</sup>:R26-YFP mice, treated with TAM, immunized with MOG<sub>35-55</sub> 6 weeks later, and sacrificed at day 17. Data are representative of two independent experiments.
- (B) MHCII expression levels of blood B cells in Cx3cr1<sup>CreER</sup>:I-ab<sup>fl/-</sup>, I-ab<sup>fl/-</sup> and I-ab<sup>-/-</sup> mice. Data are representative of 5 mice analyzed, from one experiment.
- (C) Number of CD4<sup>+</sup> and CD8<sup>+</sup> T cells numbers in blood of Cx3cr1<sup>CreER</sup>:I-ab<sup>fl/-</sup>, I-ab<sup>fl/-</sup> and I-ab<sup>-/-</sup> mice. Data are representative of 5 mice analyzed, from one experiment.
- (D) MHCII expression levels of splenic classical DC of Cx3cr1<sup>CreER</sup>:I-ab<sup>fl/-</sup> mice, 1 or 6 weeks post TAM administration, compared with I-ab<sup>-/-</sup> mice for reference. Data are representative of 4 mice analyzed, from one experiment.
- (E) Area under curve of figure 7B for Cx3cr1<sup>CreER</sup>:I-ab<sup>fl/-</sup> and I-ab<sup>fl/-</sup> mice.
- (F) Linear regression of figure 7B for Cx3cr1<sup>CreER</sup>:I-ab<sup>fl/-</sup> and I-ab<sup>fl/-</sup> mice.
- (G) Flow cytometry analysis of Th1 vs. Th17 cells in spinal cord of sick (score 3) Cx3cr1<sup>CreER</sup>:I-ab<sup>fl/-</sup> and I-ab<sup>fl/-</sup> mice, re-stimulated with PMA/ Ionomycin for 6 hours and stained intracellular for IFN- $\gamma$  and IL-17A. n=5-6. Data are from one experiment.
- (H) Analysis of blood monocytes 13 days post MOG<sub>35-55</sub> immunization with (right, red) or without (left, black) MC21 co-administration at day 9 and 12.
- (I-J) EAE disease course (right) and maximal score (left) in immunized mice vs. immunized MC21-cotreated mice. Data represent three independent experiments. n=7-9.

### **Supplementary Figure 9. Microglial transcriptome is unaffected by MHCII absence**

- (A) Gating strategy for sorting microglia under EAE.
- (B) X-y analysis of transcriptomes of isolated microglia of Cx3cr1<sup>CreER</sup>:I-ab<sup>fl/-</sup> and I-ab<sup>fl/-</sup> mice under EAE.
- (C) Expression of selected pro-inflammatory genes as analyzed by RNA-seq of Cx3cr1<sup>CreER</sup>:I-ab<sup>fl/-</sup> and I-ab<sup>fl/-</sup> mice under EAE.

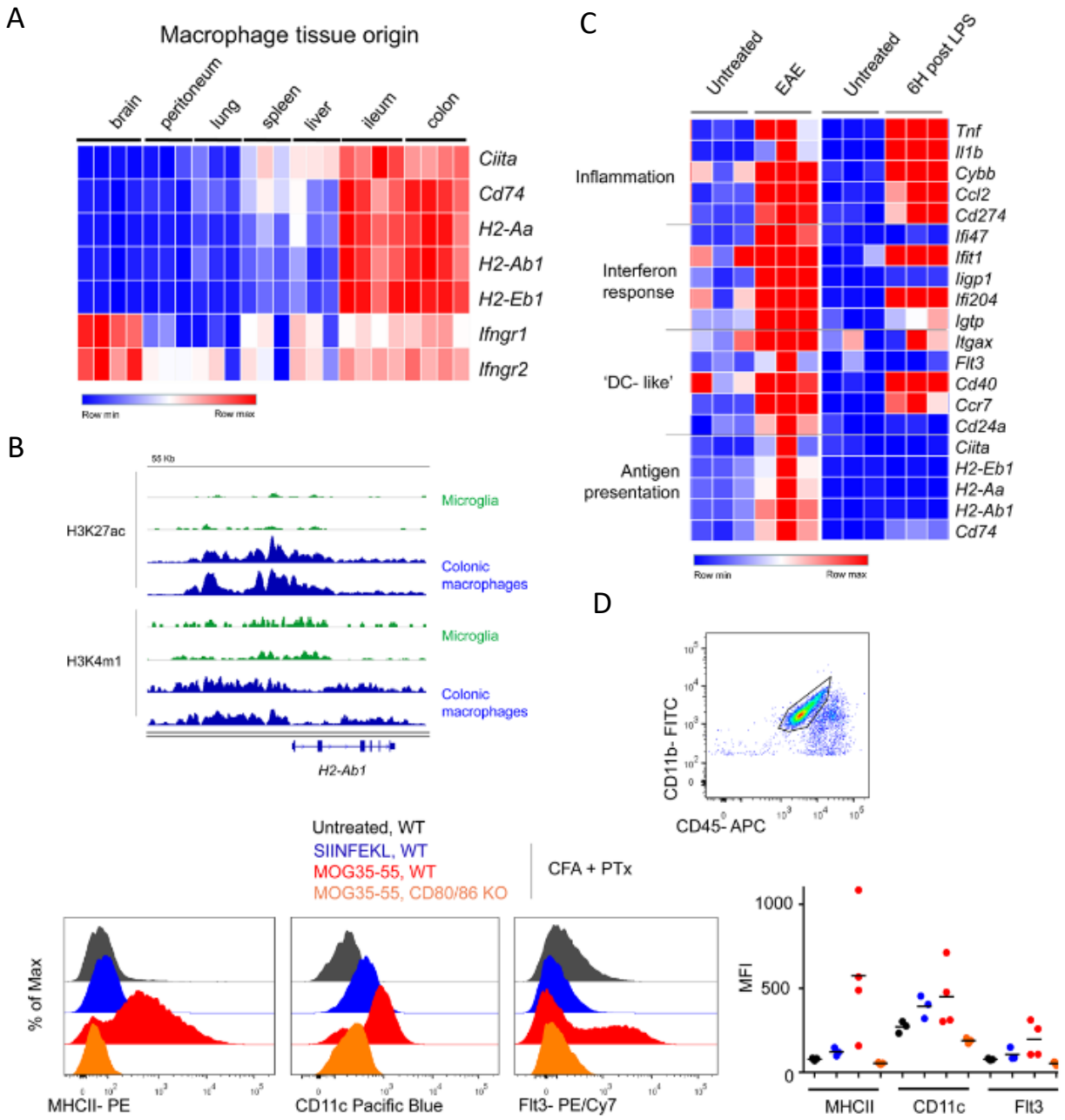


Figure 6. Microglial MHCII is elevated under specific conditions

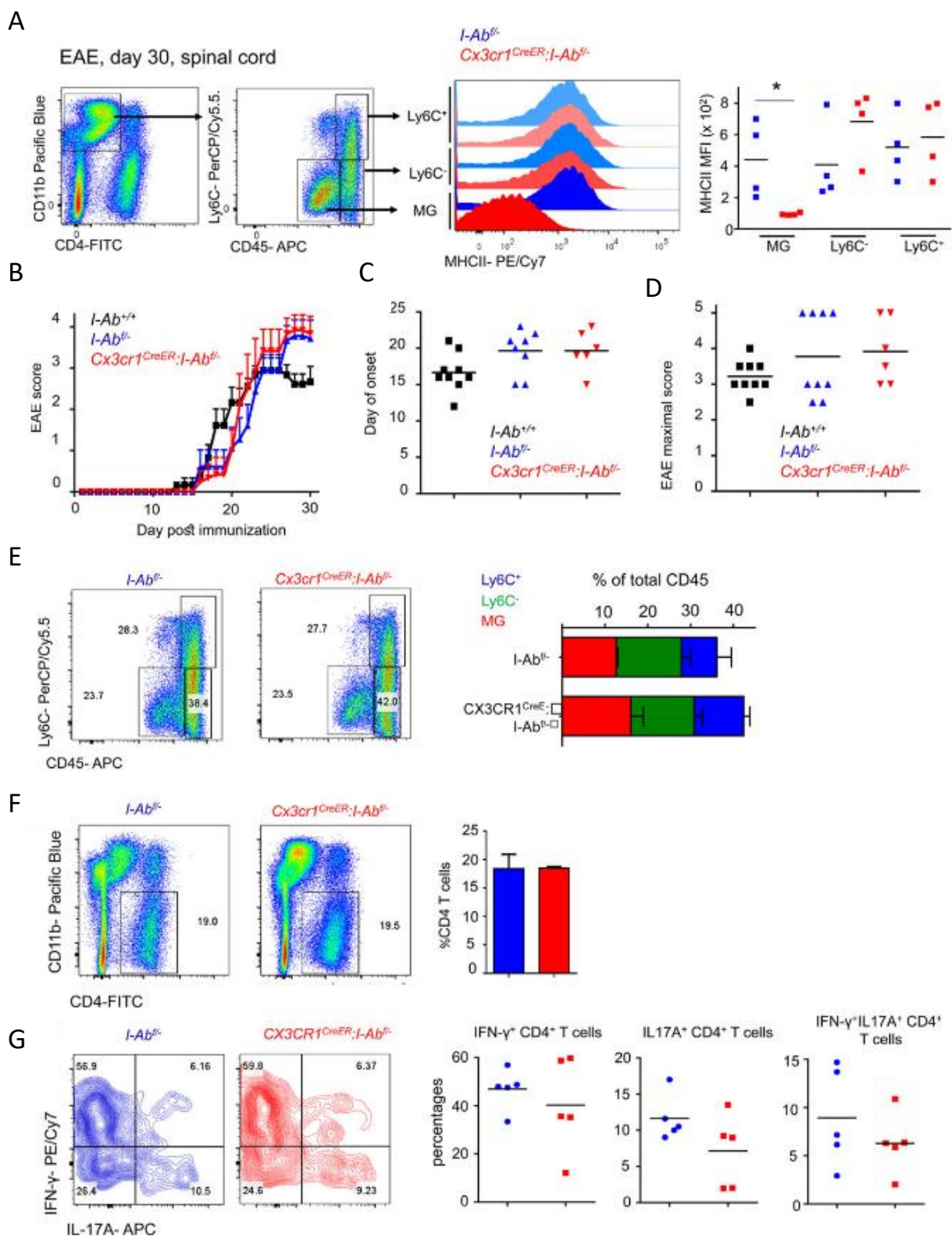
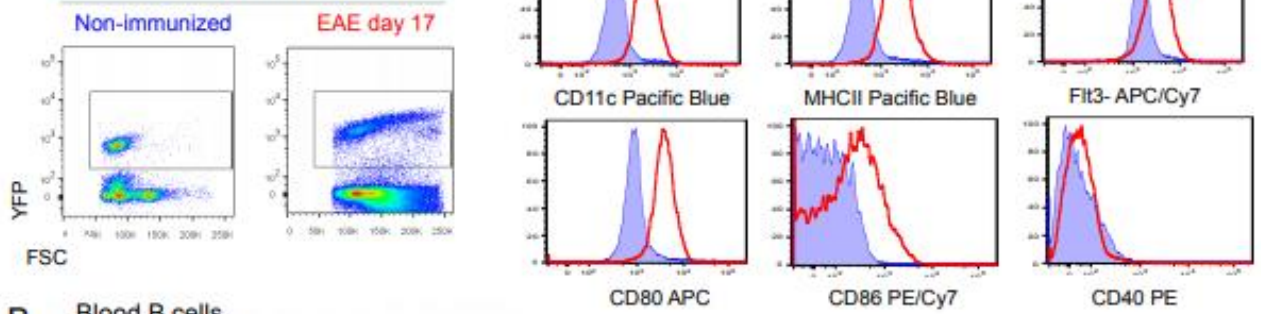
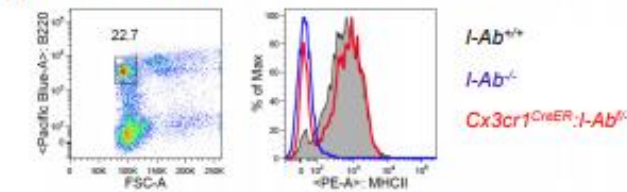


Figure 7. Microglial MHCII is not required for development of EAE

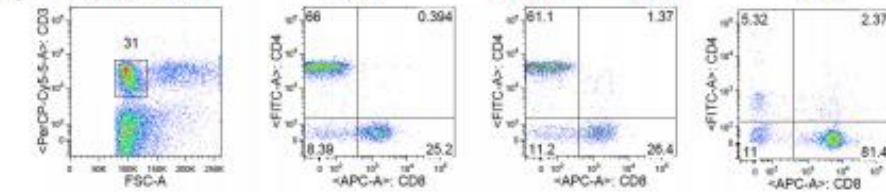
**A** TAM-treated CX3CR1<sup>CreER</sup>:R26-YFP  
2 months post treatment



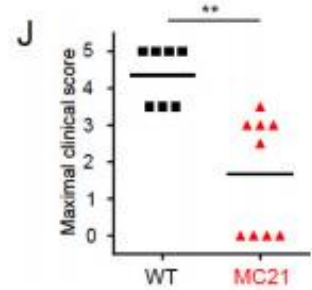
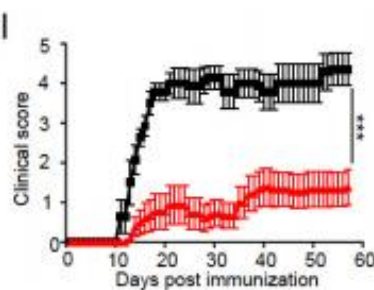
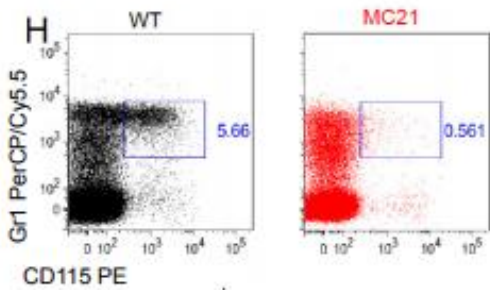
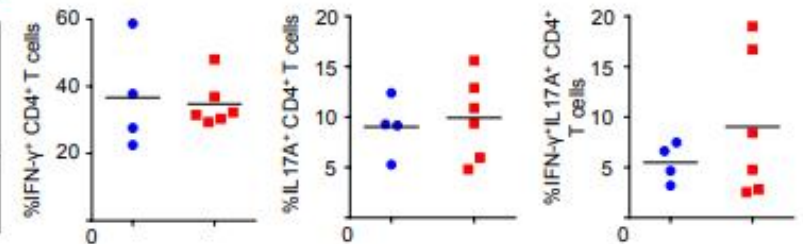
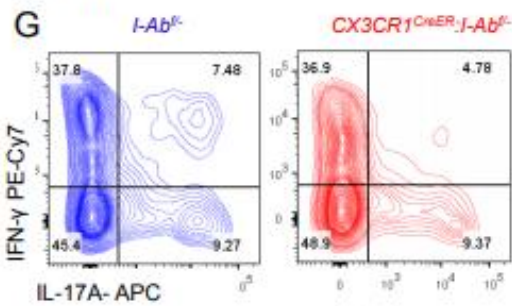
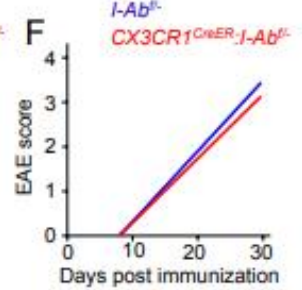
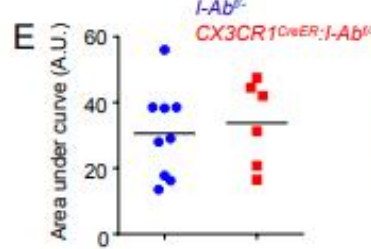
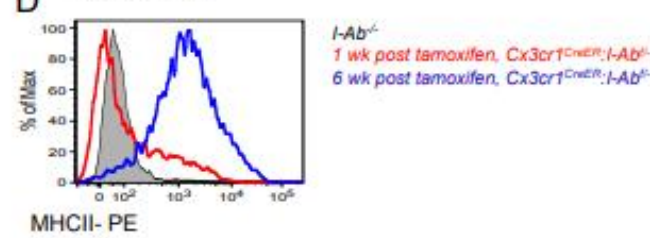
**B** Blood B cells

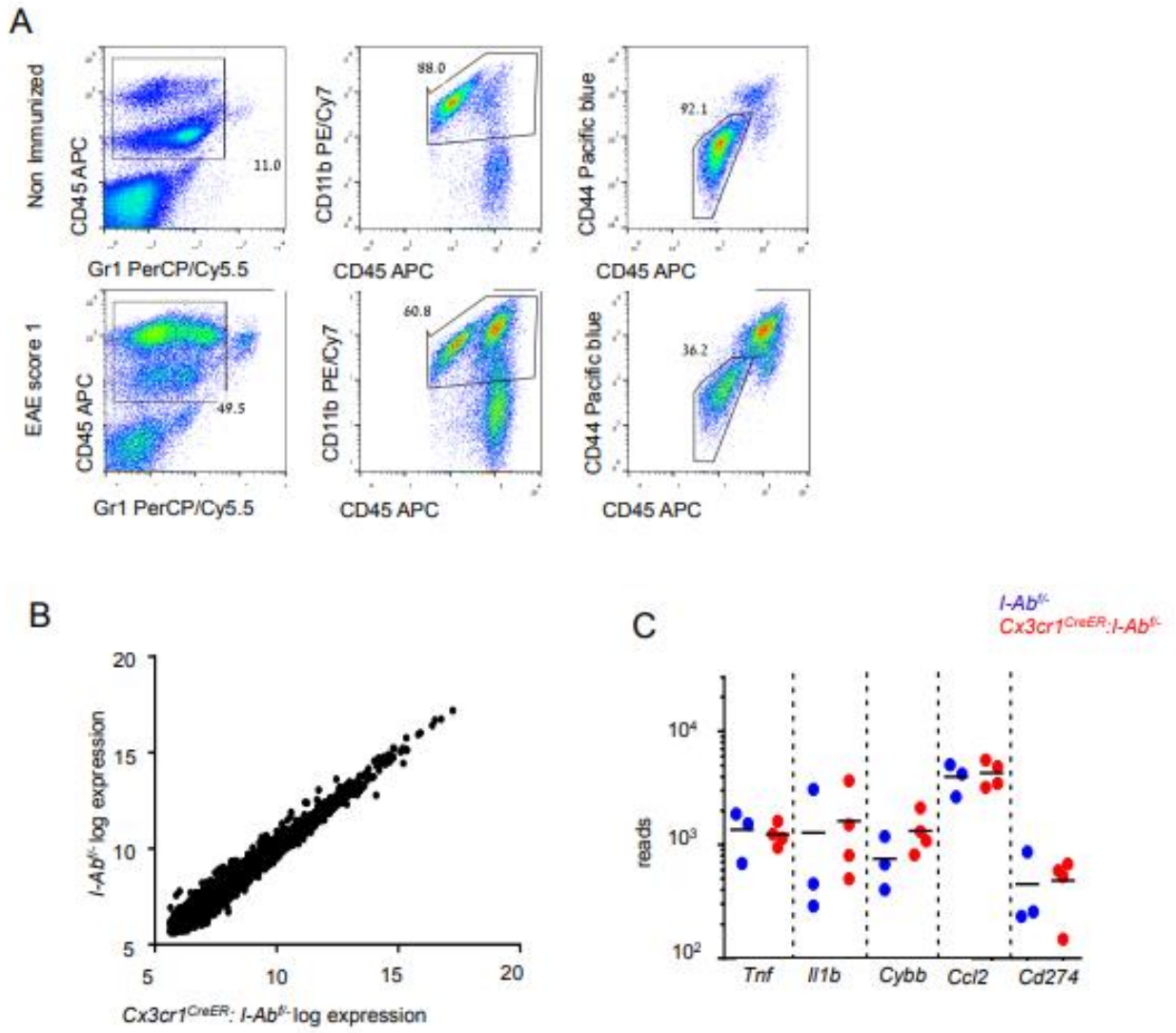


**C** Blood T cells



**D** Splenic DCs





Supplementary Figure 9. Microglial transcriptome is unaffected by MHCII absence

## Project III: The role of microglia- and macrophage-derived IL-23 in EAE induction

### *Introduction*

Following activation, microglia produce and secrete multiple cytokines that can affect EAE progression.<sup>123</sup> Two extensively studied pro-inflammatory cytokines are the IL12 superfamily cytokines - IL12, the family founding member, and the more recently discovered cytokine IL23. Both IL12 and IL23 are heterodimers that share a common p40 subunit. In IL12, p40 is covalently attached to a p35 polypeptide, while IL23 is composed of a p40/p19 heterodimer.<sup>124</sup> IL12 that is secreted by APC causes CD4<sup>+</sup> T cells to differentiate into Th1 cells, whereas IL23 secretion promotes the maintenance of Th17 cells.<sup>29</sup> Th1 cells express the master transcription factor T-bet and play a major role in the host defense against intracellular pathogens. Contribution of Th1 cells to autoimmune disorders are mainly due to their key effector cytokine IFN $\gamma$ .<sup>125</sup> Th17 cells depend on the transcription factor ROR $\gamma$ t for their generation.<sup>126</sup>

Mice deficient for p40 were shown to be EAE-resistant,<sup>127</sup> and it was originally believed that this is due to their inability to produce IL12 and generate encephalitogenic Th1 cells. However, with the discovery of IL23 and its unique subunit p19,<sup>124</sup> this perception has changed.<sup>128</sup> In fact, mice lacking p19, rather than animals lacking the IL12 subunit p35, were found to resist EAE development.<sup>30</sup> IL23 is hence now confirmed as the major pathogenic agent in EAE, as it is crucial for proliferation, expansion, and survival of pathogenic T cells in the CNS.<sup>30,31,32</sup>

As mentioned earlier, it appears that various APC, including microglia, can secrete IL23 under inflammatory conditions.<sup>30</sup> Activated CD4<sup>+</sup> T cells exposed to TGF $\beta$ , IL6, and IL21 were reported to upregulate IL23 receptor, rendering them responsive to IL23 and establishing a stable Th17 cell phenotype.<sup>129,130,131</sup> Mature Th17 cells secrete several different pro-inflammatory cytokines, including IL9, IL17A, IL17F, IL21, IL22, Tumor necrosis factor alpha (TNF $\alpha$ ), and Granulocyte macrophage colony-stimulating factor (GM-CSF).<sup>29</sup> Interestingly though, most of these cytokines were shown to be obsolete for EAE development,<sup>132,133</sup> while GM-CSF appears to be critical.<sup>134</sup> Furthermore, it has been shown that GM-CSF is secreted by Th17 cells as a result of IL23 secretion by APCs, and these two factors are hence forming a positive feedback loop.<sup>135</sup> Recently, fate mapping studies of Th17 cells<sup>136,137</sup> in EAE have revealed that most of these cells shut off IL17 production in early stages of the disease, and secrete IFN $\gamma$  and other pro-inflammatory cytokines including GM-

CSF, instead. These cells were termed ‘ex-Th17’ cells. Indeed, this scenario may have contributed to the misconception of the role of Th1 cells in EAE. Importantly, this cytokine switch was shown to be IL23-dependent.<sup>136</sup>

Despite the eminent role of IL23 in EAE, the cellular source of this cytokine that is critical for disease induction is still unknown. Moreover, whether IL23 expression is mandatory only during peripheral activation of T cells or also in the CNS itself is still under debate.<sup>138,139</sup>

Our findings suggest that peripheral macrophages, and not microglia, are responsible for the critical IL23 needed for EAE development.

## Results

### Microglial IL23 is dispensable for EAE induction and progression

To examine the role of microglial IL23 in EAE, we crossed  $CX_3CR1^{CreER}$  animals to mice harboring a conditional p19 allele ( $p19^{fl/fl}$ ).<sup>138</sup> Microglia-restricted impairment of p19 transcription was validated in sorted cells (**Fig. 8A, B**). To examine whether IL23 produced by microglia is necessary for the disease development and progression, we induced EAE in  $CX_3CR1^{CreER};p19^{fl/fl}$  mice and their littermate controls 6 weeks after TAM treatment. No significant differences were observed between the two groups in the mean clinical scores (**Fig. 8C**) or mean day of disease onset (**Fig. 8D**). This suggests that microglial IL23 is dispensable for the development of EAE.

While not critical for the induction of the disease, microglial IL23 could play a role in the transformation of Th17 to 'ex-Th17' cells.<sup>136,137</sup> We therefore isolated T cells from SC of MOG-challenged mice on d12 post-immunization and performed an *in vitro* re-stimulation in presence of MOG peptide. We observed less  $IFN\gamma^+$  MOG-specific T cells in cultures of cells isolated from  $CX_3CR1^{CreER};p19^{fl/fl}$  mice, than in their controls (**Fig. 8E**). These preliminary results suggest that although microglial IL23 does not appear to be essential for the induction of the disease, it may play a role in the cytokine shift of Th17 to  $IFN\gamma$ -secreting 'ex-Th17' cells in the SC during EAE.

### $CX_3CR1^{Cre};p19^{fl/fl}$ mice are resistant to EAE induction

We next aimed to examine the contribution of IL23 produced by peripheral cells. For that purpose, we used  $CX_3CR1^{Cre}$  mice, which display constitutively active Cre recombinase in  $CX_3CR1^+$  cells, resulting in spontaneous rearrangement of 'floxed' alleles.<sup>25</sup> As a result, in  $CX_3CR1^{Cre};p19^{fl/fl}$  mice the gene encoding p19 is deleted in all  $CX_3CR1^+$  cells, as well as cells derived from  $CX_3CR1^+$  precursors, including pre-macrophages, monocytes and all tissue macrophages.<sup>25</sup> Surprisingly,  $CX_3CR1^{Cre};p19^{fl/fl}$  mice were completely resistant to EAE development, similarly to  $IL23^{-/-}$  mice,<sup>30</sup> whereas littermate controls developed clinical symptoms (**Fig. 9A**). These results indicate that peripheral cells or CNS infiltrating, potentially monocyte-derived cells, rather than resident microglia, constitute a critical source of IL23 for induction of CNS autoimmunity.

McGeachy and colleagues reported that IL23 expression in the LN is essential for the terminal differentiation of effector Th17 cells.<sup>140</sup> Thus, IL23 receptor-deficient T cells produced less IL-17 and failed to proliferate and accumulate in the CNS following MOG-

immunization. Indeed, also we observed in the LN of CX<sub>3</sub>CR1<sup>Cre</sup>:p19<sup>fl/fl</sup> mice less IL17<sup>+</sup> and IFN $\gamma$ <sup>+</sup>IL17<sup>+</sup> ‘ex-Th17’ cells on d18 post-immunization (**Fig. 9B**). In accordance, a significant reduction in CD4 T cell infiltrates was observed in the SC of the mutants (**Fig. 9C**).

### **Monocyte-derived IL23 is not critical for EAE development**

As mentioned earlier, the CX<sub>3</sub>CR1<sup>Cre</sup> system also targets blood monocytes.<sup>25</sup> To examine whether inflammatory Ly6C<sup>hi</sup> monocytes, which we observed to infiltrate the LN in significant numbers after MOG injection (**Fig. 10A**), contribute to IL23 production, we used an anti-CCR2 antibody-based ablation approach.<sup>112</sup> In a preliminary experiment on WT mice we verified that *Il23* mRNA peaks at d4 post-immunization (**Fig. 10C**). However, depletion of blood monocytes using an anti-CCR2 antibody (**Fig. 10B**) did not significantly affect IL23 mRNA levels following immunization (**Fig. 10D**). Taken together, these findings imply that resident LN macrophages, rather than infiltrating monocyte-derived cells, are the critical cellular source of IL23 for CNS autoimmunity.

### **Antigen presentation and IL-23 production are performed by two distinct cell populations**

As mentioned earlier, DC were assumed to both present the myelin peptide and secrete IL23 – two functions necessary for the induction of EAE. However, our above findings suggest that LN resident macrophages, and not DC, might be the critical IL23 producers. In order to separate between these two functions, i.e. antigen presentation and IL23 production, we generated a number of different mixed BM chimeras: In group 1, WT recipients were engrafted with a mixed BM of WT and CX<sub>3</sub>CR1<sup>Cre</sup>:p19<sup>fl/fl</sup> mice. This group is expected to display EAE symptoms upon MOG-immunization, since they were reconstituted with WT cells, which are able to present antigen and also secrete IL23. In group 2, recipients were engrafted with a mixed BM of CX<sub>3</sub>CR1<sup>Cre</sup>:p19<sup>fl/fl</sup> and MHCII<sup>-/-</sup> mice. Here the two functions are separated: BM cells derived from the CX<sub>3</sub>CR1<sup>Cre</sup>:p19<sup>fl/fl</sup> mouse will not be able to produce IL23, but are able to present antigen (as they express MHCII); BM cells derived from the MHCII<sup>-/-</sup> mouse will not be able to present antigen, but are able to produce IL23.

As expected, group 1 indeed developed symptoms (**Fig. 11A**). Group 2, however, were protected from EAE (**Fig. 11A**). However, when examining the spleens of group 2, we observed no MHCII<sup>+</sup> cells, as the MHCII<sup>-/-</sup> cells took over for a yet unknown reason over (**Fig. 11B**). We hence generated another, similar group, group 3: here WT recipients were engrafted with a BM mix of CX<sub>3</sub>CR1<sup>Cre</sup>:p19<sup>fl/fl</sup> and CD80/86<sup>-/-</sup> mice (as CD80/86 co-

stimulatory signal is required for T cell activation). Surprisingly, EAE was not induced in this group upon MOG-immunization (**Fig. 11A**). This suggest that two separate cellular compartments are responsible for antigen presentation and IL23 production.

## *Discussion*

IL23 is known to be the effector cytokine driving EAE pathophysiology.<sup>29</sup> In the periphery, naïve CD4 T cells require IL23 signaling in order to expand as differentiated pathogenic Th17 cells<sup>140</sup>. These T cells can then invade the CNS, where they secrete critical GM-CSF for the pathogenicity and function of effector Ly6C<sup>hi</sup> monocytes,<sup>141</sup> the cells initiating the demyelination process itself.<sup>142</sup> Although both peripheral DC and CNS resident microglia were suggested to secrete IL23, it remains unclear whether the cytokine is required only in the periphery or also in the CNS, in order to induce EAE.

By ablation of IL23 in microglia using CX3CR1<sup>CreER</sup>:p19<sup>fl/fl</sup> mice, we could rule out microglia as the crucial source of IL23 in this system, as TAM-treated mice developed EAE symptoms which were comparable to those of littermate controls. Surprisingly, CX3CR1<sup>Cre</sup>:p19<sup>fl/fl</sup> remained symptom-free post-MOG immunization, suggesting a critical role of either peripheral macrophages or circulating monocytes, both targeted in the constitutive Cre system.<sup>25</sup> Although our preliminary data suggest that monocytes are not key players in that respect, as depletion of CCR2+Ly6C<sup>hi</sup> monocytes did not alter IL23 mRNA in the LN following immunization, further experimentation will be required to substantiate this conclusion.

Importantly, our findings challenge the current dogma, according to which IL23 is produced mainly by DC residing in the LN. By transferring mixed BM cells from CX3CR1<sup>Cre</sup>:p19<sup>fl/fl</sup> and CD80/86 KO origins and induction of EAE in the recipients, we showed that these T cell activation and IL23 production are performed by two separated cell entities. As DC were demonstrated to be effective APC in the LN post-immunization,<sup>143</sup> our data suggest that other cells in the LN are the source of IL23.

We hypothesized that LN resident macrophages could be prime candidates for IL23 production. Upon immunization, T cells accumulate in the LN - in the entering process they only briefly interact with subcapsular sinus macrophages,<sup>144</sup> and then colonize the T cell zone, where they interact and are activated by cognate interaction with DC.<sup>143</sup> Since IL23 secretion occurs only later (d4-5 post-immunization), we postulated that the cells required for IL23 secretion reside in the T cell zone. However, only 3 resident macrophage populations in the LN were described, none of which in the T cell zone.<sup>144</sup> Recently, Baratin and colleagues have reported of another, novel macrophage population which indeed resides in the T cell zone, now termed as T zone macrophages (TZM).<sup>145</sup> This population might fit the profile of

the cells require for IL23 production, as they express CX<sub>3</sub>CR1 but display a rather fast turnover, as most of them were replaced 6 weeks post-TAM treatment.<sup>145</sup> This might explain our results that CX<sub>3</sub>CR1<sup>CreER</sup>:p19<sup>fl/fl</sup> mice develop EAE (in which MOG was administered 6 weeks post-TAM), whereas CX<sub>3</sub>CR1<sup>Cre</sup>:p19<sup>fl/fl</sup> are resistant. Moreover, TZM were shown to lack the ability to activate T cells, as they do not express MHCII.<sup>145</sup> This would support our finding that the cells secreting IL23 are not the same cells that activate T cells following MOG challenge.

In future experiments we intent to characterize TZM upon MOG-immunization, and examine whether these cells are indeed the critical source of IL23 for induction of CNS autoimmunity. Furthermore, we would like to generalize our finding to other settings, for example *Candida albicans* infection. In contrast to EAE in which Th17 cells are the drivers of the autoimmune detrimental cascade, in the *Candida* model Th17 are required in order to induce protection against the fungi.<sup>146</sup> We therefore speculate that whereas CX<sub>3</sub>CR1<sup>Cre</sup>:p19<sup>fl/fl</sup> mice are resistant to EAE induction, they display heightened susceptibility to *Candida albicans*.

*Figure legends*

**Figure 8. Microglial IL23 is dispensable for EAE induction and progression**

(A) Gating strategy for sorting microglia and Ly6C<sup>hi</sup> monocytes. Microglia were defined as CD45<sup>int</sup>CD11b<sup>+</sup>Ly6C<sup>-</sup>. Monocytes were defined as CD45<sup>hi</sup>CD11b<sup>+</sup>Ly6C<sup>hi</sup>. Pre-gated on Ly6G<sup>-</sup>.

(B) qPCR analysis of p19 mRNA expression in the sorted microglia and Ly6C<sup>hi</sup> monocytes. Cells were sorted from TAM-treated CX<sub>3</sub>CR1<sup>CreER</sup>:p19<sup>fl/fl</sup> mice and p19<sup>fl/fl</sup> littermate controls on d18 post-immunization.

(C) Development of clinical disease in TAM-treated CX<sub>3</sub>CR1<sup>CreER</sup>:p19<sup>fl/fl</sup> mice (n=9) and p19<sup>fl/fl</sup> mice (n=10) after immunization with MOG<sub>35-55</sub> in CFA.

(D) Analysis of mean day of clinical disease onset.

(E) Quantification of flow cytometry analysis of T cell SC infiltrates in TAM-treated and EAE-induced CX<sub>3</sub>CR1<sup>CreER</sup>:p19<sup>fl/fl</sup> (n=4) and p19<sup>fl/fl</sup> (n=3) mice on day 12 post-immunization. Isolated T cells were stimulated *ex vivo* with MOG<sub>35-55</sub>, incubated with Brefeldin A, and stained for IFN $\gamma$  and IL-17 intracellular expression. Gated on CD4<sup>+</sup>CD45<sup>hi</sup>CD44<sup>+</sup>CD40L<sup>hi</sup>. Intracellular expression of IFN $\gamma$  (left), p<0.01 and IL-17 (right), p>0.05 (student's t test) in MOG-specific T cells.

**Figure 9. CX<sub>3</sub>CR1<sup>Cre</sup>: p19<sup>fl/fl</sup> mice are protected from EAE**

(A) Development of clinical disease in CX<sub>3</sub>CR1<sup>Cre</sup>:p19<sup>fl/fl</sup> (n=6) and p19<sup>fl/fl</sup> (n=5) mice after immunization with MOG<sub>35-55</sub> in CFA. Representative of 3 independent experiments.

(B) Flow cytometry analysis of Th1/Th17 cells in LNs of CX<sub>3</sub>CR1<sup>Cre</sup>:p19<sup>fl/fl</sup> and p19<sup>fl/fl</sup> mice on day 18 post-immunization. Isolated T cells were stimulated *ex vivo* with MOG<sub>35-55</sub>, incubated with brefeldin A, and stained for IFN $\gamma$  and IL-17 intracellular expression. Gated on CD4<sup>+</sup>CD45<sup>hi</sup>CD11b<sup>+</sup>CD44<sup>+</sup>CD40L<sup>hi</sup>.

(C) Flow cytometry analysis of CD4 T cells in the SC of CX<sub>3</sub>CR1<sup>Cre</sup>:p19<sup>fl/fl</sup> and p19<sup>fl/fl</sup> mice on day 18 post-immunization. Gated on CD4<sup>+</sup>CD45<sup>hi</sup>CD11b<sup>-</sup>.

**Figure 10. Depletion of blood monocytes does not alter IL-23 mRNA expression in the LN**

- (A) Flow cytometry analysis of LN of non-immunized WT (left) and MOG-immunized WT (right) 6d post-immunization. Gated on CD45<sup>+</sup>.
- (B) Flow cytometry analysis of blood of MOG-immunized (left) and MOG-immunized mouse 24hrs after MC21 injection (right), for depletion of Ly6C<sup>hi</sup> monocytes. Gated on CD45<sup>+</sup>CD11b<sup>+</sup>.
- (C) qCPR analysis of p19 mRNA expression in total inguinal LN of WT mice either non-immunized, d2 or d4 post-MOG immunization (n=2).
- (D) qPCR analysis of p19 mRNA expression in total inguinal LN of non-immunized WT mice, and d4 post-immunization in CX<sub>3</sub>CR1<sup>Cre</sup>:p19<sup>fl/fl</sup>, WT, and WT mice treated with MC21 (n=3-6).

**Figure 11. Antigen presentation and IL23 production are performed by two distinct cell populations**

- (A) Development of clinical disease in mixed BM chimeras: CX<sub>3</sub>CR1<sup>Cre</sup>:p19<sup>fl/fl</sup> + WT (blue), CX<sub>3</sub>CR1<sup>Cre</sup>:p19<sup>fl/fl</sup> + MHCII<sup>-/-</sup> (red), and CX<sub>3</sub>CR1<sup>Cre</sup>:p19<sup>fl/fl</sup> + CD80/86<sup>-/-</sup> (black).
- (A) Flow cytometry analysis of spleens to detect MHCII<sup>+</sup> cells in WT mouse transplanted with CX<sub>3</sub>CR1<sup>Cre</sup>:p19<sup>fl/fl</sup> BM (left), MHCII<sup>-/-</sup> mouse (middle), and WT mouse transplanted with a mix of CX<sub>3</sub>CR1<sup>Cre</sup>:p19<sup>fl/fl</sup> and MHCII<sup>-/-</sup> BM (right).

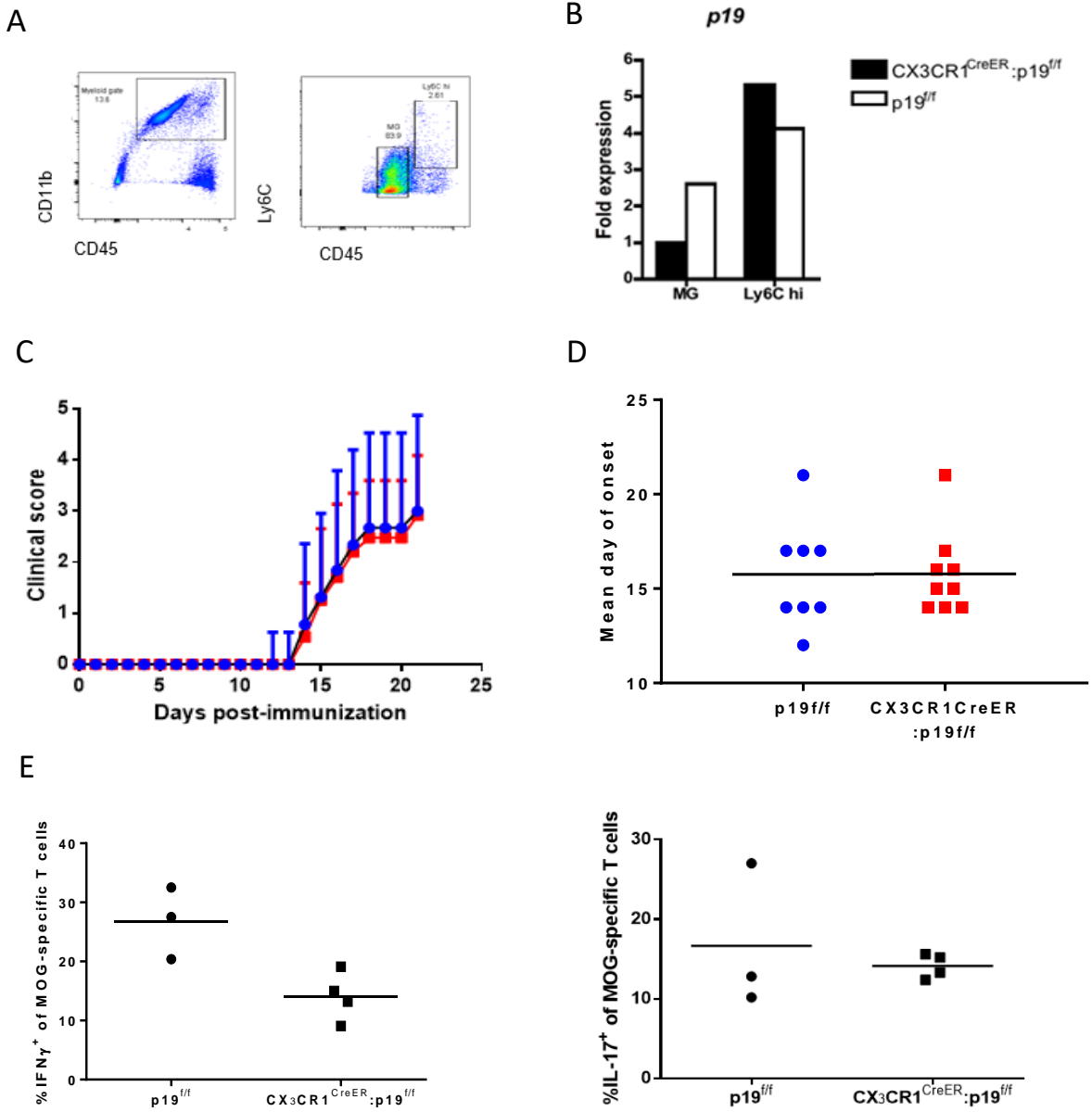


Figure 8. Microglial IL23 is dispensable for EAE induction and progression

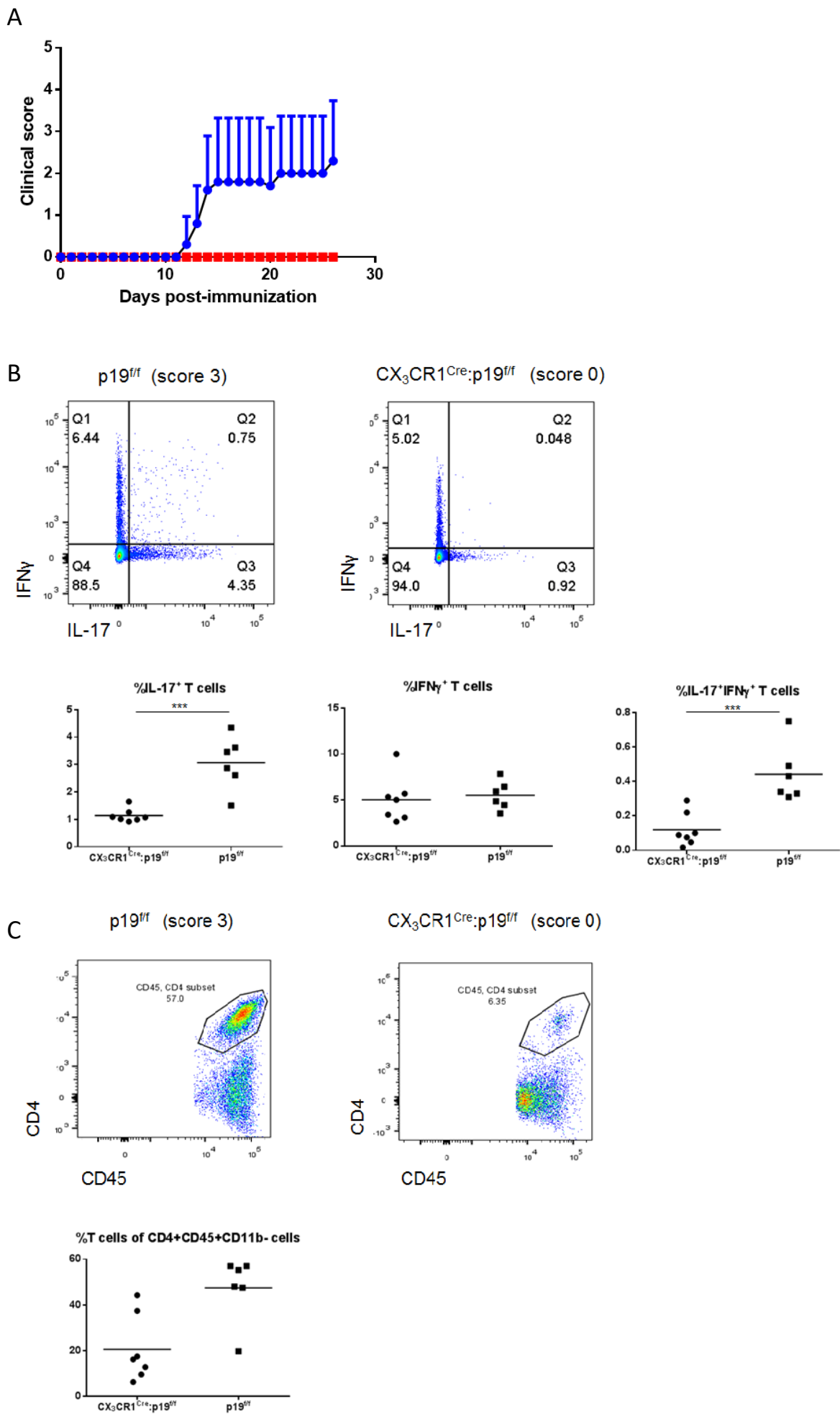


Figure 9. CX<sub>3</sub>CR1<sup>Cre</sup>:p19<sup>fl/fl</sup> mice are protected from EAE

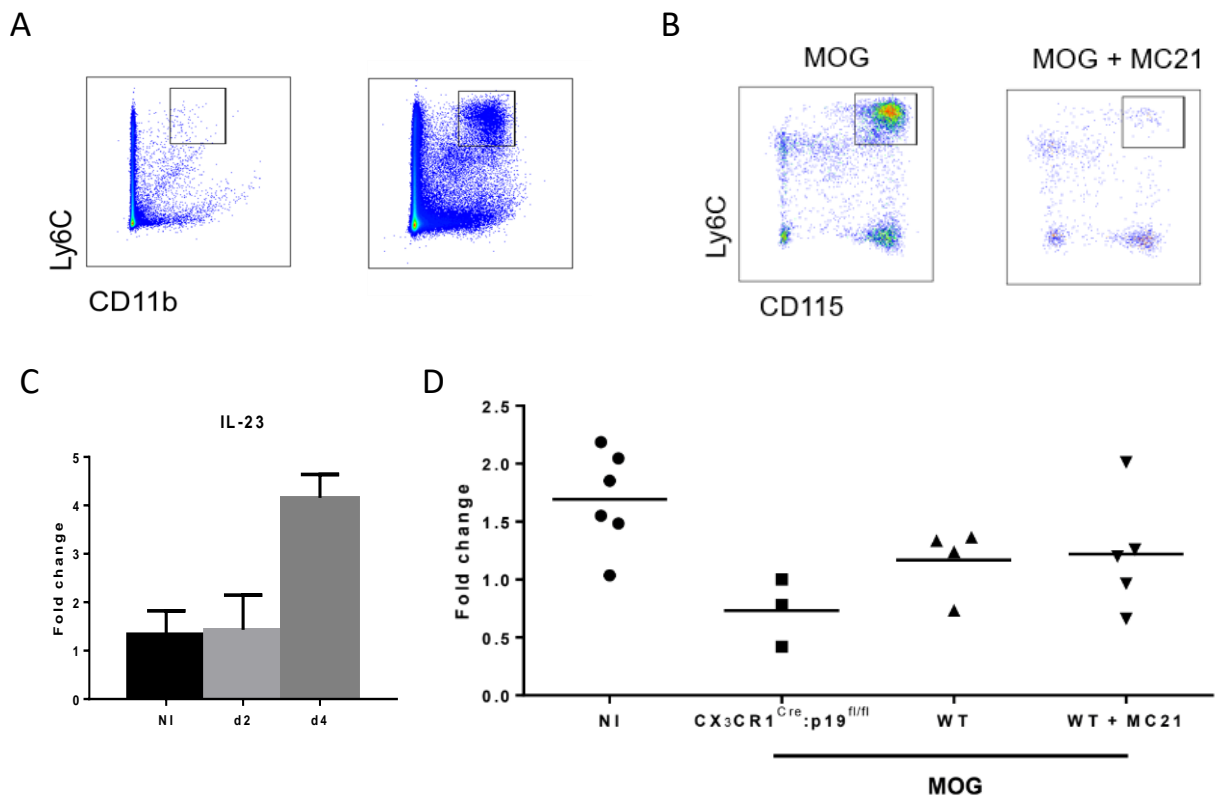
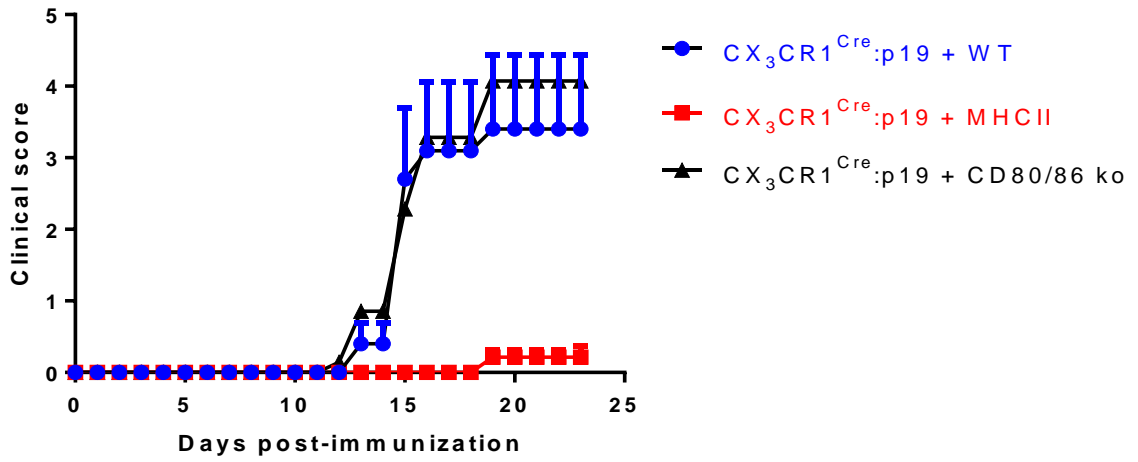


Figure 10. Depletion of blood monocytes does not alter IL-23 mRNA expression in the LN

A



B

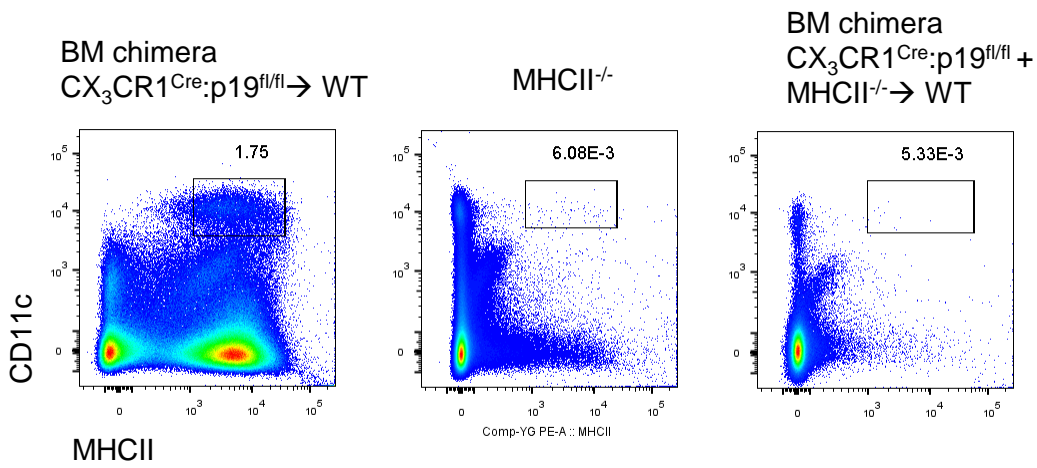


Figure 11. Antigen presentation and IL23 production are performed by two distinct cell populations

## Project IV: Studying the role of the IL-10 axis in microglia

### *Introduction*

As discussed in detail earlier, recent studies have suggested that specific CNS pathologies are associated with different microglia activation modules.<sup>33</sup> For instance, the MgND signature,<sup>34,35</sup> was linked to neurodegenerative diseases, such as AD and ALS, whereas other, distinct microglia activation profiles were linked to EAE and LPS challenge. The revealing of distinct patterns implies towards possible for targeted therapy for specific brain pathologies.<sup>33</sup> However, modules that restrain microglia activation, and are therefore crucial for CNS homeostasis, are far less studied. As mentioned earlier, microglia quiescence require expression of Sall1, Tgf $\beta$  receptor, as well as CD200 Ligand-receptor interaction.<sup>39,40,41</sup> Recently It was shown that homeostatic phagocytic functions of microglia in the aging brain could be restored by CD22 blockade.<sup>147</sup>

The cytokine IL10 plays a major role in controlling hyperactivation of lymphoid and myeloid immune cells.<sup>42</sup> IL10 can be produced by T cells, B cells, and macrophages, as well as certain non-hematopoietic cells, usually after activating stimuli. Most hematopoietic cells also can sense IL10 via expression of a dedicated IL10R, composed of an IL10-binding chain (IL-10Ra) and an accessory molecule, IL10Rb, shared with other receptors of the IL10 superfamily. Binding of IL10 to its receptor triggers the Janus kinase (JAK) signal transducer and activator of transcription (STAT) pathway, particularly by STAT3 to curb cytokine gene expression and down-regulate antigen presentation capacity the expression of MHCII and thus antigen presentation to T cells.<sup>148</sup> Microglia hyperactivation has been shown to be associated with neurodegenerative disorders, from AD and Parkinson's diseases to MS. In *in vitro* cultures, IL10 was shown to inhibit production of proinflammatory cytokines by microglia and other glia.<sup>42</sup> Prevention of deleterious microglia hyperactivation following SC injury has been reported to require monocyte-derived IL10.<sup>149</sup> IL-10 originated from regulatory T cells and acting on microglia was shown to ameliorating the outcome of intracerebral hemorrhage.<sup>150</sup>

IL10 is also critical to maintain gut homeostasis. Specifically, children that lack IL10R expression develop severe early onset colitis<sup>151</sup> assumed to result from unrestrained activation of gut macrophages.<sup>152</sup> Supporting this notion, also mice that harbor an IL10Ra deficiency in gut macrophages develop fulminant colitis.<sup>43,44</sup>

Here we used the paradigm of peripheral endotoxin challenge to establish and characterize the critical role of the IL10 axis in restoring microglia quiescence in the mouse. We reveal that microglia harbors a robust ability to revert to homeostasis. The latter is impaired when microglia are unable to sense IL10 due to uncontrolled TNF expression. Microglia hyperactivation results in fatal sickness and neuronal impairment. Collectively, our data highlight a critical control module for CNS health.

## Results

### **Microglial IL10 sensing is dispensable for CNS homeostasis despite prominent microglial IL-10R expression**

As mentioned earlier, IL10 is critical to maintain gut homeostasis since macrophage-restricted ablation of IL10R leads to spontaneous colitis.<sup>43,44</sup> Interestingly, microglia display prominent of both subunits of the IL10R expression which is acquired during development alongside the establishment of their characteristic gene expression signature, such as Sall1 induction (**Fig. 12A, B**).<sup>54,55</sup> In contrast to gut macrophages though, microglia do not express IL10 (**Fig. 12A, B**).

To investigate a potential role of the IL10 axis for microglia homeostasis and microglia function following challenge, we generated *Cx3cr1<sup>CreER</sup>:IL10ra<sup>fl/fl</sup>* mice in which TAM treatment allows introduction of an IL10R deficiency in long-lived *Cx3cr1<sup>+</sup>* macrophages.<sup>25,91</sup> The cells targeted with this system include microglia and non-parenchymal CNS macrophages,<sup>76,77</sup> as well as selected peripheral tissue macrophages,<sup>153</sup> but notably exclude shorter lived monocytes and their derivatives.<sup>25</sup> Analysis of sorted microglia of *Cx3cr1<sup>CreER</sup>:IL10ra<sup>fl/fl</sup>* mice 6 weeks post TAM treatment confirmed efficient deletion of the *IL10ra* gene from the cells (**Fig. 12C, D**). TAM-treated C57BL/6 mice lacking microglial IL10R expression did not display signs of gut inflammation or other overt phenotypes (data not shown). To probe for a direct molecular impact of the deficiency on microglia we analyzed the transcriptomes of cells sorted from the brains of the respective mice. As seen in the volcano blot (**Fig. 12E**), *IL10ra* deficient microglia of TAM-treated *Cx3cr1<sup>CreER</sup>:IL10ra<sup>fl/f</sup>* mice did not display significantly DEG over *IL10ra<sup>fl/fl</sup>* littermate control microglia, except for *Il10ra*, the targeted gene, and *Cx3cr1*, due to the heterozygosity resulting from the *CreER* transgene insertion. These data suggest that in animals kept under SPF hyper-hygienic housing conditions, microglia are not exposed to IL10 and establish that microglial IL10 sensing is under these circumstances obsolete for the maintenance of brain homeostasis.

### **Microglia display a robust, but transient global response to peripheral endotoxin challenge**

Sepsis and bacteremia result in bacterial LPS exposure that causes a complex systemic response, which involves multiple organs and cells.<sup>154</sup> Peripheral endotoxin challenge of primates and mice has been shown to result in microglia activation.<sup>38,86,155,156,157</sup> Rather than

responding to the TLR ligand which does not reach the brain parenchyma in significant amounts,<sup>158</sup> microglia are believed to sense a robust but transient serum cytokine storm, including TNF, IL6 and IL1<sup>159</sup> and/ or exposure to serum factors due to a transient limited impairment of the BBB.<sup>160,161</sup> Global RNAseq analysis of microglia sorted from C57BL/6 brains at different time points following an intra-peritoneal (i.p.) LPS challenge (2.5 mg/kg) revealed a robust response with the up- and downmodulation of 1294 and 1394 genes, respectively (**Fig 13A, D**). Genes induced by 6hrs included *Itgax*, *Ch25h*, *Spp1*, *Tnf*, *Saa3*, *Tnfaip3* and *Cd40* (**clusters 1a, b, c, 2a**) (**Fig. 13A, B**) A second group of genes displayed delayed induction, 24 or 48hrs after the LPS bolus (**clusters 2b, c**) (**Fig. 12A, B**). This list comprised genes encoding ribosomal subunits, *Marco* and *Saa3*. **Cluster 2c** also included *Tspo*, encoding a translocator protein, whose expression can be measured by PET and was used to demonstrate the global response of human microglia to peripheral endotoxin exposure.<sup>156</sup> Corroborating earlier studies, down regulated genes included the ‘microglia signature’,<sup>40</sup> including as *Sall1*, *Tgfbr* and *P2yr12*, as well as *HexB*, *Tlr4* and *Trem2* (**cluster 4a**). Interestingly, our analysis revealed that the extended microglia response to endotoxin challenge did include induction of genes whose expression had previously been thought to be restricted to settings of neurodegeneration,<sup>33,162</sup> such as *ApoE*, *Axl*, *Ctsll* and *Sspl* (**Suppl. Fig. 10A**).

The analysis of the microglial response over time revealed that by 48hrs post LPS, most up and down-modulated mRNAs had reverted to their steady state levels, either completely or close to the original configuration (**Fig 13A, C, D**). Notable exceptions were late induced transcripts and genes in **clusters 2a, 3a and 4c**, which included *Il1b* and *Ccl5*. Seven days post the LPS challenge, most the microglia had restored to the transcriptome status before the challenge, with only 204 DEG upregulated and 14 genes downregulated, as compared to the untreated control cells (**Fig 13C, D**). Collectively these data show that microglia harbor a robust propensity to restore quiescence following peripheral endotoxin challenge.

Microglia activation was also reflected in changes in the chromatin landscape, as assessed by ATACseq, that identifies open chromatin regions by virtue of their accessibility for “tagmentation” by transposases.<sup>69</sup> Loci that displayed induced expression, such as *Tnf* (cluster 1), displayed induced ATAC signals, while loci encoding genes that were downregulated, such as *Sall1* and *P2ry12* (cluster 4) did not display changes (**Fig. 13E**). Taken together, these data corroborate earlier reports that microglia respond rapidly to a peripheral endotoxin challenge,<sup>38,86,157</sup> including induced expression of pro-inflammatory genes and a

loss of ‘microglia signature genes. Importantly, our detailed time course analysis revealed that this cellular compartment to display a robust ability to restore its steady state transcriptome configuration.

### **IL10 receptor-deficient microglia are hyperactive after peripheral LPS challenge and fail to return to quiescence**

IL10 is well known to control macrophage activation.<sup>43,42,163</sup> To probe for a potential role of IL10 in curbing the microglia response to the cytokine pulse induced by the peripheral LPS challenge, we performed a side by side comparison of microglia isolated from *Cx3cr1<sup>CreER</sup>:IL10ra<sup>fl/fl</sup>* and *IL10ra<sup>fl/fl</sup>* littermate control mice, 6, 24 and 48hrs after the i.p. LPS bolus (**Fig. 14B, C**). Beyond the 48hrs time point, a major fraction of the mutant animals succumbed the LPS challenge precluding the analysis of a later time point (**Fig. 14A**). PCA revealed that while ‘wild type’ microglia showed a transient response but reverted by 48hrs largely to the steady state transcriptome configuration, IL10Ra deficient microglia failed to restore quiescence (**Fig. 14B**). K-means clustering of the RNAseq data revealed 9 clusters with distinct gene expression dynamics (**Fig. 14C**).

Except for **cluster 5 and 6**, gene expression 48hrs post LPS bolus was significantly impaired when microglia were unable to sense IL10. Specifically, expression of 1975 induced genes failed in mutant microglia to be silenced. This included *Tnf*, *Ccl5*, *Ssp1* and *Cd69* indication microglia hyperactivation. Likewise, expression of downmodulated genes that was in control transiently reduced failed to recover in mutant microglia, including the microglia signature genes *P2ry12* and *Sall1*, as well as *Mef2c*, *Tmem119*, *Tgfbr*, and *Il10rb*. These data establish a critical role of IL10 for microglia to restore homeostasis following the LPS challenge. Interestingly, **cluster 1**, comprised induced 326 genes, that displayed at 48hrs higher expression in controls than in mutant microglia. This included *Ccr5*, which had previously been reported to be induced by IL10 in human monocytes.<sup>164</sup>

### **Mice with microglial IL-10R deficiency exhibit prolonged sickness behavior and impaired neuronal function post-LPS administration**

Septic shock and the associated endotoxin exposure result in sickness behavior, a centrally organized response, including reduced motility, appetite loss and social withdrawal.<sup>154</sup>

Several studies imply microglia as regulator of these symptoms and other related conditions.<sup>165,166,167</sup> To probe for an impact of the IL10R deficiency-associated microglia hyperactivation on this response, TAM-treated CX<sub>3</sub>CR1<sup>CreER</sup>:IL-10R<sup>fl/fl</sup> mice and littermate controls were placed in an automated Home Cage Locomotion system. Before challenge, both groups of mice displayed similar activity in light and dark cycles (**Fig. 15A**). Both CX<sub>3</sub>CR1<sup>CreER</sup>:IL-10R<sup>fl/fl</sup> and control mice, treated with a reduced LPS bolus (0.5 mg/kg) to improve survival of the mutants, showed significantly impaired motility (**Fig. 15A**). However, whereas controls resumed some level of activity within 24hrs and returned to baseline activity by 4 days, mutant mice failed to recover during this time frame and some mice had to be sacrificed (**Fig. 15A**). In line with their exacerbated and extended sickness behavior, CX<sub>3</sub>CR1<sup>CreER</sup>:IL-10R<sup>fl/fl</sup> mice consumed significantly less food after the challenge compared to the controls (**Fig. 15B**). This establishes that restoration of microglia quiescence is critical to limit the sickness response to endotoxin challenge. Conversely, the exacerbated and extended activation of IL10R deficient microglia results in pathology.

Systemic endotoxin challenges were shown to transiently impair the response of hippocampal neurons to repeated synapse stimulation, known as long-term potentiation (LTP).<sup>168,169,170</sup> Specifically, TNF, potentially derived from microglia, has been suggested to contribute to LTP impairment.<sup>171</sup> To probe for an impact of the IL10R-deficient, hyperactive microglia on neuronal fitness, we performed extracellular electrophysiological recordings on acute slices prepared from dorsal hippocampi of TAM-treated CX<sub>3</sub>CR1<sup>CreER</sup>:IL-10R<sup>fl/fl</sup> mice and littermate controls.<sup>169</sup> We examined LTP 12 and 24hrs after the peripheral LPS stimulus (**Fig. 15C, D**). Neurons of mice harboring IL10R proficient and deficient microglia displayed comparable LTP before the LPS challenge (**Fig. 15D**). However, 12 hours post-LPS hippocampi of the mutant animals displayed a greater LTP impairment than controls (**Fig. 15D**). Moreover, 24 hours after the LPS bolus, this LTP impairment persisted in CX<sub>3</sub>CR1<sup>CreER</sup>:IL-10R<sup>fl/fl</sup> animals, whereas control mice showed significant recovery (**Fig. 15D**). These findings establish that hyperactivation of microglia, that includes uncontrolled Tnf expression, causes prolonged impairment of neuronal function in the hippocampus.

### **Defining the source of IL10**

Microglia isolated from unchallenged CX<sub>3</sub>CR1<sup>CreER</sup>:IL-10R<sup>fl/fl</sup> mice and littermate controls displayed essentially no differentially expressed genes (**Fig. 12E**). Moreover, even by 6hrs post the LPS bolus, transcriptomes of IL10R deficient and proficient microglia showed with

86 DEG only minor differences (**Fig. 14E**). This suggest that the cells are in steady state not exposed to IL10, but rather that expression of the anti-inflammatory cytokine is induced by the endotoxin challenge. Microglia themselves to not produce IL10 (**Fig. 12A**). Accordingly, TAM-treated CX<sub>3</sub>CR1<sup>CreER</sup>:IL-10<sup>fl/fl</sup> mice<sup>172</sup> which lack the *IL10* gene in microglia displayed a controlled sickness behavior like their littermates (**Fig. 16A**).

Astrocytes, the majority of glial cells in the brain, were reported to produce IL10 upon challenge.<sup>42,173</sup> In order to examine if this is the case upon LPS treatment, we sorted astrocytes and microglia in steady state and 12hrs post LPS using GFAP<sup>CreER</sup>:tdTomato<sup>fl/fl</sup> mice,<sup>174</sup> in which astrocytes are labeled following TAM administration. RNAseq analysis confirmed that only microglia expressed *Cx3cr1* transcripts, whereas the expression of *Aldh1l1* was restricted to astrocytes (**Fig. 16A**), validating our sorting strategy of Tomato<sup>+</sup> astrocytes. Interestingly, *Il10ra* was expressed only in microglia, whereas *Il10* was not expressed in neither astrocytes or microglia populations (in microglia upon LPS challenge – below threshold), suggesting astrocytes are not the source of IL10 in the CNS post-LPS bolus (**Fig. 16A**). Indeed, when ablating IL10 in a more specific system to target astrocytes, the *Aldh1l1*<sup>CreER</sup> mouse,<sup>175</sup> also these mice displayed a controlled sickness response, similar to littermate controls (**Fig. 16B**).

We have previously reported that in a model of SC injury, infiltrating monocytes and monocyte-derived macrophages seem to provide critical IL-10.<sup>149</sup> To investigate which cell provides IL10 to curb microglial activation following LPS challenge, we isolated different fractions of hematopoietic cells from the CNS of challenged WT mice and untreated controls. In this preliminary study, we sorted and compared microglia, T cells, and all other (non T, non microglia) CD45<sup>+</sup> cells 12hrs post-injection (**Fig. 16C**). In order to increase cell numbers of rather small populations such as brain T cells, we pooled two brains together to constitute one sample. RT-PCR confirmed that microglia do not express IL10 mRNA in either steady state or post-LPS challenge (**Fig. 16C**). In contrast, upon challenge but not in steady state, IL10 transcripts were detected in the T cell fraction, and at even in higher levels in the CD45<sup>+</sup> fraction (**Fig. 16C**). This suggested that other immune cells in the CNS, but not microglia, are providing IL10 necessary to maintain quiescence of microglia under pathological conditions, and therefore contribute to maintenance of tissue homeostasis. Of note, *Tnf* transcripts were detected only in LPS-challenged microglia, but not in T cells or the other hematopoietic cells (CD45<sup>+</sup>) (**Fig. 16C**). Collectively, these results suggest that neither microglia or astrocytes are the source of IL10 in the CNS following LPS treatment.

Furthermore, although T cells produce IL10 upon challenge, the major source of the anti-inflammatory cytokine is a different CD45<sup>+</sup> population in the CNS, potentially monocytes or resident perivascular macrophages.

### **Impairment of microglial TNF production restores the ability of IL10R-deficient microglia to re-establish quiescence and prevents associated pathologies**

IL10R-deficient microglia fail to restore quiescence following their activation in response to the peripheral LPS challenge. We hypothesized that the hyperactivation of the microglia compartment in the mutant animals could be intrinsic and result from pro-inflammatory factors the cells themselves secrete and that might perpetuate the activation. A prime candidate for such a scenario would be TNF, a factor that has been implied in CNS pathologies.<sup>176</sup> Both control microglia and IL10R-deficient cells prominently expressed *Tnf* mRNA following challenge, although induction in mutant cells was more robust, in contrast to WT cells, and did also not recede with time (**Fig. 17A**). This exacerbated TNF expression of mutant microglia was also reflected on the protein level as shown by flow cytometric analysis (**Fig. 17B**). To test if microglial TNF is not only a part, but a critical driver of the observed microglia hyperactivation and pathology, we crossed a ‘floxed’ *Tnf* allele<sup>177</sup> onto the *Cx3cr1*<sup>CreER</sup>:*IL-10ra*<sup>fl/fl</sup> background. Upon TAM treatment, microglia of the resulting animals will not be able to sense IL10, but concomitantly fail to produce TNF.

Notably, TNF is among the serum cytokines that are considered to trigger the microglia activation.<sup>159</sup> We therefore first tested whether serum TNF levels would be affected in *Cx3cr1*<sup>CreER</sup>:*IL-10ra*<sup>fl/fl</sup>:*Tnf*<sup>fl/fl</sup> animals. As seen in **Fig. 17C**, serum TNF levels were comparable and transient in double mutant, single mutant and control mice. This indicates that the peripheral *Tnf* source is not targeted by the *Cx3cr1* promoter-driven inducible <sup>CreER</sup> recombinase transgene. In line with the unimpaired induction of serum *Tnf*, microglia of TAM-treated *Cx3cr1*<sup>CreER</sup>:*IL-10ra*<sup>fl/fl</sup>:*Tnf*<sup>fl/fl</sup> animals displayed 6 hours post the LPS bolus a robust response that was indistinguishable from littermate controls (**Fig. 17D, F**). Moreover and in stark contrast to *Cx3cr1*<sup>CreER</sup>:*IL-10ra*<sup>fl/fl</sup> animals, the double mutant *Cx3cr1*<sup>CreER</sup>:*IL-10ra*<sup>fl/fl</sup>:*Tnf*<sup>fl/fl</sup> mice were like the controls able to restore microglia quiescence by 48hrs following the challenge (**Fig. 17D, E, F**).

Impairment of microglial *Tnf* production restored the ability of IL10Ra deficient microglia to revert to a steady state transcriptome configuration. We next asked whether

*Cx3cr1<sup>CreER</sup>:IL-10ra<sup>fl/fl</sup>:Tnf<sup>fl/fl</sup>* mice would also be protected from the pathologies, including the extended sickness behavior and neuronal deficits. TAM-treated *CX<sub>3</sub>CR1<sup>CreER</sup>:IL-10R<sup>fl/fl</sup>:Tnf<sup>fl/fl</sup>* mice and littermate controls were challenged with LPS (0.5 mg/kg) and monitored for locomotion. Both groups of mice were equally affected by the LPS bolus and displayed a withdrawal response but recovered within a few days (**Fig. 18A**), unlike the single IL10Ra mutant animals (**Fig. 15A**). This establishes that microglial TNF is critically driving the LPS-induced sickness behavior in response to the peripheral endotoxin challenge.

TNF has already been implied in the endotoxin-associated impairment of the LTP response,<sup>171</sup> although the exact cytokine source remained undefined.

Electrophysiological measurements on acute hippocampal slices of LPS treated mice corroborated our earlier finding that TAM-treated *Cx3cr1<sup>CreER</sup>:IL-10R<sup>fl/fl</sup>* mice display enhanced LTP impairment as compared to controls (**Fig. 18B**). In stark contrast, in hippocampi of mice whose microglia were in addition to the IL10R mutation unable to produce Tnf, no LTP impairment was observed. These data establish that the neuronal impairment is caused by TNF secreted by microglia and corroborate that exacerbated TNF levels are responsible for the persevering LTP impairment caused by the microglial IL10ra deficiency.

Since monocytes are considered the main source of peripheral TNF upon LPS challenge,<sup>154</sup> we hypothesized that monocyte depletion would affect microglial activation post-LPS. However, depletion of CCR2<sup>+</sup> inflammatory blood monocytes had no effect on activation of microglia 6 hrs post-LPS (**Fig. 19A**). Indeed, we then confirmed that levels of serum TNF post-LPS injection were comparable in untreated and monocyte-depleted WT mice (**Fig. 19B**). Our data imply towards a different cell population, other than monocytes, to be responsible for the pronounced TNF protein elevation in the serum following LPS treatment.

## Discussion

Sepsis and bacteremia trigger a complex response of the central nervous system, including microglia activation. Using this paradigm of a robust but transient response to endotoxin challenge with an ensuing serum cytokine pulse, we establish here the critical role of IL10 exposure for microglia to return to homeostasis.

An important feature of the peripheral LPS challenge is the brain wide response, as indicated from the quantitative loss of gene expression of for instance the microglia signature genes. A similar robust global acute CNS response has been shown for humans by PET.<sup>156</sup> Microglia are thought to react to serum cytokines that are induced in the periphery; in addition, there could a limited impairment of the BBB that leads to exposure to serum factors that have been shown to activate microglia.<sup>160,161</sup>

Several studies have implicated defective IL10 production or signaling in patients and animal models of neurological diseases, ranging from MS to AD or Parkinson's disease.<sup>42</sup> However, the direct involvement of microglia in the *in vivo* context has not been established. Conversely, an IL10 deficiency was shown to mitigate Alzheimer pathology by boosting microglial  $\text{A}\beta$  phagocytosis.<sup>178,179</sup>

Recent studies have suggested that different challenges can be associated with distinct microglia activation modules.<sup>33</sup> A transcriptomic signature, termed DAM or MgND<sup>34,35</sup> was proposed to be associated with neurodegenerative diseases, such as AD and ALS. A fundamental assumption of this notion is that genes associated with this signature are not induced in other paradigms. Here we show that a significant number of the genes proposed to be associated with neurodegeneration and pathology are also induced following systemic endotoxin challenge, albeit transiently. The identification of disease-specific microglia signatures is clearly attractive as they might bear potential as future therapeutic targets, however our data indicate that definition of this modules will require further refinement.

The literature holds that microglia express IL10. However, this notion is largely based on the analysis of microglia *in vitro* cultures.<sup>180</sup> Importantly, it was recently shown, that cultured microglia lose their characteristic tissue imprint and adopt a distinct gene expression signature akin prototype macrophage.<sup>45,53</sup> Here we establish that *in situ*, microglia neither express IL10 in steady state nor upon challenge. Indeed, a screen of the relevant literature that reports transcriptome analysis of acutely isolated microglia isolated from challenges as distinct as cuprizone-induced demyelination,<sup>99</sup> EAE,<sup>142</sup> and ALS<sup>181</sup> supports our conclusion.

Moreover, we had reported earlier that recovery from SC injury was dependent on IL10 which was provided by monocyte infiltrates, as microglia were unable to produce this factor.<sup>149</sup> On the other hand, it has been reported that microglia isolated from LPS-challenged animals do express Il10 although the cells were in this study merely defined by density.<sup>182</sup> Nevertheless, the ability of microglia to produce Il10 could differ between inbred mouse strains and be affected by housing conditions and clearly merits further investigation. Of note, it is the absence of microglial IL10 production which allows the robust response by cells that are seem otherwise uniquely prepared to sense the cytokine through high receptor expression. This feature seems to be in stark contrast to other tissue macrophages and it is hence tempting to speculate, that this scenario is of importance for the unique CNS physiology. Future studies should genomic regulatory elements that suppress microglial Il10 production and conversely test the impact of a removal of this restriction.

Microglia constitutively express high levels of the Il10 receptor, suggesting that they might be subject to recurrent activation that requires control by the anti-inflammatory cytokine. Interestingly, mild bacteremia which is associated with transient endotoxin exposure has been shown to be associated with mastication, toothbrushing and dental extraction<sup>183</sup> and has been discussed to potentially have systemic effects.<sup>184</sup>

Inherited deficiencies of the IL-10R lead to immune dysregulation with life-threatening early-onset enterocolitis.<sup>151</sup> Because the disease driving culprit in these patients is of the hematopoietic lineage and their colitis is resistant to standard immunosuppressive therapy, early hematopoietic stem cell transplantation (HSCT) is considered as curative therapeutic option.<sup>185</sup> Interesting though, microglia are relatively resistant to irradiation and busulfan treatment used for myeloablation in pediatric and adult patients. While intestinal macrophages in patients with Il10Ra mutations are replaced and colitis is cured, Il10Ra deficient microglia cells hence likely persist in these patients. Our finding that Il10 sensing is critical to prevent microglia hyperactivation during septic shock or bacteremia warrants studies that investigate whether the patients that underwent a transplant suffer from CNS pathologies.

Notably, Il10-deficient animals display impaired gut homeostasis<sup>186</sup> and also animals that harbor a largely macrophage-restricted systemic Il10Ra deficiency develop colitis that can affect the CNS<sup>43</sup>. To circumvent this potentially confounding complication we take here advantage of TAM-treated Cx3cr1<sup>CreER</sup> animals that target long-lived Cx3cr1<sup>+</sup> macrophages

that include microglia but also border-associated macrophages (BAM) in the CNS.<sup>25,76,91</sup> We currently cannot exclude that IL10R-deficient BAM contribute to the hyperactivation.

TNF plays a dual role in the paradigm of endotoxin-induced sickness behavior. Together with other proinflammatory factors is part of a robust but rapid cytokine pulse that causes the CNS response. In addition, we show here that locally produced TNF acts in the CNS paracrine or autocrine driver of microglia activation. Moreover, we show that if unchecked by the Il10 axis, microglial Tnf results in persistent deleterious sickness behavior and neuronal defects. These data are well in line with a recent study that showed using whole body IL10 KO animals in combination with a novel multivariate analysis of microglial morphology that IL-10 was sufficient to impede the recovery from TNF $\alpha$ -mediated inflammation.<sup>187</sup> Our study corroborates the earlier notion of cognitive deficits in LPS-challenged Il10-deficient mice<sup>188</sup> and establishes that the lengthy sickness behavior syndrome results from a CNS-intrinsic deleterious circuit driven by unchecked hyperactive microglia.

Collectively, we establish the critical roles of microglial TNF and non-microglial Il10 in orchestrating the ability of microglia to restore quiescence following a peripheral endotoxin challenge. Given the emergence evidence for a central role of microglia in CNS disorders, our findings should have major implications for our understanding of CNS homeostasis and pathology, and might reveal novel strategies for therapeutic intervention.

*Figure legends*

**Figure 12. Microglial IL10 sensing is dispensable for CNS homeostasis despite prominent microglial IL-10R expression**

- (A) Comparative transcriptome analysis of colon macrophages (green) and CNS-resident microglia (pink) displaying normalized counts of *Il10ra*, *Il10rb*, and *Il10*. Reads. Data were taken from *Lavin et al., 2014*.<sup>52</sup>
- (B) Comparative transcriptome analysis of microglia during development displaying normalized counts for *Sall1*, *Il10ra*, *Il10rb*, and *Il10*. Data were taken from *Matcovitch-Natan et al., 2016*.<sup>54</sup>
- (C) Scheme illustrating conditional TAM-induced mutagenesis in microglia using  $Cx3cr1^{CreER}:IL-10R^{fl/fl}$  mice.
- (D) Sorting strategy of microglia for genomic PCR. Microglia were defined as  $CD45^{int}CD11b^{+}Ly6C/G^{-}$  cells.
- (E) Genomic PCR of microglia sorted from  $Cx3cr1^{CreER}:IL-10R^{fl/fl}$  mice (n=2) and *Il10rfl/fl* controls (n=2) 6 weeks post-TAM administration. Mutant microglia show only KO band (280 kb), whereas controls show only the ‘flox’ band (450 kb)
- (F) Volcano plot of statistical significance ( $-\log_{10}$  P value) against  $\log_2$  ratio of microglia sorted from TAM-treated  $Cx3cr1^{CreER}:IL-10R^{fl/fl}$  mice (n=9) and *Il10rfl/fl* (n=6) littermate controls, based on RNAseq data. Significantly differentially expressed genes (fold change >2; adj. P < 0.05) are in black, and non-significant genes are in gray.

**Figure 13. Microglia display a robust, but transient global response to peripheral endotoxin challenge**

- (A) RNAseq analysis of microglia isolated from *Il10ra*<sup>fl/fl</sup> ‘wild type’ C57Bl/6 mice untreated, 6, 24, 48 hours, and 7 days following a peripheral LPS challenge (2.5 mg/kg) (n=4-6).
- (B) Examples genes displayed in (A)
- (C) Principal component analysis (PCA) based on the RNAseq data shown in (A)
- (D) Table of differentially expressed genes shown in (A)
- (E) IGV tracks of selected loci showing ATAC signals in untreated microglia and microglia retrieved from mice at indicated times post LPS challenge.

**Figure 14. IL10 receptor-deficient microglia are hyperactive after peripheral LPS challenge and fail to return to quiescence**

- (A) Survival curve of Cx3cr1<sup>CreER</sup>:IL-10R<sup>fl/fl</sup> mice (n=11) and Il10rfl/fl littermate controls (n=7) treated with LPS (2.5 mg/kg).
- (B) Principal component analysis (PCA) based on RNAseq data of microglia isolated from TAM-treated Cx3cr1<sup>CreER</sup>:IL-10R<sup>fl/fl</sup> mice and Il10rfl/fl littermate controls, untreated and at indicated times after LPS challenge (2.5 mg/kg).
- (C) Heatmap of microglia isolated from TAM-treated Cx3cr1<sup>CreER</sup>:IL-10R<sup>fl/fl</sup> mice and Il10rfl/fl littermate controls, untreated and at indicated times after LPS challenge (2.5 mg/kg).
- (D) Examples genes displayed in (C)
- (E) Table of differentially expressed genes displayed in (C)

**Figure 15. Microglial IL-10R deficiency causes prolonged sickness behavior and impaired neuronal function post-LPS administration**

- (A) Home cage locomotion assay of Cx3cr1<sup>CreER</sup>:IL-10R<sup>fl/fl</sup> mice (n=11) and Il10rfl/fl littermate controls (n=7) treated with LPS (0.5 mg/kg). Representative of three independent experiments
- (B) Food intake after LPS challenge of the mice from the locomotion experiment shown in (A)
- (C) Graphical description of LTP measurement protocol. Stimulation of Schaffer's collaterals was evoked using a pulse stimulator and delivered through a bipolar nichrome electrode.
- (D) LTP analysis on Schaffer collateral cornu ammonis 1 (CA1) region synapses probed in acute hippocampal slices isolated from either untreated, 12hrs post LPS-, or 24hrs post LPS-treated Cx3cr1<sup>CreER</sup>:IL-10R<sup>fl/fl</sup> mice and controls (n=5). Averaged EPSP are plotted versus time. Data are expressed as mean  $\pm$  SEM and statistically analyzed with two-way ANOVA on time point 60 considering the type of treatment, genotype, and the interaction between the two factors (\*p < 0.05, \*\*p < 0.01 represent the significance of interaction). Representative traces at indicated times (a, b) are shown on top of each section. Upward arrows indicate the time of high-frequency stimulation (HFS).

### Figure 16. The source of IL10

- (A) Example genes from RNAseq of isolated microglia and astrocytes from TAM-treated GFAP<sup>CreER</sup>:tdTomato<sup>fl/fl</sup> mice, either untreated or 12hrs post-LPS (2.5 mg/kg). Gating strategy of the left: Microglia were defined as CD45<sup>int</sup>CD11b<sup>+</sup>; Astrocytes were defined as CD45<sup>-</sup>CD11b<sup>-</sup>Tomato<sup>+</sup>.
- (B) Home cage locomotion assay of *Cx3cr1*<sup>CreER</sup>:*IL-10*<sup>fl/fl</sup> mice, *Aldh1l1*<sup>CreER</sup>:*IL-10*<sup>fl/fl</sup> mice and Il10r<sup>fl/fl</sup> littermate controls treated with LPS (0.5 mg/kg).
- (C) RT-PCR analysis of indicated cell populations isolated from brain of WT mice, either untreated or 12hrs post-LPS (2.5 mg/kg) . Gating strategy of the left: Microglia were defined as CD45<sup>int</sup>CD11b<sup>+</sup>; T cells were defined as CD45<sup>hi</sup>CD11b<sup>-</sup>TCRb/TCRgd<sup>+</sup>; Other CD45<sup>+</sup> cells were defined as CD45<sup>+</sup> which are not microglia or T cells.

### Figure 17. Microglial TNF drives the hyperactivation

- (A) Expression patten on Tnf of microglia isolated from untreated and LPS treated *Cx3cr1*<sup>CreER</sup>:*IL-10*<sup>fl/fl</sup> animals and littermate controls. Normalized reads.
- (B) Flowcytometric analysis of intracellular TNF expression in microglia of *Cx3cr1*<sup>CreER</sup>:*IL-10*<sup>fl/fl</sup> animals and littermate controls, untreated or 24hrs post in vivo LPS challenge.
- (C) Serum TNF levels in LPS treated *Cx3cr1*<sup>CreER</sup>:*IL-10*<sup>fl/fl</sup> , *Cx3cr1*<sup>CreER</sup>:*IL-10*<sup>fl/fl</sup>:*Tnf*<sup>fl/fl</sup> animals and littermate controls.
- (D) Principal component analysis (PCA) of RNAseq data of isolated micoglia from *Cx3cr1*<sup>CreER</sup>:*IL-10*<sup>fl/fl</sup>:*Tnf*<sup>fl/fl</sup> animals and littermate controls, either untreated or 6 and 48hrs post-LPS challenge (2.5 mg/kg).
- (E) Volcano blots comparing microglia transcriptomes of *Cx3cr1*<sup>CreER</sup>:*IL-10*<sup>fl/fl</sup>:*Tnf*<sup>fl/fl</sup> animals and littermate controls, untreated (left) or 48 hours after LPS challenge (right).
- (F) Examples genes from RNAseq data described in (D).

**Figure 18. Addition of a microglial Tnf deficiency rescues *Cx3cr1<sup>CreER</sup>:IL-10<sup>fl/fl</sup>* animals from pathologies**

- (A) Home cage locomotion assay of *Cx3cr1<sup>CreER</sup>:IL-10<sup>fl/fl</sup>:Tnf<sup>fl/fl</sup>* animals and littermate controls, treated with LPS (0.5 mg/kg). Representative of two independent experiments.
- (B) LTP analysis on Schaffer collateral cornu ammonis 1 (CA1) region synapses probed in acute hippocampal slices isolated from *Cx3cr1<sup>CreER</sup>:IL-10<sup>fl/fl</sup>*, *Cx3cr1<sup>CreER</sup>:IL-10<sup>fl/fl</sup>:Tnf<sup>fl/fl</sup>* animals and littermate controls in steady state (left), 12hrs post LPS (middle), and 24hrs post-LPS (right) (1 mg/kg).

**Figure 19. Circulating monocytes are not the source of peripheral TNF upon LPS intraperitoneal injection**

- (A) PCA of RNAseq data of microglia isolated from brain of WT mice, wither untreated, treated with LPS (2.5 mg/kg), treated with MC21, or treated both LPS and MC21.
- (B) Serum TNF levels in LPS treated, WT mice, either untreated or pre-treated with MC21 for monocyte depletion.

**Supplementary Figure 10. Expression of ‘DAM’ genes upon LPS treatment**

- (A) Heatmap of selected genes that have been proposed to be induced in association with neurodegeneration, but not endotoxin challenge.<sup>33,162</sup> Microglia was isolated from controls or LPS-treated *I10ra<sup>fl/fl</sup>* ‘wild type’ C57Bl/6 mice at indicated times post treatment.

### *Final discussion*

My thesis focused on studying microglial activation and its contributions in two different pathological settings – autoimmune neurodegeneration (EAE) and bacteremia-associated endotoxin challenge. Microglia research has gained significant clinical motivation in recent years, with the rise and increased awareness to so-called ‘microgliopathies’. These diseases in which microglia are suggested to be the drivers of pathological cascade in patients, include inflammatory, neurodegenerative, and psychiatric disorders.<sup>12</sup> Not surprisingly, a suggested treatment to these conditions includes replacement of mutant detrimental microglia by WT cells, for example through HSC transplantation.<sup>17</sup> Partial microglia replacement is also a side product of BM transplantation as pediatric treatment of monogenic immune-deficiencies. Whether these HSC/BM-derived brain macrophages can reliably replace microglia is therefore of considerable clinical relevance.

In *project I*, we have shown that although BM-derived brain macrophages acquire microglial characteristics, such as radio-resistance, longevity and microglial morphology, they remain distinct from host microglia in their transcriptome and epigenome.<sup>18</sup> Furthermore, host microglia and BM-derived engrafted macrophages respond differently to the same immune challenge, LPS, and are hence functionally distinct. This might be one of the reasons that patients after BMT are more susceptible to CNS infections.<sup>189</sup> Further experimentation is required to probe the capability of BM-derived engrafted macrophages to perform under various pathological conditions, for example during pathology-associated demyelination, and healing processes that dependent on proper function and phagocytosis by microglia.<sup>114</sup>

In *project II*, we have probed the role of microglia as APC in the initiation of EAE and local restimulation of pathogenic T cells. Microglia upregulate MHCII expression upon CNS autoimmunity and thus presumably can present myelin antigen. We have utilized the inducible CX3CR1<sup>CreER</sup> system introduced by our group<sup>25</sup> to ablate MHCII in microglia while sparing other APC, and demonstrated that symptoms in the preclinical EAE model were unaltered.<sup>28</sup> This provides critical evidence that microglial MHCII is dispensable for the induction of EAE. Together with two other recent publications, we showed that infiltrating monocyte-derived cells are responsible for T cell stimulation upon MOG-immunization.<sup>28,190,191</sup> Furthermore, we have demonstrated that microglial MHCII does also not play a role in the cuprizone-induced non-autoimmune demyelination model, in which T cell are not involved.<sup>28</sup>

In *project III*, we aimed to determine the critical source of IL23 for induction of EAE. IL23 is now established as the key effector cytokine for development of CNS autoimmunity,<sup>29</sup> and was shown to be critical for the terminal differentiation and expansion of pathogenic Th17 cells.<sup>140</sup> IL23 KO mice are essentially resistant to induction of EAE,<sup>30</sup> but whether IL23 is needed only in the periphery or also in the CNS remained unclear. Using the CX<sub>3</sub>CR1<sup>CreER</sup> and CX<sub>3</sub>CR1<sup>Cre</sup> systems,<sup>25</sup> we have excluded microglia as critical IL23 producers, implying a critical role of either monocytes or peripheral macrophages in that respect. Moreover, using an antibody-based approach to deplete circulating monocytes, we show that also these cells seem dispensable for EAE induction. Our data support a previously unnoticed crucial role of peripheral macrophages, possible in LNs, where activation and expansion of pathogenic Th17 cells occur. Further characterization of these TZM<sup>145</sup> is required in order to determine whether these are indeed critical regulators of CNS autoimmunity.

Finally, in *project IV*, we have revealed a novel role for IL10 in curbing detrimental hyperactivation of microglia following peripheral endotoxin challenge. Furthermore, we demonstrated that this hyperactivation is driven by uncontrolled production of TNF of microglia themselves, which results in fatal sickness and neuronal impairment. Few studies have suggested a microglial involvement in sickness response,<sup>165,166</sup> although no mechanism was proposed. In addition, IL-10-deficient mice were reported to display an exaggerated sickness behavior post LPS treatment.<sup>188</sup> Our data provide evidence that microglia are critical regulators of sickness response, and require IL10 sensing in order to modulate excess TNF secretion, which might be neurotoxic.

IL10R-sufficient microglia display a robust ability to return to quiescence post a peripheral endotoxin challenge, in contrast to persistent activation modules described for chronic pathologies.<sup>34,35</sup> Our findings are of relevance for severe settings, as sepsis and bacteremia. Furthermore, the high IL10R expression on microglia in steady state suggests that these cells might be subject to recurrent activation that requires control by the anti-inflammatory cytokine. Interestingly, mild bacteremia which involves transient endotoxin exposure has been shown to be associated with mastication, toothbrushing and dental extraction<sup>183</sup> and has been discussed to potentially have systemic effects.<sup>184</sup> Collectively, our data define the kinetics of the microglia response to peripheral endotoxin challenge, including their

activation and robust silencing, and highlight the critical role of non-microglial I10 in preventing otherwise deleterious microglia hyperactivation.

To summarize, this thesis focused on exploring the contribution of microglial activation to different pathological models, and examining novel circuits to control microglial hyperactivation. These data will hopefully contribute to better understanding of microglia functions, and open new possibilities to novel research of these fascinating cells, which are now revealed as key players in different CNS pathologies, from Alzheimer's Disease to depression.

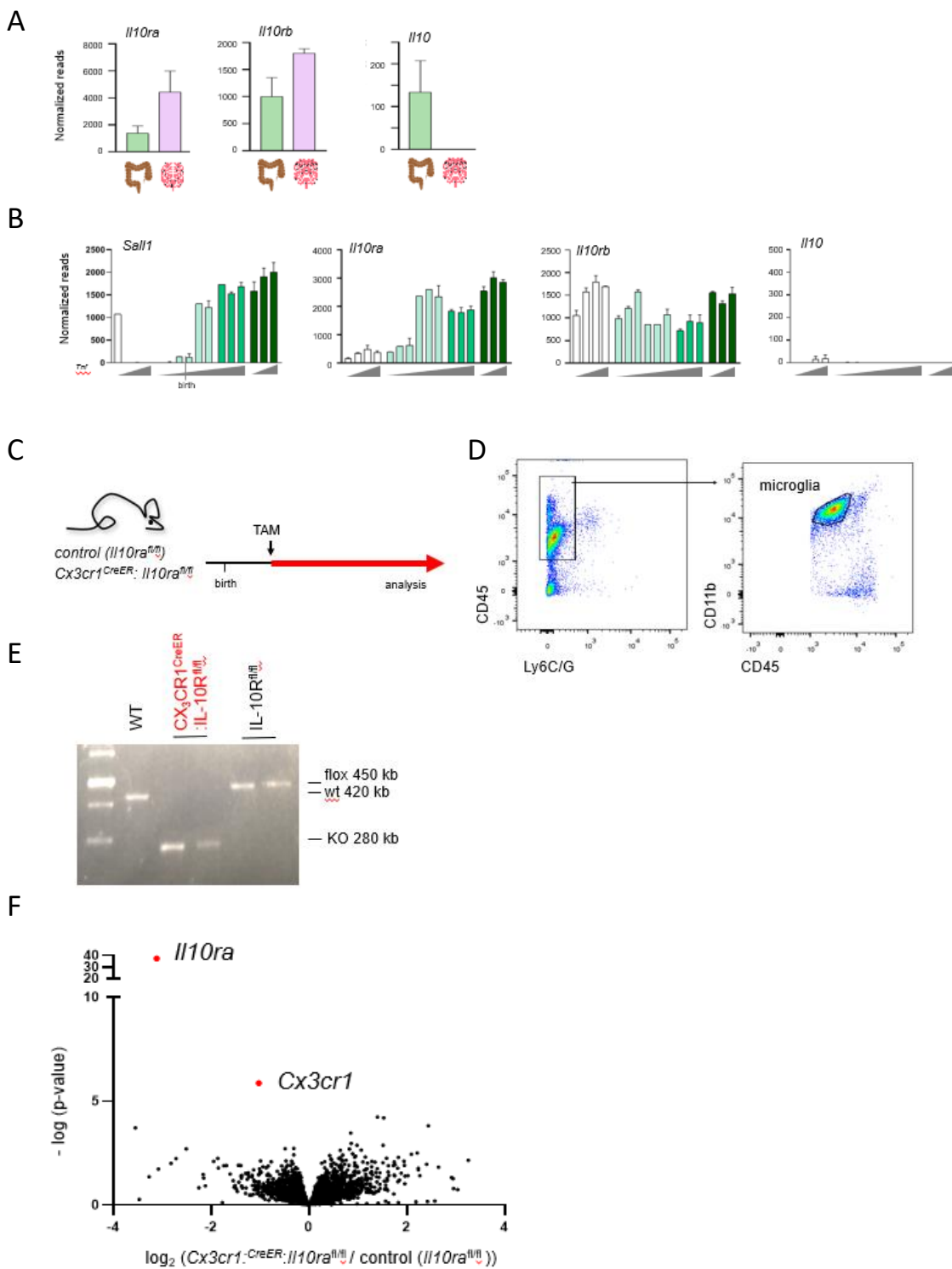
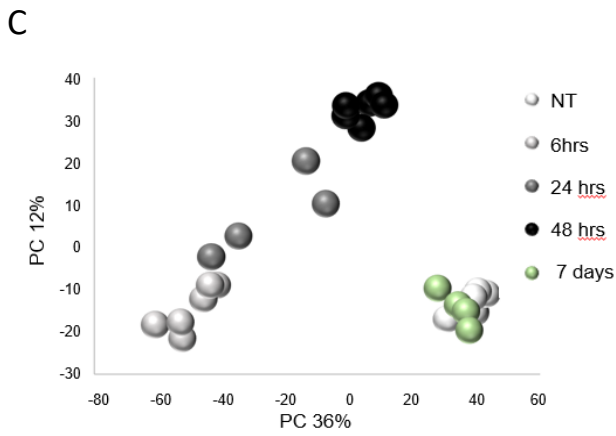
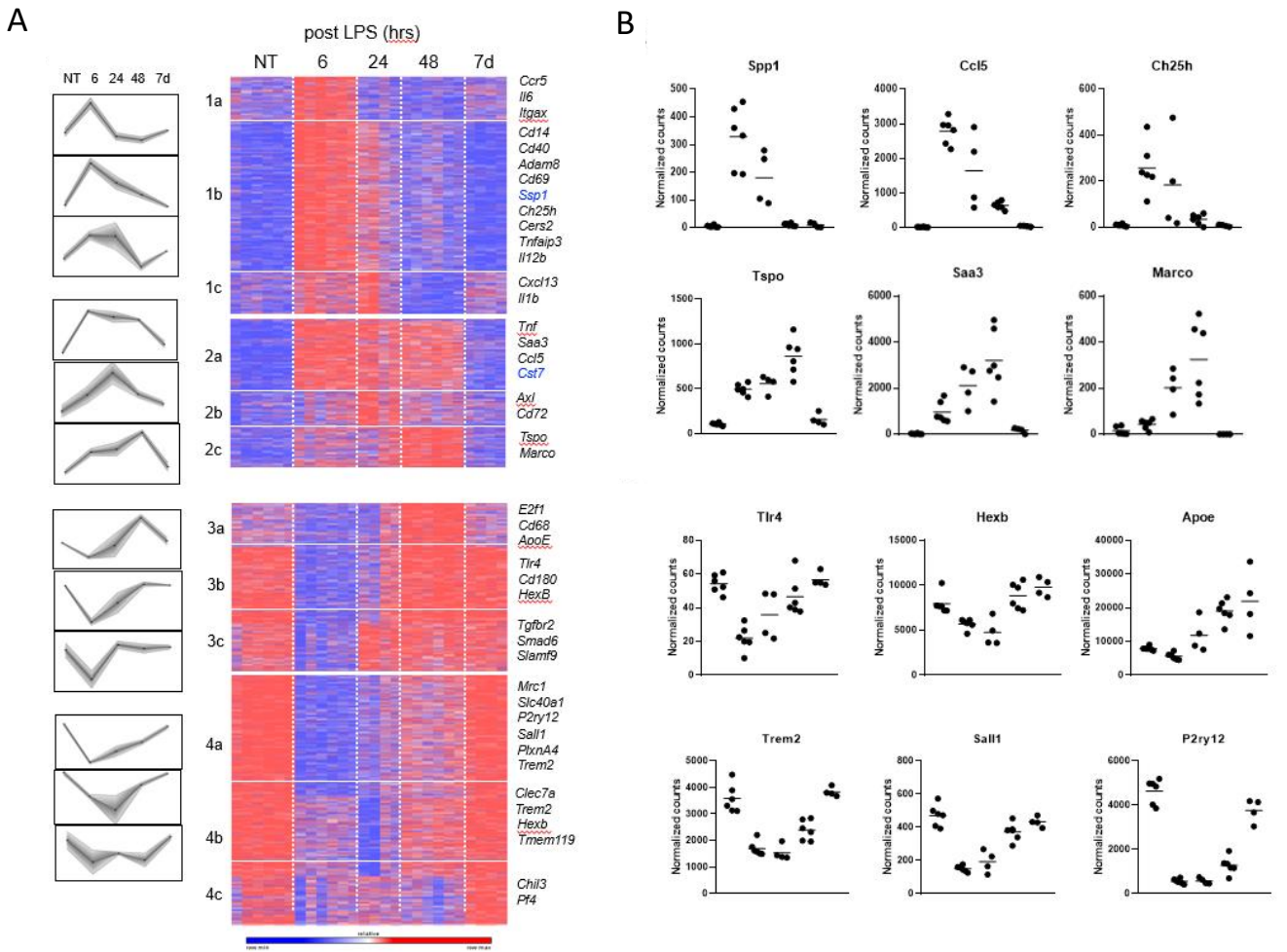


Figure 12. Microglial IL10 sensing is dispensable for CNS homeostasis despite prominent microglial IL10R expression



**D**

Comparison	DEG up	DEG down	Total DEG
6 hrs vs. NT	1294	1394	2688
24 hrs vs. NT	884	861	1745
48 hrs vs. NT	677	386	1063
7d vs. NT	204	14	218

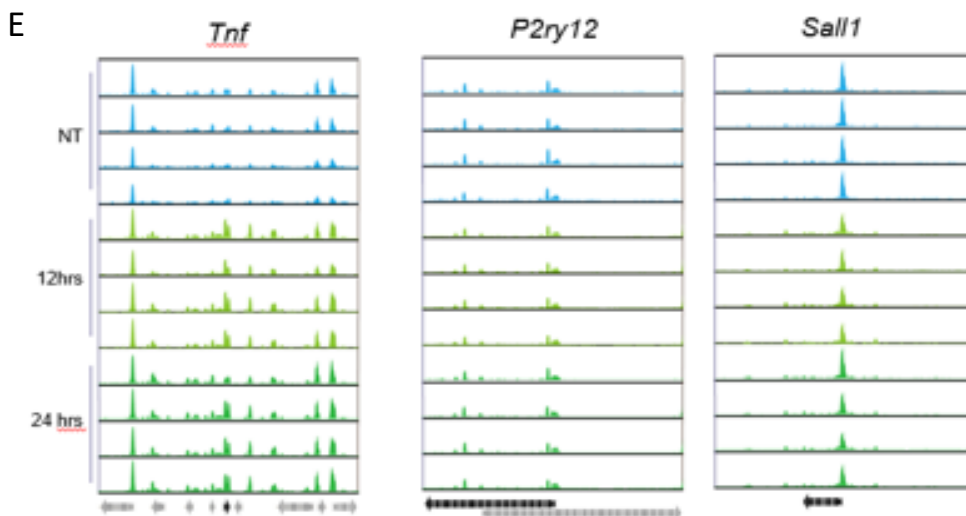


Figure 13. Microglia display a robust, but transient global response to peripheral endotoxin challenge

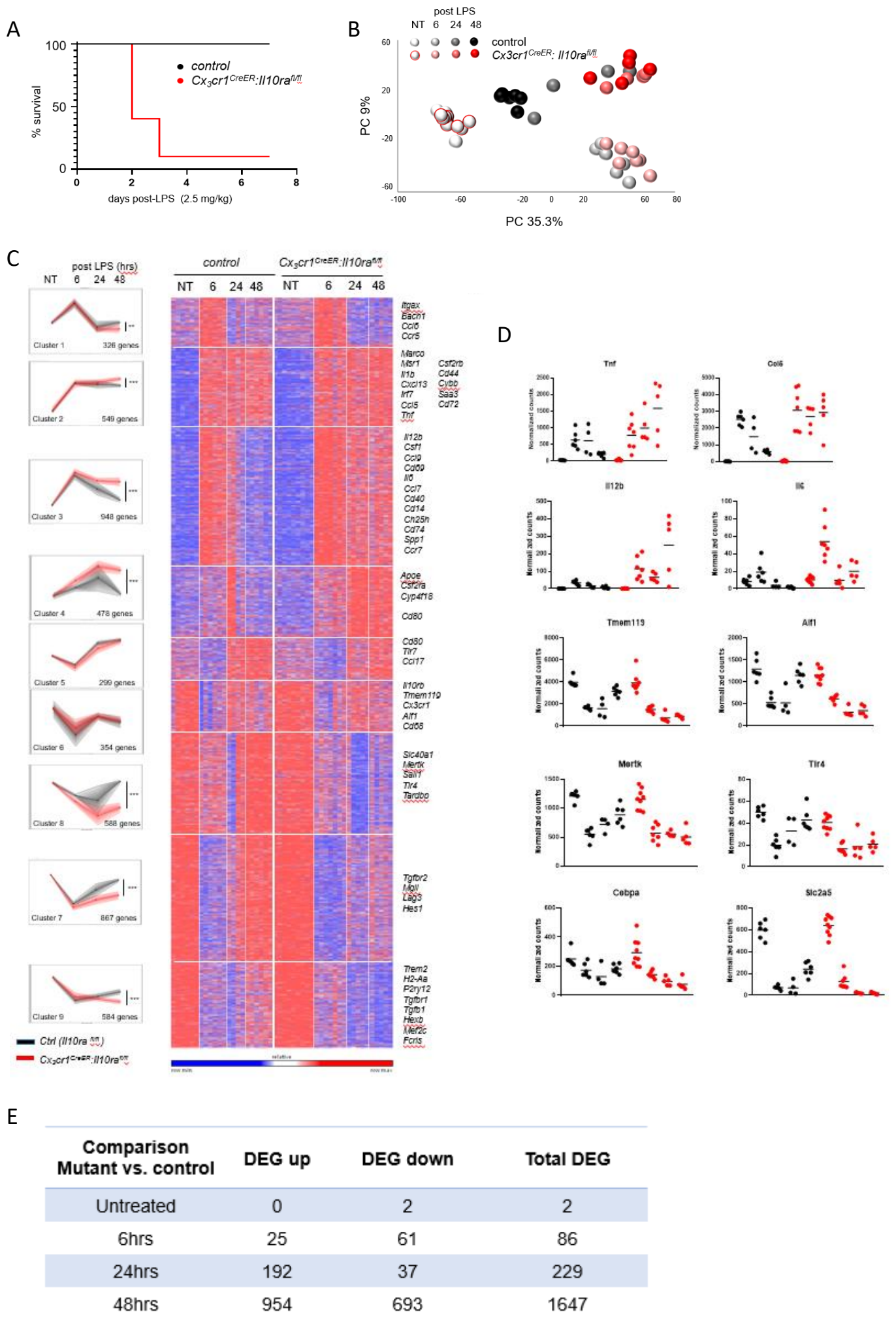


Figure 14. Il10 receptor-deficient microglia are hyperactive after peripheral LPS challenge and fail to return to quiescence

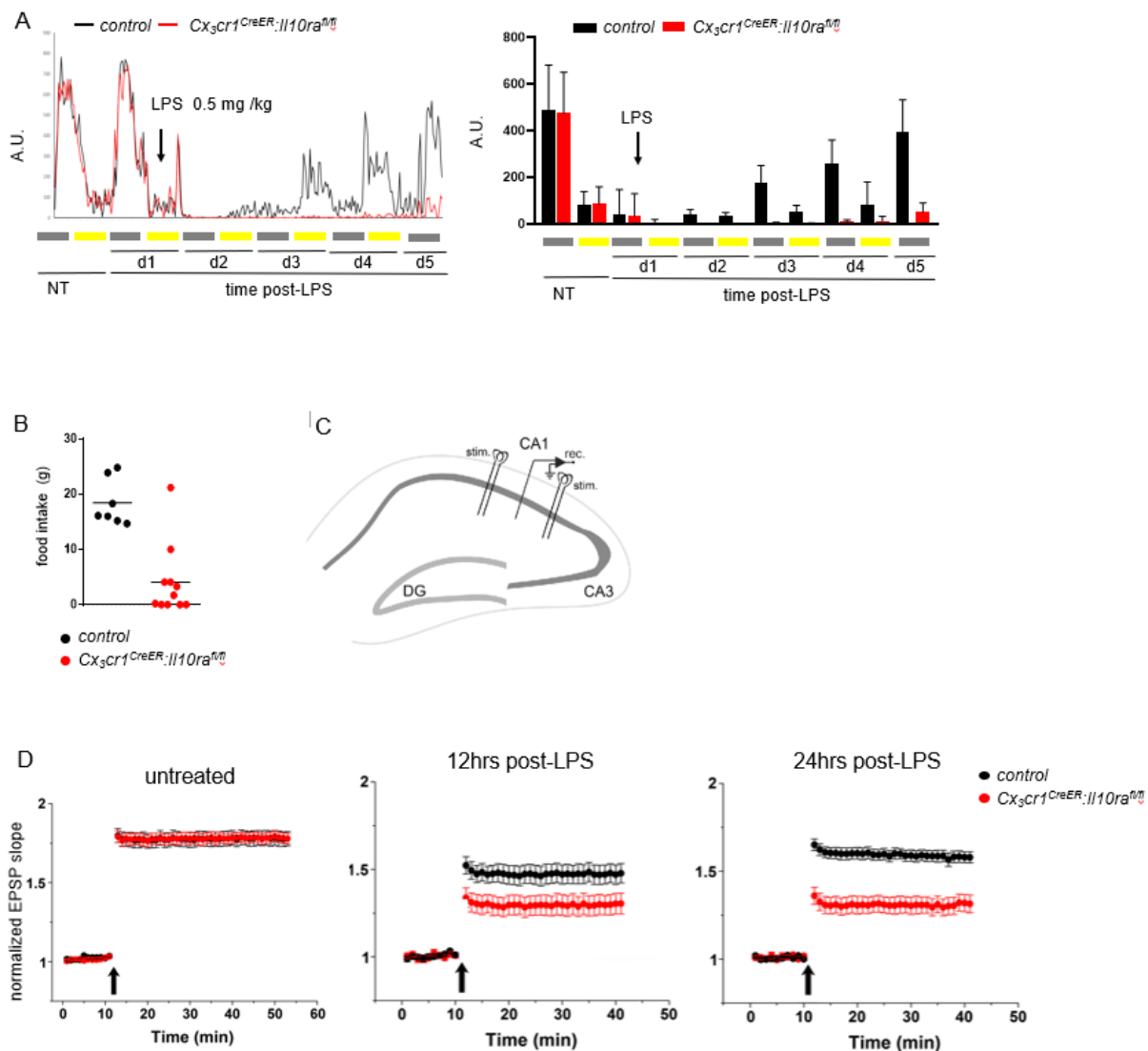


Figure 15. Microglial IL-10R deficiency causes prolonged sickness behavior and impaired neuronal function post-LPS administration

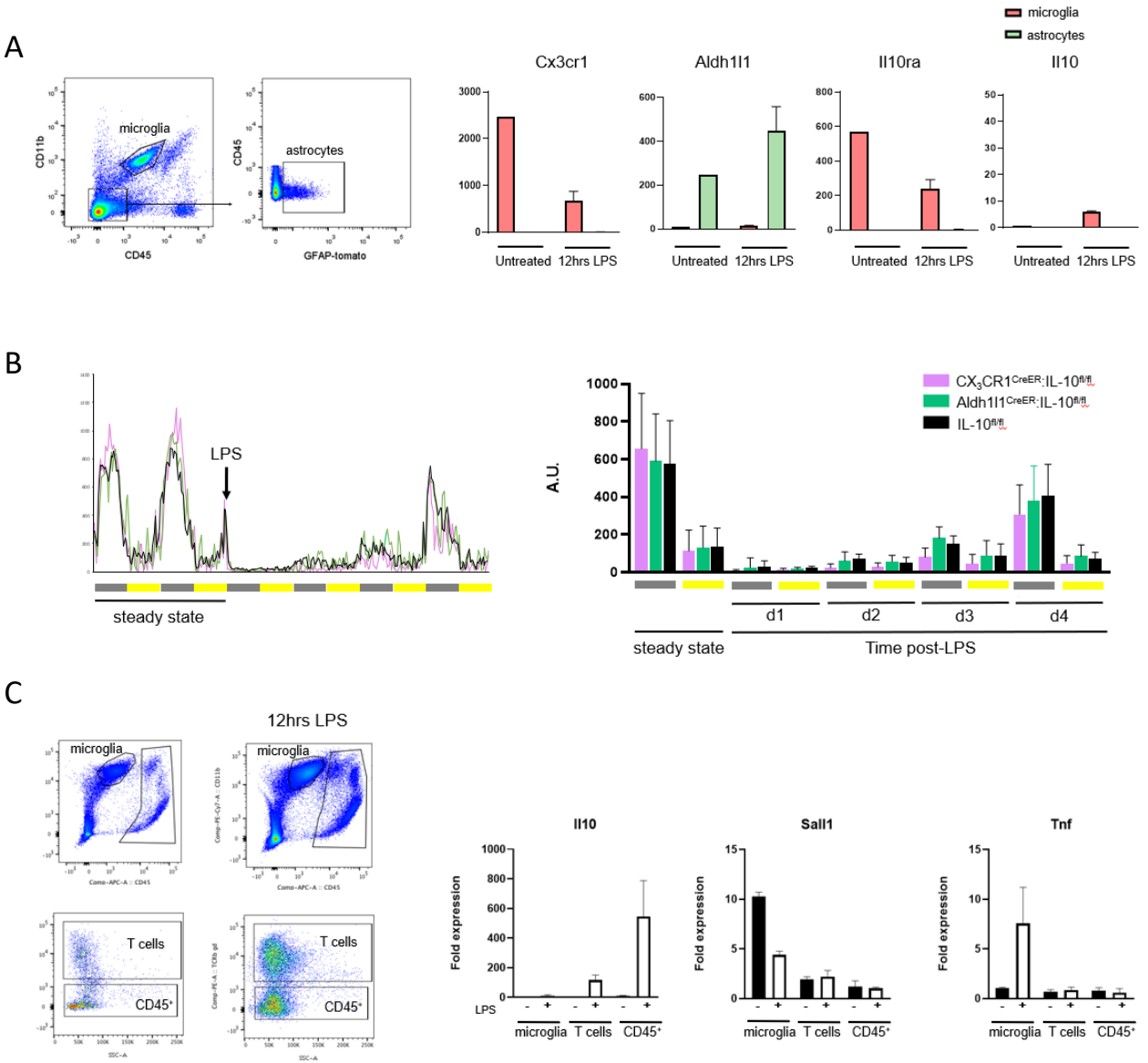


Figure 16. The source of IL10

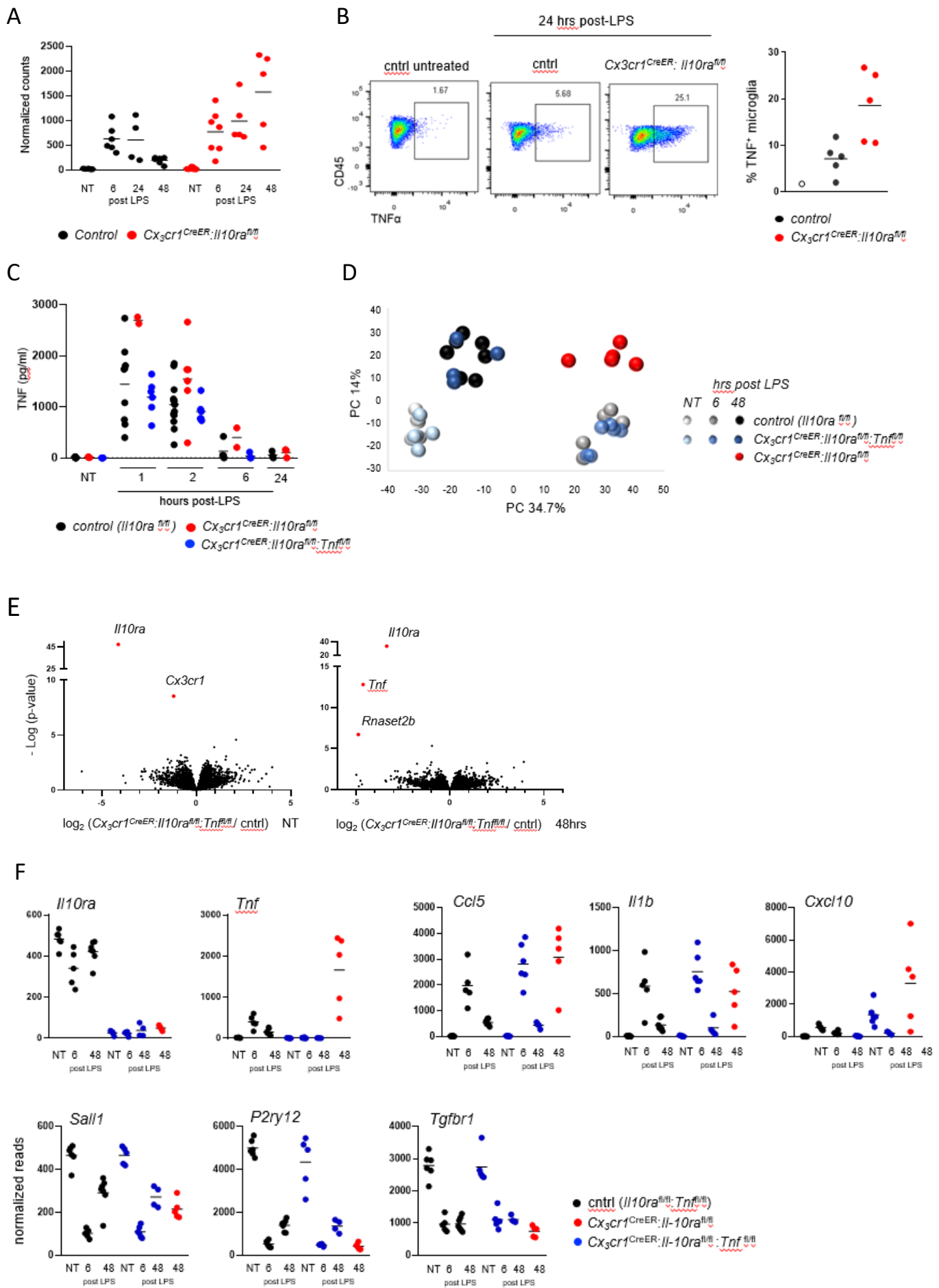


Figure 17. Microglial TNF drives the hyperactivation

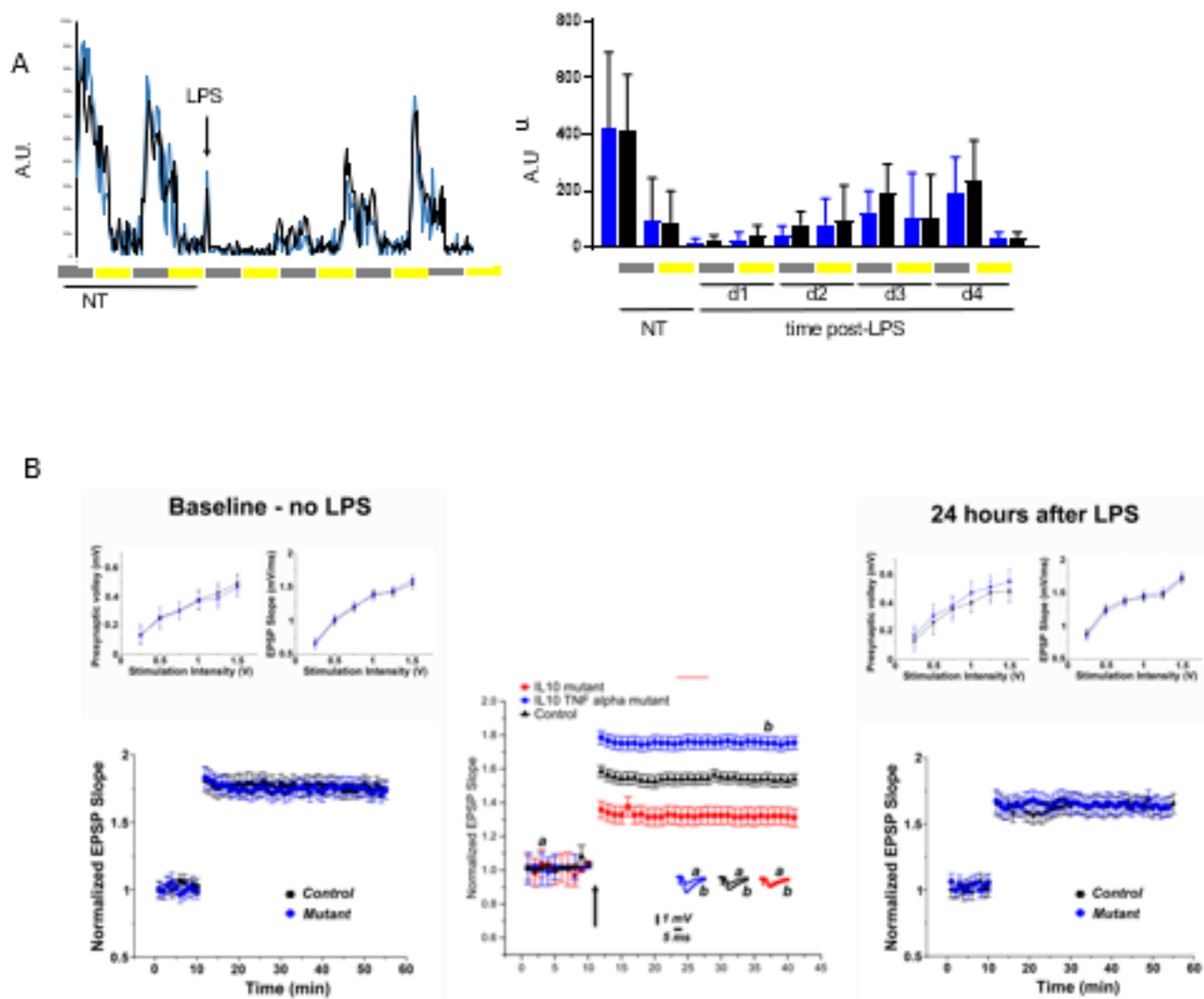


Figure 18. Addition of a microglial *Tnf* deficiency rescues  $Cx3cr1^{CreER};IL-10^{fl/fl}$  animals from pathologies

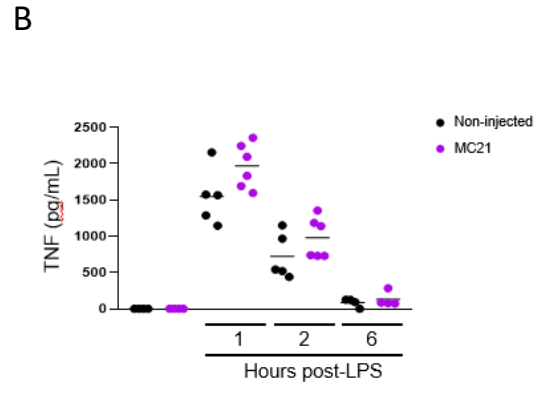
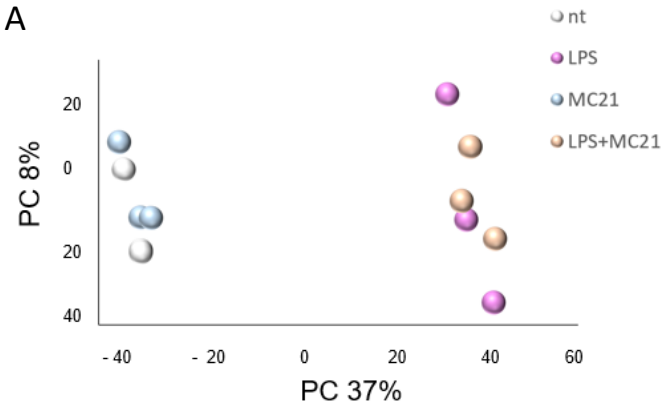
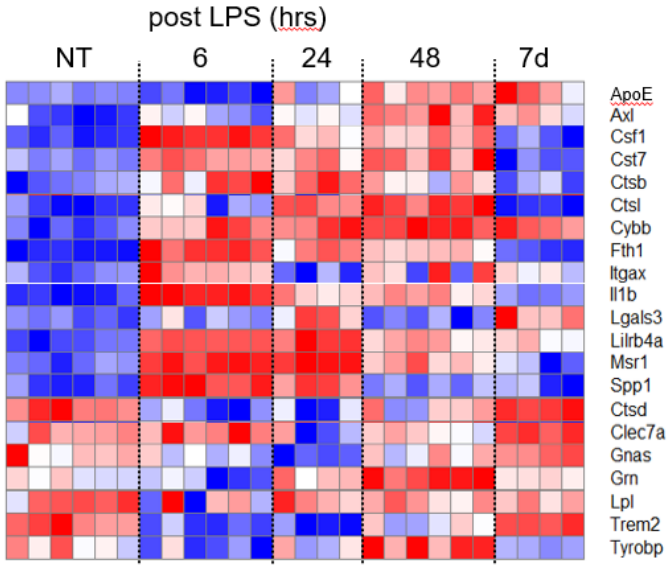


Figure 19. Circulating monocytes are not the source of peripheral TNF upon LPS treatment

A



### *Final discussion*

My thesis focused on studying microglial activation and its contributions in two different pathological settings – autoimmune neurodegeneration (EAE) and bacteremia-associated endotoxin challenge. Microglia research has gained significant clinical motivation in recent years, with the rise and increased awareness to so-called ‘microgliopathies’. These diseases in which microglia are suggested to be the drivers of pathological cascade in patients, include inflammatory, neurodegenerative, and psychiatric disorders.<sup>12</sup> Not surprisingly, a suggested treatment to these conditions includes replacement of mutant detrimental microglia by WT cells, for example through HSC transplantation.<sup>17</sup> Partial microglia replacement is also a side product of BM transplantation as pediatric treatment of monogenic immune-deficiencies. Whether these HSC/BM-derived brain macrophages can reliably replace microglia is therefore of considerable clinical relevance.

In *project I*, we have shown that although BM-derived brain macrophages acquire microglial characteristics, such as radio-resistance, longevity and microglial morphology, they remain distinct from host microglia in their transcriptome and epigenome.<sup>18</sup> Furthermore, host microglia and BM-derived engrafted macrophages respond differently to the same immune challenge, LPS, and are hence functionally distinct. This might be one of the reasons that patients after BMT are more susceptible to CNS infections.<sup>189</sup> Further experimentation is required to probe the capability of BM-derived engrafted macrophages to perform under various pathological conditions, for example during pathology-associated demyelination, and healing processes that dependent on proper function and phagocytosis by microglia.<sup>114</sup>

In *project II*, we have probed the role of microglia as APC in the initiation of EAE and local restimulation of pathogenic T cells. Microglia upregulate MHCII expression upon CNS autoimmunity and thus presumably can present myelin antigen. We have utilized the inducible CX3CR1<sup>CreER</sup> system introduced by our group<sup>25</sup> to ablate MHCII in microglia while sparing other APC, and demonstrated that symptoms in the preclinical EAE model were unaltered.<sup>28</sup> This provides critical evidence that microglial MHCII is dispensable for the induction of EAE. Together with two other recent publications, we showed that infiltrating monocyte-derived cells are responsible for T cell stimulation upon MOG-immunization.<sup>28,190,191</sup> Furthermore, we have

demonstrated that microglial MHCII does also not play a role in the cuprizone-induced non-autoimmune demyelination model, in which T cell are not involved.<sup>28</sup>

In *project III*, we aimed to determine the critical source of IL23 for induction of EAE. IL23 is now established as the key effector cytokine for development of CNS autoimmunity,<sup>29</sup> and was shown to be critical for the terminal differentiation and expansion of pathogenic Th17 cells.<sup>140</sup> IL23 KO mice are essentially resistant to induction of EAE,<sup>30</sup> but whether IL23 is needed only in the periphery or also in the CNS remained unclear. Using the CX<sub>3</sub>CR1<sup>CreER</sup> and CX<sub>3</sub>CR1<sup>Cre</sup> systems,<sup>25</sup> we have excluded microglia as critical IL23 producers, implying a critical role of either monocytes or peripheral macrophages in that respect. Moreover, using an antibody-based approach to deplete circulating monocytes, we show that also these cells seem dispensable for EAE induction. Our data support a previously unnoticed crucial role of peripheral macrophages, possible in LNs, where activation and expansion of pathogenic Th17 cells occur. Further characterization of these TZM<sup>145</sup> is required in order to determine whether these are indeed critical regulators of CNS autoimmunity.

Finally, in *project IV*, we have revealed a novel role for IL10 in curbing detrimental hyperactivation of microglia following peripheral endotoxin challenge. Furthermore, we demonstrated that this hyperactivation is driven by uncontrolled production of TNF of microglia themselves, which results in fatal sickness and neuronal impairment. Few studies have suggested a microglial involvement in sickness response,<sup>165,166</sup> although no mechanism was proposed. In addition, IL-10-deficient mice were reported to display an exaggerated sickness behavior post LPS treatment.<sup>188</sup> Our data provide evidence that microglia are critical regulators of sickness response, and require IL10 sensing in order to modulate excess TNF secretion, which might be neurotoxic.

IL10R-sufficient microglia display a robust ability to return to quiescence post a peripheral endotoxin challenge, in contrast to persistent activation modules described for chronic pathologies.<sup>34,35</sup> Our findings are of relevance for severe settings, as sepsis and bacteremia. Furthermore, the high IL10R expression on microglia in steady state suggests that these cells might be subject to recurrent activation that requires control by the anti-inflammatory cytokine. Interestingly, mild bacteremia which involves transient endotoxin exposure has been shown to be

associated with mastication, toothbrushing and dental extraction<sup>183</sup> and has been discussed to potentially have systemic effects.<sup>184</sup> Collectively, our data define the kinetics of the microglia response to peripheral endotoxin challenge, including their activation and robust silencing, and highlight the critical role of non-microglial Il10 in preventing otherwise deleterious microglia hyperactivation.

To summarize, this thesis focused on exploring the contribution of microglial activation to different pathological models, and examining novel circuits to control microglial hyperactivation. These data will hopefully contribute to better understanding of microglia functions, and open new possibilities to novel research of these fascinating cells, which are now revealed as key players in different CNS pathologies, from Alzheimer's Disease to depression.

## *Materials and methods*

### **Mice**

For generation of BM chimeras, wild type C57BL/6 J mice (Harlan) were used as recipients, Cx3cr1<sup>GFP</sup> or CX<sub>3</sub>CR1<sup>Cre</sup>:R26-RFP<sup>fl/fl</sup> mice<sup>25,26</sup> were used as donors. Recipient mice were lethally irradiated with a single dose of 950 cGy using an XRAD 320 machine (Precision X-Ray (PXi)) and reconstituted the next day by i.v. injection of 5 x 10<sup>6</sup> donor BM cells per mouse.

This study also involved the following animals, all on C57BL/6 background: CX<sub>3</sub>CR1<sup>Cre</sup>:mice and CX<sub>3</sub>CR1<sup>CreER</sup>:mice<sup>25</sup>; I-A<sup>b fl/fl</sup> mice<sup>109</sup>; IL-23p19<sup>fl/fl</sup> mice<sup>138</sup>; IL-10R<sup>fl/fl</sup> mice<sup>192</sup>; IL-10<sup>fl/fl</sup> mice<sup>172</sup>; TNF<sup>fl/fl</sup> mice<sup>177</sup>; GFAP<sup>CreER</sup> mice<sup>174</sup>; Aldh111<sup>CreER</sup> mice<sup>175</sup>. All animals bred at the Weizmann animal facility were maintained under specific pathogen-free conditions and handled according to protocols approved by the Weizmann Institute Animal Care Committee as per international guidelines.

### **Tamoxifen treatment**

To induce gene recombination in CreER transgenic mice, tamoxifen (TAM) was dissolved in warm corn oil (Sigma) and administered orally via gavage for four times every other day. All animals were TAM-treated first at 5–6 weeks of age. Each oral application consisted of 5 mg at a concentration of 0.1 mg/μl. Mice were examined 6-8 weeks after treatment.

### **Lipopolysaccharide challenge**

For lipopolysaccharide (LPS) treatment, mice were injected intra-peritoneally (i.p.) with a single dose of LPS as indicated (0.2, 1, or 2.5 mg/kg, *E. coli* 0111:B4; Sigma).

### **EAE induction and assessment**

For EAE induction, mice were injected into each flank with 100 ul emulsion containing 1mg/ml MOG<sub>35-55</sub> peptide (GeneScript,USA), 1:4 PBS and 1:2 Freund's incomplete adjuvant (Sigma) enriched with killed *M. tuberculosis* (BD), supplemented with 250ng pertussis toxin (Sigma) administered *i.p.* on day 0 and 2. EAE was assessed according to accepted assessment described below. The mice were monitored daily by being held at the base of the tail. The index is as follows: 0 - no symptoms; 0.5 - partial tail limp; 1 - complete tail limp; 1.5 - impaired gait; 2 -

lose of pinch reflex in hind-limbs; 2.5 - one hind limb paralysis; 3 -complete hind limb paralysis; 3.5 - one forelimb paralysis; 4 - complete fore limb paralysis; 5 - death.

### **Monocyte depletion**

For monocyte ablation, the anti-CCR2 antibody MC21 was a kind gift of M. Mack (Regensburg, Germany) manufactured in-house by the Weizmann antibody unit, and 200ul of MC21 containing medium was administered *ip*.

### **Microglia isolation**

To isolate microglia and BM-derived parenchymal CNS macrophages, mice were perfused using ice-cold phosphate buffered saline (PBS) and brains or spinal cords were harvested. Brains were dissected, homogenized by pipetting and incubated for 20 min at 37°C in a 1 ml HBSS solution containing 2% BSA, 1 mg/ml Collagenase D (Sigma) and 1 mg/ml DNase1 (Sigma). The homogenate was then filtered through a 100 µm mesh and centrifuged at 2200 RPM, at 4°C, for 5 min. For the enrichment of microglia and BM-derived cells, the pellet was re-suspended with a 40% percoll solution (Sigma) and centrifuged at 2200 RPM, room temperature for 15 min. The cell pellet was next subjected to antibody labeling and flow-cytometry analysis.

### **Blood and spleen extraction**

Blood was collected by tail bleeds; mononuclear cells were enriched by ficoll density gradient centrifugation (1000 x g. 15 min at 20°C with low acceleration and no brake). For spleen analysis, tissue was collected and digested for 1 hour with 1 mg/ml collagenase D (Roche) in PBS containing magnesium and calcium (PBS +/+; Beit Ha'emek, Israel), then macerated mechanically and filtered through a 70 µm mesh.

### **T cells ex-vivo stimulation**

For Th1/17 stimulation, spinal cord or lymph nodes samples were prepared as the above protocol for microglia enrichment, and were incubated for 3 hours in RPMI medium containing 10% fetal calf serum, 1:100 pen strep antibiotic, 1:100 -glutamine, 1:100 MEM and 1:100 sodium pyruvate (Beit Ha'emek, Israel) supplemented with 20ug/ml MOG<sub>35-55</sub> peptide (GeneScript, USA) or PMA/Ionomycin (Sigma). The cell suspensions were then further

incubated with the same solution as above, supplemented with 1ug/ml Brefeldin A (Sigma-Aldrich) for 3 additional hours, prior to antibody staining.

### **Flow cytometry and cell sorting**

Cells were stained with primary antibodies against CD45 (clone 30-F11), CD45.1 (A20), CD45.2 (104), CD11b (M1/70), Ly6C (AL-21), Ly6G (1A8), B220 (RA3-6B2), Gr-1 (RB6-8C5), CD4 (H129.19), IL17A (TC11-18H10.1), IFN-gamma (XMG1.2), CD11c (N418), MHCII (M5/114.15.2), CD8 (53-6.7), Flt3 (A2F10), CD44 (IM7), TNFa (MP6-XT22), - all from Biologend, San Diego, CA, USA. After incubation with the Abs at 4°C for 15 min, cells were washed and sorted using a FACSAria (BD, Erembodegem, Belgium) flow cytometer. Data were acquired with FACSdiva software (Becton Dickinson). Post-acquisition analysis was performed using FlowJo software (Tree Star, FlowJo LLC; Ashland, Oregon).

### **Genomic PCR of sorted cells**

5,000-10,000 cells were sorted, and DNA was isolated using the DNeasy Blood and tissue kit (Qiagen) according to the manufacturer instructions. PCR for the WT, IL-10R flox, and IL-10R KO alleles was performed with the following primers: 5'-ACTGAAGAGGCATCTGAGTG-3'; 5'-ACTTTACCCACTCCTCAGCTC-3'; 5'-ACCCTGCTTGTCTACACAGAC-3'.

### **qPCR of sorted cells**

RNA was isolated from 5,000 to 10,000 cells sorted into 40 µl of lysis buffer (Life Technologies). Dynabeads mRNA Direct Purification Kit (Life Technologies) was used following manufacturer's guidelines. RNA was reverse transcribed with High Capacity cDNA Transcription Kit (Applied Biosystems). PCR were performed with Platinum SYBR Green qPCR SuperMix (Life Technologies) and QuantStudio 6 Flex (Applied Biosystems). Quantification of the PCR signals of each sample was performed by comparing the cycle threshold values (Ct), in duplicate, of the gene of interest with the Ct values of the Actb housekeeping.

### **Lymph node extraction and RNA isolation**

Inguinal lymph nodes were harvested, mechanically disrupted by a syringe plunger and incubated for 30 min with collagenase D (Roche) at 37°C. Cell suspensions were filtered through a 100 µm

mesh. RNA was isolated using the RNeasy Micro kit (Qiagen) according to the manufacturer's instructions.

### **TNF serum analysis**

Blood was extracted from the heart and centrifuged at 1000 RPM at room temperature for 15 min. TNF was measured using the DuoSet kit (R&D Systems). ELISA was performed according to the manufacturer's instructions.

### **RNAseq analysis**

RNA-seq of populations was performed as described previously (Lavin 2014). In brief,  $10^3$  -  $10^5$  cells from each population were sorted into 50  $\mu$ L of lysis/binding buffer (Life Technologies) and stored at 80 C. mRNA was captured with Dynabeads oligo(dT) (Life Technologies) according to manufacturer's guidelines. We used a derivation of MARS-seq<sup>68</sup> to prepare libraries for RNA-seq. Briefly, RNA was reversed transcribed with MARS-seq barcoded RT primer in a 10  $\mu$ L volume with the Affinity Script kit (Agilent). Reverse transcription was analyzed by qRT-PCR and samples with a similar CT were pooled (up to 8 samples per pool). Each pool was treated with Exonuclease I (NEB) for 30 min at 37 C and subsequently cleaned by 1.2X volumes of SPRI beads (Beckman Coulter). Subsequently, the cDNA was converted to double-stranded DNA with a second strand synthesis kit (NEB) in a 20 mL reaction, incubating for 2 hr at 16 C. The product was purified with 1.4X volumes of SPRI beads, eluted in 8  $\mu$ L and in vitro transcribed (with the beads) at 37 C overnight for linear amplification using the T7 High Yield RNA polymerase IVT kit (NEB). Following IVT, the DNA template was removed with Turbo DNase I (Ambion) 15 min at 37 C and the amplified RNA (aRNA) purified with 1.2 volumes of SPRI beads. The aRNA was fragmented by incubating 3 min at 70 C in  $Zn^{2+}$  RNA fragmentation reagents (Ambion) and purified with 2X volumes of SPRI beads. The aRNA was ligated to the MARS-seq ligation adaptor with T4 RNA Ligase I (NEB).” The reaction was incubated at 22 C for 2 hr. After 1.5X SPRI cleanup, the ligated product was reverse transcribed using Affinity Script RT enzyme (Agilent) and a primer complementary to the ligated adaptor. The reaction was incubated for 2 min at 42 C, 45 min at 50 C, and 5 min at 85 C. The cDNA was purified with 1.5X volumes of SPRI beads. The library was completed and amplified through a nested PCR reaction with 0.5 mM of P5\_Rd1 and P7\_Rd2 primers and PCR ready mix (Kappa Biosystems). The amplified pooled library was purified with 0.7X volumes of SPRI beads to remove primer

leftovers. Library concentration was measured with a Qubit fluorometer (Life Technologies) and mean molecule size was determined with a 2200 TapeStation instrument. RNA-seq libraries were sequenced using the Illumina NextSeq 500. Raw reads were mapped to the genome (NCBI37/mm9) using hisat (version 0.1.6). Only reads with unique mapping were considered for further analysis. Gene expression levels were calculated and normalized using the HOMER software package (analyzeRepeats.pl rna mm9 -d < tagDir > -count exons -condenseGenes -strand + -raw) (Heinz et al., 2010). Differential expressed genes were selected using a 2-fold change cutoff between at least two populations and adjusted p value for multiple gene testing > 0.05. Gene expression matrix was clustered using k-means algorithm (MATLAB function kmeans) with correlation as the distance metric. The value of k was chosen by assessing the average silhouette (MATLAB function silhouette) (3) for a range of possible values (4–15).

### **ATACseq analysis**

20,000-50,000 cells were used for ATAC-seq<sup>69</sup> applying described changes.<sup>193</sup> Briefly, nuclei were obtained by lysing the cells with cold lysis buffer (10 mM Tris-HCl pH 7.4, 10 mM NaCl, 3 mM MgCl<sub>2</sub>, 0.1% Igepal CA-630) and nuclei were pelleted by centrifugation for 20 min at 500 g, 4 C using a swing rotor. Supernatant was discarded and nuclei were re-suspended in 25 µL reaction buffer containing 2 µL of Tn5 transposase and 12.5 µL of TD buffer (Nextera Sample preparation kit from Illumina). The reaction was incubated at 37 C for 1 hr. DNA was released from chromatin by adding 5 µL of clean up buffer (900 mM NaCl, 300 mM EDTA, 1.1% SDS, 4.4 mg/ml Proteinase K (NEB)) followed by an incubation for 30 min at 40 C. Tagmented DNA was isolated using 2X volumes of SPRI beads and eluted in 21 µl. For library amplification, two sequential PCRs (9 cycles, followed by an additional 6 cycles) were performed in order to enrich small tagmented DNA fragments. We used the indexing primers as described by Buenrostro et al., 2013 and KAPA HiFi HotStart ready mix. After the first PCR, the libraries were size-selected using double SPRI bead selection (0.65X followed by 1.8X). Then the second PCR was performed with the same conditions in order to obtain the final library. DNA concentration was measured with a Qubit fluorometer (Life Technologies) and library sizes were determined using TapeStation (Agilent Technologies). Libraries were sequenced on the Illumina NextSeq 500 obtaining an average of 20 million reads per sample. Putative open chromatin regions (peaks) were called using HOMER (using parameters compatible with IDR

analysis:  $-L 0 -C 0 -fdr 0.9$ ). The Irreproducible Discovery Rate (IDR) was computed for each peak using the Homer peak score for each replicate experiment (<https://github.com/nboley/idr>); peaks with  $IDR > 0.05$  were filtered away. Normalization and differential expression analysis was done using the DESeq2 R-package.

### **Locomotion and food intake analysis**

Homecage locomotion was assessed using the InfraMot system (TSE Systems). Measurements of locomotion consisted of 5-6 light and 5-6 dark cycles, collected at 30-min intervals. Each individually-housed mouse was supplied with 50 g of chaw, and the food left at the end of the locomotion experiment was weighted to determine food consumption.

### **Electrophysiology on brain slices (LTP)**

Extracellular recordings in acute slices prepared from dorsal hippocampus were performed as previously described.<sup>194</sup> Following anesthesia with ketamine/xylazine (0.13/0.01 mg/g body weight), animals were rapidly decapitated, the brain removed, and 400  $\mu$ m slices prepared using a vibroslicer. Slices were incubated for 1.5 hr in a humidified, carbonated (5% CO<sub>2</sub> and 95% O<sub>2</sub>) gas atmosphere at  $33 \pm 1$  °C and perfused with artificial cerebrospinal fluid (ACSF) containing: 124mM NaCl, 2mM KCl, 26mM NaHCO<sub>3</sub>, 1.24mM KH<sub>2</sub>PO<sub>4</sub>, 2.5mM CaCl<sub>2</sub>, 2mM MgSO<sub>4</sub>, and 10mM glucose (pH 7.4) in a standard interface chamber. Recordings were made with a glass pipette containing 0.75M NaCl (4 MU) placed in stratum radiatum of CA1. Stimulation of Schaffer's collaterals was evoked using a pulse stimulator and delivered through a bipolar nichrome electrode. Input-output curves were run on each slice prior to beginning of each experiment. Before applying the tetanic stimulation, baseline values were recorded at a frequency of 0.033 Hz. LTP was induced by high-frequency stimulation (HFS) consisting of 100 pulses at twice the test intensity, delivered at a frequency of 100 Hz (1 s). Responses were digitized at 5 kHz and stored on a computer. Spike 2 software (Cambridge Electronic Design) was used for data acquisition.

### **Statistical analysis**

Mean data are shown. Mann-Whitney test, D'Agostino-Pearson test, two-tailed unpaired *t*-test, and Welch's *t*-test were performed in GraphPad Prism7. Statistical significance was taken at  $P < 0.05$ .

## References

1. Prinz M, Jung S, Priller J. Microglia Biology: One Century of Evolving Concepts. *Cell*. 2019;179(2):292-311. doi:10.1016/j.cell.2019.08.053
2. Sierra A, Encinas JM, Deudero JJP, et al. Microglia shape adult hippocampal neurogenesis through apoptosis-coupled phagocytosis. *Cell Stem Cell*. 2010;7(4):483-495. doi:10.1016/j.stem.2010.08.014
3. Squarzoni P, Oller G, Hoeffel G, et al. Microglia Modulate Wiring of the Embryonic Forebrain. *Cell Reports*. 2014;8(5):1271-1279. doi:10.1016/j.celrep.2014.07.042
4. Schafer DP, Lehrman EK, Kautzman AG, et al. Microglia Sculpt Postnatal Neural Circuits in an Activity and Complement-Dependent Manner. *Neuron*. 2012;74(4):691-705. doi:10.1016/j.neuron.2012.03.026
5. Tremblay MÈ, Lowery RL, Majewska AK. Microglial interactions with synapses are modulated by visual experience. *PLoS Biology*. 2010;8(11). doi:10.1371/journal.pbio.1000527
6. Hanisch UK, Kettenmann H. Microglia: Active sensor and versatile effector cells in the normal and pathologic brain. *Nature Neuroscience*. 2007;10(11):1387-1394. doi:10.1038/nn1997
7. Ginhoux F, et al. Fate mapping analysis reveals that adult microglia derive from primitive macrophages. *Science*. 2010;330(6005).
8. Schulz C, et al. A lineage of myeloid independent of Myb and hematopoietic stem cells. *Science*. 2012;336(6077).
9. Varol C, Mildner A, Jung S. Macrophages: Development and Tissue Specialization. *Annual Review of Immunology*. 2015;33(1):643-675. doi:10.1146/annurev-immunol-032414-112220
10. Ajami B, Bennett JL, Krieger C, McNagny KM, Rossi FMV. Infiltrating monocytes trigger EAE progression, but do not contribute to the resident microglia pool. *Nature Neuroscience*. 2011;14(9):1142-1150. doi:10.1038/nn.2887
11. Wong WT. Microglial aging in the healthy CNS: Phenotypes, drivers, and rejuvenation. *Frontiers in Cellular Neuroscience*. 2013;(MAR). doi:10.3389/fncel.2013.00022
12. Prinz M, Priller J. Microglia and brain macrophages in the molecular age: From origin to neuropsychiatric disease. *Nature Reviews Neuroscience*. 2014;15(5):300-312. doi:10.1038/nrn3722
13. Rademakers R, Baker M, Nicholson AM, et al. Mutations in the colony stimulating factor 1 receptor (CSF1R) gene cause hereditary diffuse leukoencephalopathy with spheroids. *Nature Genetics*. 2012;44(2):200-205. doi:10.1038/ng.1027
14. Guerreiro R, Wojtas A, Bras J, et al. TREM2 variants in Alzheimer's disease. *New England Journal of Medicine*. 2013;368(2):117-127. doi:10.1056/NEJMoa1211851

15. Hollingworth P, Harold D, Sims R, et al. Common variants at ABCA7, MS4A6A/MS4A4E, EPHA1, CD33 and CD2AP are associated with Alzheimer's disease. *Nature Genetics*. 2011;43(5):429-436. doi:10.1038/ng.803
16. Griciuc A, Serrano-Pozo A, Parrado AR, et al. Alzheimer's disease risk gene cd33 inhibits microglial uptake of amyloid beta. *Neuron*. 2013;78(4):631-643. doi:10.1016/j.neuron.2013.04.014
17. Biffi A. Hematopoietic Gene Therapies for Metabolic and Neurologic Diseases. *Hematology/Oncology Clinics of North America*. 2017;31(5):869-881. doi:10.1016/j.hoc.2017.06.004
18. Shemer A, Grozovski J, Tay TL, et al. Engrafted parenchymal brain macrophages differ from microglia in transcriptome, chromatin landscape and response to challenge. *Nature Communications*. 2018;9(1). doi:10.1038/s41467-018-07548-5
19. Lisak RP. *Neurodegeneration in Multiple Sclerosis Defining the Problem.*; 2007.
20. Fletcher JM, Lalor SJ, Sweeney CM, Tubridy N, Mills KHG. T cells in multiple sclerosis and experimental autoimmune encephalomyelitis. *Clinical and Experimental Immunology*. 2010;162(1):1-11. doi:10.1111/j.1365-2249.2010.04143.x
21. Marik C, Felts PA, Bauer J, Lassmann H, Smith KJ. Lesion genesis in a subset of patients with multiple sclerosis: A role for innate immunity? *Brain*. 2007;130(11):2800-2815. doi:10.1093/brain/awm236
22. Mendel L, Kerlero De Rosbo N, Ben-Nun A. *PMOG 35-55 Induces Chronic Nohi-Remitting EAE in H-2h Mice A Myelin Oligodendrocyte Glycoprotein Peptide Induces Typical Chronic Experimental Autoimmune Encephalomyelitis in H-2b Mice: Fine Specificity and T Cell Receptor Vp Expression of Encephalitogenic T Cells*. Vol 25.; 1995.
23. Bhasin M, Wu M, Tsirka SE. Modulation of microglial/macrophage activation by macrophage inhibitory factor (TKP) or tuftsin (TKPR) attenuates the disease course of experimental autoimmune encephalomyelitis. *BMC Immunology*. 2007;8. doi:10.1186/1471-2172-8-10
24. Heppner FL, Greter M, Marino D, et al. Experimental autoimmune encephalomyelitis repressed by microglial paralysis. *Nature Medicine*. 2005;11(2):146-152. doi:10.1038/nm1177
25. Yona S, Kim KW, Wolf Y, et al. Fate Mapping Reveals Origins and Dynamics of Monocytes and Tissue Macrophages under Homeostasis. *Immunity*. 2013;38(1):79-91. doi:10.1016/j.immuni.2012.12.001
26. Jung S, et al. Analysis of Fractalkine Receptor CX<sub>3</sub>CR1 Function by Targeted Deletion and Green Fluorescent Protein Reporter Gene Insertion. *Molecular and Cell Biology*. 2000;20(11):4106-4114.
27. Hickey WF, Kimura H. Perivascular microglial cells of the CNS are bone marrow-derived and present antigen in vivo. *Science*. 1988;239(4837):290-292. doi:10.1126/science.3276004

28. Wolf Y, Shemer A, Levy-Efrati L, et al. Microglial MHC class II is dispensable for experimental autoimmune encephalomyelitis and cuprizone-induced demyelination. *European Journal of Immunology*. 2018;48(8):1308-1318. doi:10.1002/eji.201847540
29. Croxford AL, Mair F, Becher B. IL-23: One cytokine in control of autoimmunity. *European Journal of Immunology*. 2012;42(9):2263-2273. doi:10.1002/eji.201242598
30. Cua DJ, Sherlock J, Chen Y, et al. *Interleukin-23 Rather than Interleukin-12 Is the Critical Cytokine for Autoimmune Inflammation of the Brain.*; 2003. www.nature.com/nature.
31. Das R, Chen X, Komorowski R, Hessner MJ, Drobyski WR. Interleukin-23 secretion by donor antigen-presenting cells is critical for organ-specific pathology in graft-versus-host disease. 2009. doi:10.1182/blood
32. Gyölvézi G, Haak S, Becher B. IL-23-driven encephalo-tropism and Th17 polarization during CNS-inflammation in vivo. *European Journal of Immunology*. 2009;39(7):1864-1869. doi:10.1002/eji.200939305
33. Song WM, Colonna M. The identity and function of microglia in neurodegeneration. *Nature Immunology*. 2018;19(10):1048-1058. doi:10.1038/s41590-018-0212-1
34. Keren-Shaul H, Spinrad A, Weiner A, et al. A Unique Microglia Type Associated with Restricting Development of Alzheimer's Disease. *Cell*. 2017;169(7):1276-1290.e17. doi:10.1016/j.cell.2017.05.018
35. Krasemann S, Madore C, Cialic R, et al. The TREM2-APOE Pathway Drives the Transcriptional Phenotype of Dysfunctional Microglia in Neurodegenerative Diseases. *Immunity*. 2017;47(3):566-581.e9. doi:10.1016/j.immuni.2017.08.008
36. Ajami B, Samusik N, Wieghofer P, et al. Single-cell mass cytometry reveals distinct populations of brain myeloid cells in mouse neuroinflammation and neurodegeneration models. *Nature Neuroscience*. 2018;21(4):541-551. doi:10.1038/s41593-018-0100-x
37. Mrdjen D, Pavlovic A, Hartmann FJ, et al. High-Dimensional Single-Cell Mapping of Central Nervous System Immune Cells Reveals Distinct Myeloid Subsets in Health, Aging, and Disease. *Immunity*. 2018;48(2):380-395.e6. doi:10.1016/j.immuni.2018.01.011
38. Holtman IR, Raj DD, Miller JA, et al. Induction of a common microglia gene expression signature by aging and neurodegenerative conditions: a co-expression meta-analysis. *Acta neuropathologica communications*. 2015;3:31. doi:10.1186/s40478-015-0203-5
39. Buttgereit A, Lelios I, Yu X, et al. Sall1 is a transcriptional regulator defining microglia identity and function. *Nature Immunology*. 2016;17(12):1397-1406. doi:10.1038/ni.3585
40. Butovsky O, Jedrychowski MP, Moore CS, et al. Identification of a unique TGF- $\beta$ -dependent molecular and functional signature in microglia. *Nature Neuroscience*. 2014;17(1):131-143. doi:10.1038/nn.3599

41. Lyons A, Downer EJ, Crotty S, Nolan YM, Mills KHG, Lynch MA. CD200 ligand-receptor interaction modulates microglial activation in vivo and in vitro: A role for IL-4. *Journal of Neuroscience*. 2007;27(31):8309-8313. doi:10.1523/JNEUROSCI.1781-07.2007
42. Lobo-Silva D, Carriche GM, Castro AG, Roque S, Saraiva M. Balancing the immune response in the brain: IL-10 and its regulation. *Journal of Neuroinflammation*. 2016;13(1). doi:10.1186/s12974-016-0763-8
43. Zigmund E, Bernshtein B, Friedlander G, et al. Macrophage-restricted interleukin-10 receptor deficiency, but not IL-10 deficiency, causes severe spontaneous colitis. *Immunity*. 2014;40(5):720-733. doi:10.1016/j.immuni.2014.03.012
44. Bernshtein B, Curato C, Ioannou M, et al. *INFLAMMATION IL-23-Producing IL-10R $\alpha$ -Deficient Gut Macrophages Elicit an IL-22-Driven Proinflammatory Epithelial Cell Response*. Vol 4.; 2019. <http://immunology.sciencemag.org/>.
45. Bohlen CJ, Bennett FC, Tucker AF, Collins HY, Mulinyawe SB, Barres BA. Diverse Requirements for Microglial Survival, Specification, and Function Revealed by Defined-Medium Cultures. *Neuron*. 2017;94(4):759-773.e8. doi:10.1016/j.neuron.2017.04.043
46. Stremmel C, Schuchert R, Wagner F, et al. Yolk sac macrophage progenitors traffic to the embryo during defined stages of development. *Nature Communications*. 2018;9(1). doi:10.1038/s41467-017-02492-2
47. Guilliams M, Scott CL. Does niche competition determine the origin of tissue-resident macrophages? *Nature Reviews Immunology*. 2017;17(7):451-460. doi:10.1038/nri.2017.42
48. Scott CL, Zheng F, de Baetselier P, et al. Bone marrow-derived monocytes give rise to self-renewing and fully differentiated Kupffer cells. *Nature Communications*. 2016;7. doi:10.1038/ncomms10321
49. Gibbings SL, Goyal R, Desch AN, et al. Transcriptome analysis highlights the conserved difference between embryonic and postnatal-derived alveolar macrophages. *Blood*. 2015;126(11):1357-1366. doi:10.1182/blood-2015-01-624809
50. Bruttger J, Karram K, Wörtge S, et al. Genetic Cell Ablation Reveals Clusters of Local Self-Renewing Microglia in the Mammalian Central Nervous System. *Immunity*. 2015;43(1):92-106. doi:10.1016/j.immuni.2015.06.012
51. van de Laar L, Saelens W, de Pijck S, et al. Yolk Sac Macrophages, Fetal Liver, and Adult Monocytes Can Colonize an Empty Niche and Develop into Functional Tissue-Resident Macrophages. *Immunity*. 2016;44(4):755-768. doi:10.1016/j.immuni.2016.02.017
52. Lavin Y, Winter D, Blecher-Gonen R, et al. Tissue-resident macrophage enhancer landscapes are shaped by the local microenvironment. *Cell*. 2014;159(6):1312-1326. doi:10.1016/j.cell.2014.11.018

53. Gosselin D, Link VM, Romanoski CE, et al. Environment drives selection and function of enhancers controlling tissue-specific macrophage identities. *Cell*. 2014;159(6):1327-1340. doi:10.1016/j.cell.2014.11.023
54. Matcovitch-Natan O, Winter DR, Giladi A, et al. Microglia development follows a stepwise program to regulate brain homeostasis. *Science*. 2016;353(6301). doi:10.1126/science.aad8670
55. Mass E, Ballesteros I, Farlik M, et al. Specification of tissue-resident macrophages during organogenesis. *Science*. 2016;353(6304). doi:10.1126/science.aaf4238
56. T'Jonck W, Guilliams M, Bonnardel J. Niche signals and transcription factors involved in tissue-resident macrophage development. *Cellular Immunology*. 2018;330:43-53. doi:10.1016/j.cellimm.2018.02.005
57. Fourceaud L, Traves PG, Tufail Y, et al. TAM receptors regulate multiple features of microglial physiology. *Nature*. 2016;532(7598):240-244. doi:10.1038/nature17630
58. Klein RS, Hunter CA. Protective and Pathological Immunity during Central Nervous System Infections. *Immunity*. 2017;46(6):891-909. doi:10.1016/j.immuni.2017.06.012
59. Ajami B, Bennett JL, Krieger C, Tetzlaff W, Rossi FMV. Local self-renewal can sustain CNS microglia maintenance and function throughout adult life. *Nature Neuroscience*. 2007;10(12):1538-1543. doi:10.1038/nn2014
60. Hashimoto D, Chow A, Noizat C, et al. Tissue-resident macrophages self-maintain locally throughout adult life with minimal contribution from circulating monocytes. *Immunity*. 2013;38(4):792-804. doi:10.1016/j.immuni.2013.04.004
61. Mildner A, Schmidt H, Nitsche M, et al. Microglia in the adult brain arise from Ly-6ChiCCR2+ monocytes only under defined host conditions. *Nature Neuroscience*. 2007;10(12):1544-1553. doi:10.1038/nn2015
62. Priller J, et al. Targeting gene-modified hematopoietic cells to the central nervous system: use of green fluorescent protein uncovers microglial engraftment. *Nature Medicine*. 2001;7(12):1356-1361.
63. Lassmann, ' , Mascha Schmied, ' H, Vass K, Hickey<sup>3</sup> WF. *Bone Marrow Derived Elements and Resident Microglia in Brain Inflammation*.
64. Capotondo A, Milazzo R, Politi LS, et al. Brain conditioning is instrumental for successful microglia reconstitution following hematopoietic stem cell transplantation. *Proceedings of the National Academy of Sciences of the United States of America*. 2012;109(37):15018-15023. doi:10.1073/pnas.1205858109
65. Askew K, Li K, Olmos-Alonso A, et al. Coupled Proliferation and Apoptosis Maintain the Rapid Turnover of Microglia in the Adult Brain. *Cell Reports*. 2017;18(2):391-405. doi:10.1016/j.celrep.2016.12.041

66. Tay TL, Mai D, Dautzenberg J, et al. A new fate mapping system reveals context-dependent random or clonal expansion of microglia. *Nature Neuroscience*. 2017;20(6):793-803. doi:10.1038/nn.4547
67. Aranyosy T, Thielecke L, Glauche I, Fehse B, Cornils K. Genetic Barcodes Facilitate Competitive Clonal Analyses in Vivo. *Human Gene Therapy*. 2017;28(10):926-937. doi:10.1089/hum.2017.124
68. Jaitin DA, et al. Massively parallel single-cell RNA-seq for marker-free decomposition of tissues into cell types. *Science*. 2014;343(6172)-776-779.
69. Buenrostro JD, Giresi PG, Zaba LC, Chang HY, Greenleaf WJ. Transposition of native chromatin for fast and sensitive epigenomic profiling of open chromatin, DNA-binding proteins and nucleosome position. *Nature Methods*. 2013;10(12):1213-1218. doi:10.1038/nmeth.2688
70. Mildner A, Schönheit J, Giladi A, et al. Genomic Characterization of Murine Monocytes Reveals C/EBP $\beta$  Transcription Factor Dependence of Ly6C<sup>-</sup> Cells. *Immunity*. 2017;46(5):849-862.e7. doi:10.1016/j.immuni.2017.04.018
71. Paolicelli RC, Jawaid A, Henstridge CM, et al. TDP-43 Depletion in Microglia Promotes Amyloid Clearance but Also Induces Synapse Loss. *Neuron*. 2017;95(2):297-308.e6. doi:10.1016/j.neuron.2017.05.037
72. Madry C, Kyrargyri V, Arancibia-Cárcamo IL, et al. Microglial Ramification, Surveillance, and Interleukin-1 $\beta$  Release Are Regulated by the Two-Pore Domain K<sup>+</sup> Channel THIK-1. *Neuron*. 2018;97(2):299-312.e6. doi:10.1016/j.neuron.2017.12.002
73. Deczkowska A, Matcovitch-Natan O, Tsitsou-Kampeli A, et al. Mef2C restrains microglial inflammatory response and is lost in brain ageing in an IFN-I-dependent manner. *Nature Communications*. 2017;8(1). doi:10.1038/s41467-017-00769-0
74. Gosselin D, Skola D, Coufal NG, et al. An environment-dependent transcriptional network specifies human microglia identity. *Science*. 2017;356(6344):1248-1259. doi:10.1126/science.aal3222
75. Bennett ML, Bennett FC, Liddel SA, et al. New tools for studying microglia in the mouse and human CNS. *Proceedings of the National Academy of Sciences of the United States of America*. 2016;113(12):E1738-E1746. doi:10.1073/pnas.1525528113
76. Goldmann T, Wieghofer P, Jordão MJC, et al. Origin, fate and dynamics of macrophages at central nervous system interfaces. *Nature Immunology*. 2016;17(7):797-805. doi:10.1038/ni.3423
77. Haimon Z, Volaski A, Orthgiess J, et al. Re-evaluating microglia expression profiles using RiboTag and cell isolation strategies /631/1647/2017 /631/1647/2017/2079 technical-report. *Nature Immunology*. 2018;19(6):636-644. doi:10.1038/s41590-018-0110-6
78. Bennett FC, Bennett ML, Yaqoob F, et al. A Combination of Ontogeny and CNS Environment Establishes Microglial Identity. *Neuron*. 2018;98(6):1170-1183.e8. doi:10.1016/j.neuron.2018.05.014

79. Cronk JC, Filiano AJ, Louveau A, et al. Peripherally derived macrophages can engraft the brain independent of irradiation and maintain an identity distinct from microglia. *Journal of Experimental Medicine*. 2018;215(6):1627-1647. doi:10.1084/jem.20180247
80. Mildner A, Huang H, Radke J, Stenzel W, Priller J. P2Y12 receptor is expressed on human microglia under physiological conditions throughout development and is sensitive to neuroinflammatory diseases. *GLIA*. 2017;65(2):375-387. doi:10.1002/glia.23097
81. Haynes SE, Hollopeter G, Yang G, et al. The P2Y12 receptor regulates microglial activation by extracellular nucleotides. *Nature Neuroscience*. 2006;9(12):1512-1519. doi:10.1038/nn1805
82. Takata K, Kozaki T, Lee CZW, et al. Induced-Pluripotent-Stem-Cell-Derived Primitive Macrophages Provide a Platform for Modeling Tissue-Resident Macrophage Differentiation and Function. *Immunity*. 2017;47(1):183-198.e6. doi:10.1016/j.immuni.2017.06.017
83. Safaiyan S, Kannaiyan N, Snaidero N, et al. Age-related myelin degradation burdens the clearance function of microglia during aging. *Nature Neuroscience*. 2016;19(8):995-998. doi:10.1038/nn.4325
84. ElAli A, Rivest S. Microglia in Alzheimer's disease: A multifaceted relationship. *Brain, Behavior, and Immunity*. 2016;55:138-150. doi:10.1016/j.bbi.2015.07.021
85. Kierdorf K, Katzmarski N, Haas CA, Prinz M. Bone Marrow Cell Recruitment to the Brain in the Absence of Irradiation or Parabiosis Bias. *PLoS ONE*. 2013;8(3). doi:10.1371/journal.pone.0058544
86. Varol D, Mildner A, Blank T, et al. Dicer Deficiency Differentially Impacts Microglia of the Developing and Adult Brain. *Immunity*. 2017;46(6):1030-1044.e8. doi:10.1016/j.immuni.2017.05.003
87. Kambayashi T, Laufer TM. Atypical MHC class II-expressing antigen-presenting cells: Can anything replace a dendritic cell? *Nature Reviews Immunology*. 2014;14(11):719-730. doi:10.1038/nri3754
88. Saijo K, Glass CK. Microglial cell origin and phenotypes in health and disease. *Nature Reviews Immunology*. 2011;11(11):775-787. doi:10.1038/nri3086
89. Holmøy T, Lise A, Hestvik K. *Multiple Sclerosis: Immunopathogenesis and Controversies in Defining the Cause*.
90. Steinman L. *Multiple Sclerosis: A Coordinated Review Immunological Attack against Myelin in the Central Nervous System*. Vol 85.; 1996.
91. Goldmann T, Wieghofer P, Müller PF, et al. A new type of microglia gene targeting shows TAK1 to be pivotal in CNS autoimmune inflammation. *Nature Neuroscience*. 2013;16(11):1618-1626. doi:10.1038/nn.3531

92. Wolf Y, Shemer A, Polonsky M, et al. Autonomous TNF is critical for in vivo monocyte survival in steady state and inflammation. *Journal of Experimental Medicine*. 2017;214(4):905-917. doi:10.1084/jem.20160499
93. Goverman J. Autoimmune T cell responses in the central nervous system. *Nature Reviews Immunology*. 2009;9(6):393-407. doi:10.1038/nri2550
94. Wu GF, Shindler KS, Allenspach EJ, et al. Limited sufficiency of antigen presentation by dendritic cells in models of central nervous system autoimmunity. *Journal of Autoimmunity*. 2011;36(1):56-64. doi:10.1016/j.jaut.2010.10.006
95. Yogev N, Frommer F, Lukas D, et al. Dendritic cells ameliorate autoimmunity in the CNS by controlling the homeostasis of PD-1 receptor+ regulatory T cells. *Immunity*. 2012;37(2):264-275. doi:10.1016/j.immuni.2012.05.025
96. Matsushima GK, Morell P. 2011. The neurotoxicant, cuprizone, as a model to study demyelination and remyelination in the central nervous system. *Brain Pathology*. 2001;11(1):107-116.
97. Skripuletz T, Bussmann JH, Gudi V, et al. Cerebellar cortical demyelination in the murine cuprizone model. *Brain Pathology*. 2010;20(2):301-312. doi:10.1111/j.1750-3639.2009.00271.x
98. Bakker DA, Ludwin SK. *Blood-Brain Barrier Permeability during Cuprizone-Induced Demyelination Implications for the Pathogenesis of Immune-Mediated Demyelinating Diseases*. Vol 78.; 1987.
99. Olah M, Amor S, Brouwer N, et al. Identification of a microglia phenotype supportive of remyelination. *GLIA*. 2012;60(2):306-321. doi:10.1002/glia.21266
100. Hiremath MM, Chen VS, Suzuki K, Ting JPY, Matsushima GK. MHC class II exacerbates demyelination in vivo independently of T cells. *Journal of Neuroimmunology*. 2008;203(1):23-32. doi:10.1016/j.jneuroim.2008.06.034
101. Arnett HA, Wang Y, Matsushima GK, Suzuki K, P-Y Ting J. *Development/Plasticity/Repair Functional Genomic Analysis of Remyelination Reveals Importance of Inflammation in Oligodendrocyte Regeneration.*; 2003. www.jneurosci.org.
102. Nabavi N, et al. Signalling through the MHC class II cytoplasmic domain is required for antigen presentation and induces B7 expression. *Nature*. 1992;360(6401):266-268.
103. Liu X, Zhan Z, Li D, et al. Intracellular MHC class II molecules promote TLR-triggered innate immune responses by maintaining activation of the kinase Btk. *Nature Immunology*. 2011;12(5):416-424. doi:10.1038/ni.2015
104. Ní Gabhann J, Jefferies CA. TLR-induced activation of Btk - Role for endosomal MHC class II molecules revealed. *Cell Research*. 2011;21(7):998-1001. doi:10.1038/cr.2011.88
105. Creighton MP, Cheng AW, Welstead GG, et al. Histone H3K27ac separates active from poised enhancers and predicts developmental state. *Proceedings of the National Academy of Sciences*. 2010;107(10):12733-12738. doi:10.1073/pnas.1005537107

*Sciences of the United States of America*. 2010;107(50):21931-21936.  
doi:10.1073/pnas.1016071107

106. Borriello F, Sethna MP, Boyd SD, Schweitzer AN, Tivol EA. *These Findings*. Vol 6.; 1997.
107. Bar-On L, Birnberg T, Kim K wook, Jung S. Dendritic cell-restricted CD80/86 deficiency results in peripheral regulatory T-cell reduction but is not associated with lymphocyte hyperactivation. *European Journal of Immunology*. 2011;41(2):291-298.  
doi:10.1002/eji.201041169
108. Madsen L, Labrecque N, Engberg J, et al. *Mice Lacking All Conventional MHC Class II Genes*. Vol 96.; 1999. www.pnas.org.
109. Hashimoto K, Joshi SK, Koni PA. A conditional null allele of the major histocompatibility IA-beta chain gene. *Genesis*. 2002;32(2):152-153. doi:10.1002/gene.10056
110. Fleming KK, Bovaird JA, Mosier MC, Emerson MR, LeVine SM, Marquis JG. Statistical analysis of data from studies on experimental autoimmune encephalomyelitis. *Journal of Neuroimmunology*. 2005;170(1-2):71-84. doi:10.1016/j.jneuroim.2005.08.020
111. Wang C, Yosef N, Gaublomme J, et al. CD5L/AIM Regulates Lipid Biosynthesis and Restrains Th17 Cell Pathogenicity. *Cell*. 2015;163(6):1413-1427. doi:10.1016/j.cell.2015.10.068
112. Mildner A, MacK M, Schmidt H, et al. CCR2+Ly-6Chi monocytes are crucial for the effector phase of autoimmunity in the central nervous system. *Brain*. 2009;132(9):2487-2500.  
doi:10.1093/brain/awp144
113. Remington LT, Babcock AA, Zehntner SP, Owens T. Microglial recruitment, activation, and proliferation in response to primary demyelination. *American Journal of Pathology*. 2007;170(5):1713-1724. doi:10.2353/ajpath.2007.060783
114. Lampron A, Larochele A, Laflamme N, et al. Inefficient clearance of myelin debris by microglia impairs remyelinating processes. *Journal of Experimental Medicine*. 2015;212(4):481-495. doi:10.1084/jem.20141656
115. Voß EV, Škuljec J, Gudi V, et al. Characterisation of microglia during de- and remyelination: Can they create a repair promoting environment? *Neurobiology of Disease*. 2012;45(1):519-528.  
doi:10.1016/j.nbd.2011.09.008
116. Greter M, Heppner FL, Lemos MP, et al. Dendritic cells permit immune invasion of the CNS in an animal model of multiple sclerosis. *Nature Medicine*. 2005;11(3):328-334.  
doi:10.1038/nm1197
117. Anandasabapathy N, Victora GD, Meredith M, et al. Flt3L controls the development of radiosensitive dendritic cells in the meninges and choroid plexus of the steady-state mouse brain. *Journal of Experimental Medicine*. 2011;208(18):1695-1705. doi:10.1084/jem.20102657

118. Ponomarev ED, Shriver LP, Maresz K, Dittel BN. Microglial cell activation and proliferation precedes the onset of CNS autoimmunity. *Journal of Neuroscience Research*. 2005;81(3):374-389. doi:10.1002/jnr.20488
119. Bartholomäus I, Kawakami N, Odoardi F, et al. Effector T cell interactions with meningeal vascular structures in nascent autoimmune CNS lesions. *Nature*. 2009;462(7269):94-98. doi:10.1038/nature08478
120. Foster JA, McVey Neufeld KA. Gut-brain axis: How the microbiome influences anxiety and depression. *Trends in Neurosciences*. 2013;36(5):305-312. doi:10.1016/j.tins.2013.01.005
121. Frei R, Steinle J, Birchler T, et al. MHC class II molecules enhance toll-like receptor mediated innate immune responses. *PLoS ONE*. 2010;5(1). doi:10.1371/journal.pone.0008808
122. Arnett HA, Mason J, Marino M, Suzuki K, Matsushima GK, Ting JPY. TNF $\alpha$  promotes proliferation of oligodendrocyte progenitors and remyelination. *Nature Neuroscience*. 2001;4(11):1116-1122. doi:10.1038/nn738
123. Ransohoff RM, Perry VH. Microglial Physiology: Unique Stimuli, Specialized Responses. *Annual Review of Immunology*. 2009;27(1):119-145. doi:10.1146/annurev.immunol.021908.132528
124. Oppmann B, Lesley R, Blom B, et al. *Novel P19 Protein Engages IL-12p40 to Form a Cytokine, IL-23, with Biological Activities Similar as Well as Distinct from IL-12 Ducing Chains. The Presence of Shared Signal-Transduc-Ing Receptors Offers an Explanation for the Overlapping Functions of IL-6-like Cytokines. Two Other IL-6-like Cytokines, G-CSF and the P35 Subunit of IL-12, Signal through Private Superfamily Re.* Vol 13.; 2000.
125. Zhu J, Paul WE. CD4 T cells: fates, functions, and faults. doi:10.1182/blood-2008
126. Ivanov II, McKenzie BS, Zhou L, et al. The Orphan Nuclear Receptor ROR $\gamma$ t Directs the Differentiation Program of Proinflammatory IL-17+ T Helper Cells. *Cell*. 2006;126(6):1121-1133. doi:10.1016/j.cell.2006.07.035
127. Leonard JP, Waldburger KE, Goldman SJ. *Prevention of Experimental Autoimmune Encephalomyelitis by Antibodies Against Interleukin 12.* <https://rupress.org/jem/article-pdf/181/1/381/495827/381.pdf>.
128. Becher B, Durell BG, Noelle RJ. Experimental autoimmune encephalitis and inflammation in the absence of interleukin-12. *Journal of Clinical Investigation*. 2002;110(4):493-497. doi:10.1172/JCI15751
129. Bettelli E, Carrier Y, Gao W, et al. Reciprocal developmental pathways for the generation of pathogenic effector TH17 and regulatory T cells. *Nature*. 2006;441(7090):235-238. doi:10.1038/nature04753
130. Nurieva R, Yang XO, Martinez G, et al. Essential autocrine regulation by IL-21 in the generation of inflammatory T cells. *Nature*. 2007;448(7152):480-483. doi:10.1038/nature05969

131. Zhou L, Ivanov II, Spolski R, et al. IL-6 programs TH-17 cell differentiation by promoting sequential engagement of the IL-21 and IL-23 pathways. *Nature Immunology*. 2007;8(9):967-974. doi:10.1038/ni1488
132. Haak S, Croxford AL, Kreymborg K, et al. IL-17A and IL-17F do not contribute vitally to autoimmune neuro-inflammation in mice. *Journal of Clinical Investigation*. 2009;119(1):61-69. doi:10.1172/JCI35997
133. Kreymborg K, Etzensperger R, Dumoutier L, et al. IL-22 Is Expressed by Th17 Cells in an IL-23-Dependent Fashion, but Not Required for the Development of Autoimmune Encephalomyelitis. *The Journal of Immunology*. 2007;179(12):8098-8104. doi:10.4049/jimmunol.179.12.8098
134. Codarri L, Gyölvészii G, Tosevski V, et al. ROR $\gamma$ t drives production of the cytokine GM-CSF in helper T cells, which is essential for the effector phase of autoimmune neuroinflammation. *Nature Immunology*. 2011;12(6):560-567. doi:10.1038/ni.2027
135. El-Behi M, Ciric B, Dai H, et al. The encephalitogenicity of TH 17 cells is dependent on IL-1- and IL-23-induced production of the cytokine GM-CSF. *Nature Immunology*. 2011;12(6):568-575. doi:10.1038/ni.2031
136. Hirota K, Duarte JH, Veldhoen M, et al. Fate mapping of IL-17-producing T cells in inflammatory responses. *Nature Immunology*. 2011;12(3):255-263. doi:10.1038/ni.1993
137. Kurschus FC, Croxford AL, Heinen A, Wörtge S, Ielo D, Waisman A. Genetic proof for the transient nature of the Th17 phenotype. *European Journal of Immunology*. 2010;40(12):3336-3346. doi:10.1002/eji.201040755
138. Thakker P, Leach MW, Kuang W, Benoit SE, Leonard JP, Marusic S. IL-23 Is Critical in the Induction but Not in the Effector Phase of Experimental Autoimmune Encephalomyelitis. *The Journal of Immunology*. 2007;178(4):2589-2598. doi:10.4049/jimmunol.178.4.2589
139. Becher B, Durell BG, Noelle RJ. IL-23 produced by CNS-resident cells controls T cell encephalitogenicity during the effector phase of experimental autoimmune encephalomyelitis. *Journal of Clinical Investigation*. 2003;112(8):1186-1191. doi:10.1172/JCI19079
140. McGeachy MJ, Chen Y, Tato CM, et al. The interleukin 23 receptor is essential for the terminal differentiation of interleukin 17-producing effector T helper cells in vivo. *Nature Immunology*. 2009;10(3):314-324. doi:10.1038/ni.1698
141. Croxford AL, Lanzinger M, Hartmann FJ, et al. The Cytokine GM-CSF Drives the Inflammatory Signature of CCR2+ Monocytes and Licenses Autoimmunity. *Immunity*. 2015;43(3):502-514. doi:10.1016/j.immuni.2015.08.010
142. Yamasaki R, Lu H, Butovsky O, et al. Differential roles of microglia and monocytes in the inflamed central nervous system. *Journal of Experimental Medicine*. 2014;211(8):1533-1549. doi:10.1084/jem.20132477

143. Chastain EML, Duncan DS, Rodgers JM, Miller SD. The role of antigen presenting cells in multiple sclerosis. *Biochimica et Biophysica Acta - Molecular Basis of Disease*. 2011;1812(2):265-274. doi:10.1016/j.bbadis.2010.07.008
144. Gray EE, Cyster JG. Lymph node macrophages. *Journal of Innate Immunity*. 2012;4(5-6):424-436. doi:10.1159/000337007
145. Baratin M, Simon L, Jorquera A, et al. T Cell Zone Resident Macrophages Silently Dispose of Apoptotic Cells in the Lymph Node. *Immunity*. 2017;47(2):349-362.e5. doi:10.1016/j.immuni.2017.07.019
146. Hernández-Santos N, Gaffen SL. Th17 cells in immunity to *Candida albicans*. *Cell Host and Microbe*. 2012;11(5):425-435. doi:10.1016/j.chom.2012.04.008
147. Pluvinage J v., Haney MS, Smith BAH, et al. CD22 blockade restores homeostatic microglial phagocytosis in ageing brains. *Nature*. 2019;568(7751):187-192. doi:10.1038/s41586-019-1088-4
148. Murray PJ. Understanding and exploiting the endogenous interleukin-10/STAT3-mediated anti-inflammatory response. *Current Opinion in Pharmacology*. 2006;6(4):379-386. doi:10.1016/j.coph.2006.01.010
149. Shechter R, London A, Varol C, et al. Infiltrating blood-derived macrophages are vital cells playing an anti-inflammatory role in recovery from spinal cord injury in mice. *PLoS Medicine*. 2009;6(7). doi:10.1371/journal.pmed.1000113
150. Zhou K, Zhong Q, Wang YC, et al. Regulatory T cells ameliorate intracerebral hemorrhage-induced inflammatory injury by modulating microglia/macrophage polarization through the IL-10/GSK3 $\beta$ /PTEN axis. *Journal of Cerebral Blood Flow and Metabolism*. 2017;37(3):967-979. doi:10.1177/0271678X16648712
151. Glocker EO, Kotlarz D, Boztug K, et al. Inflammatory bowel disease and mutations affecting the interleukin-10 receptor. *New England Journal of Medicine*. 2009;361(21):2033-2045. doi:10.1056/NEJMoa0907206
152. Shouval DS, Biswas A, Goettel JA, et al. Interleukin-10 receptor signaling in innate immune cells regulates mucosal immune tolerance and anti-inflammatory macrophage function. *Immunity*. 2014;40(5):706-719. doi:10.1016/j.immuni.2014.03.011
153. Wolf Y, Boura-Halfon S, Cortese N, et al. Brown-adipose-tissue macrophages control tissue innervation and homeostatic energy expenditure. *Nature Immunology*. 2017;18(6):665-674. doi:10.1038/ni.3746
154. Buras JA, Holzmann B, Sitkovsky M. Model organisms: Animal models of sepsis: Setting the stage. *Nature Reviews Drug Discovery*. 2005;4(10):854-865. doi:10.1038/nrd1854
155. Hannestad J, Gallezot JD, Schafbauer T, et al. Endotoxin-induced systemic inflammation activates microglia: [11C]PBR28 positron emission tomography in nonhuman primates. *NeuroImage*. 2012;63(1):232-239. doi:10.1016/j.neuroimage.2012.06.055

156. Sandiego CM, Gallezot JD, Pittman B, et al. Imaging robust microglial activation after lipopolysaccharide administration in humans with PET. *Proceedings of the National Academy of Sciences of the United States of America*. 2015;112(40):12468-12473. doi:10.1073/pnas.1511003112
157. Wendeln AC, Degenhardt K, Kaurani L, et al. Innate immune memory in the brain shapes neurological disease hallmarks. *Nature*. 2018;556(7701):332-338. doi:10.1038/s41586-018-0023-4
158. Banks WA, Robinson SM. Minimal penetration of lipopolysaccharide across the murine blood-brain barrier. *Brain, Behavior, and Immunity*. 2010;24(1):102-109. doi:10.1016/j.bbi.2009.09.001
159. Skelly DT, Hennessy E, Dansereau MA, Cunningham C. A Systematic Analysis of the Peripheral and CNS Effects of Systemic LPS, IL-1B, TNF- $\alpha$  and IL-6 Challenges in C57BL/6 Mice. *PLoS ONE*. 2013;8(7). doi:10.1371/journal.pone.0069123
160. Davalos D, Kyu Ryu J, Merlini M, et al. Fibrinogen-induced perivascular microglial clustering is required for the development of axonal damage in neuroinflammation. *Nature Communications*. 2012;3. doi:10.1038/ncomms2230
161. Ryu JK, Rafalski VA, Meyer-Franke A, et al. Fibrin-targeting immunotherapy protects against neuroinflammation and neurodegeneration. *Nature Immunology*. 2018;19(11):1212-1223. doi:10.1038/s41590-018-0232-x
162. Butovsky O, Weiner HL. Microglial signatures and their role in health and disease. *Nature Reviews Neuroscience*. 2018;19(10):622-635. doi:10.1038/s41583-018-0057-5
163. Bogdan C, Vodovotz Y, Nathan C. *Macrophage Deactivation by Interleukin 10*. <https://rupress.org/jem/article-pdf/174/6/1549/492347/1549.pdf>.
164. Houle M, Thivierge M, le Gouill C, Stankova J, Rola-Pleszczynski M. *IL-10 UP-REGULATES CCR5 GENE EXPRESSION IN HUMAN MONOCYTES*. Vol 23.; 1999.
165. Jin S, Kim JG, Park JW, Koch M, Horvath TL, Lee BJ. Hypothalamic TLR2 triggers sickness behavior via a microglia-neuronal axis. *Scientific Reports*. 2016;6. doi:10.1038/srep29424
166. Kreisel T, Frank MG, Licht T, et al. Dynamic microglial alterations underlie stress-induced depressive-like behavior and suppressed neurogenesis. *Molecular Psychiatry*. 2014;19(6):699-709. doi:10.1038/mp.2013.155
167. Yirmiya R, Rimmerman N, Reshef R. Depression as a Microglial Disease. *Trends in Neurosciences*. 2015;38(10):637-658. doi:10.1016/j.tins.2015.08.001
168. Maggio N, Shavit-Stein E, Dori A, Blatt I, Chapman J. Prolonged systemic inflammation persistently modifies synaptic plasticity in the hippocampus: Modulation by the stress hormones. *Frontiers in Molecular Neuroscience*. 2013;6(DEC). doi:10.3389/fnmol.2013.00046

169. Strehl A, Lenz M, Itsekson-Hayosh Z, et al. Systemic inflammation is associated with a reduction in Synaptopodin expression in the mouse hippocampus. *Experimental Neurology*. 2014;261:230-235. doi:10.1016/j.expneurol.2014.04.033
170. Vereker E, Campbell V, Roche E, McEntee E, Lynch MA. Lipopolysaccharide inhibits long term potentiation in the rat dentate gyrus by activating caspase-1. *Journal of Biological Chemistry*. 2000;275(34):26252-26258. doi:10.1074/jbc.M002226200
171. Maggio N, Vlachos A. Tumor necrosis factor (TNF) modulates synaptic plasticity in a concentration-dependent manner through intracellular calcium stores. *Journal of Molecular Medicine*. 2018;96(10):1039-1047. doi:10.1007/s00109-018-1674-1
172. Roers A, Siewe L, Strittmatter E, et al. T cell-specific inactivation of the interleukin 10 gene in mice results in enhanced T cell responses but normal innate responses to lipopolysaccharide or skin irritation. *Journal of Experimental Medicine*. 2004;200(10):1289-1297. doi:10.1084/jem.20041789
173. Recasens M, Shrivastava K, Almolda B, González B, Castellano B. Astrocyte-targeted IL-10 production decreases proliferation and induces a downregulation of activated microglia/macrophages after PPT. *GLIA*. 2019;67(4):741-758. doi:10.1002/glia.23573
174. Ganat YM, Silbereis J, Cave C, et al. Early postnatal astroglial cells produce multilineage precursors and neural stem cells In Vivo. *Journal of Neuroscience*. 2006;26(33):8609-8621. doi:10.1523/JNEUROSCI.2532-06.2006
175. Srinivasan R, Lu TY, Chai H, et al. New Transgenic Mouse Lines for Selectively Targeting Astrocytes and Studying Calcium Signals in Astrocyte Processes In Situ and In Vivo. *Neuron*. 2016;92(6):1181-1195. doi:10.1016/j.neuron.2016.11.030
176. McCoy MK, Tansey MG. TNF signaling inhibition in the CNS: Implications for normal brain function and neurodegenerative disease. *Journal of Neuroinflammation*. 2008;5. doi:10.1186/1742-2094-5-45
177. Grivennikov SI, Tumanov A v., Liepinsh DJ, et al. Distinct and nonredundant in vivo functions of TNF produced by T cells and macrophages/neutrophils: Protective and deleterious effects. *Immunity*. 2005;22(1):93-104. doi:10.1016/j.immuni.2004.11.016
178. Guillot-Sestier MV, Doty KR, Gate D, et al. Il10 deficiency rebalances innate immunity to mitigate Alzheimer-like pathology. *Neuron*. 2015;85(3):534-548. doi:10.1016/j.neuron.2014.12.068
179. Michaud JP, Rivest S. Anti-inflammatory Signaling in Microglia Exacerbates Alzheimer's Disease-Related Pathology. *Neuron*. 2015;85(3):450-452. doi:10.1016/j.neuron.2015.01.021
180. Lobo-Silva D, Carriche GM, Castro AG, Roque S, Saraiva M. Interferon- $\beta$  regulates the production of IL-10 by toll-like receptor-activated microglia. *GLIA*. 2017;65(9):1439-1451. doi:10.1002/glia.23172

181. Chiu IM, Morimoto ETA, Goodarzi H, et al. A neurodegeneration-specific gene-expression signature of acutely isolated microglia from an amyotrophic lateral sclerosis mouse model. *Cell Reports*. 2013;4(2):385-401. doi:10.1016/j.celrep.2013.06.018
182. Norden DM, Trojanowski PJ, Villanueva E, Navarro E, Godbout JP. Sequential activation of microglia and astrocyte cytokine expression precedes increased iba-1 or GFAP immunoreactivity following systemic immune challenge. *GLIA*. 2016;64(2):300-316. doi:10.1002/glia.22930
183. Forner L, Larsen T, Kilian M, Holmstrup P. Incidence of bacteremia after chewing, tooth brushing and scaling in individuals with periodontal inflammation. *Journal of Clinical Periodontology*. 2006;33(6):401-407. doi:10.1111/j.1600-051X.2006.00924.x
184. Teles R, Wang CY. Mechanisms involved in the association between periodontal diseases and cardiovascular disease. *Oral Diseases*. 2011;17(5):450-461. doi:10.1111/j.1601-0825.2010.01784.x
185. Engelhardt KR, Shah N, Faizura-Yeop I, et al. Clinical outcome in IL-10- and IL-10 receptor-deficient patients with or without hematopoietic stem cell transplantation. *Journal of Allergy and Clinical Immunology*. 2013;131(3). doi:10.1016/j.jaci.2012.09.025
186. Kohn R, Löhler I, Rennick D, Rajewsky K, Moiler W. *Interleukin-10-Deficient Mice Develop Chronic Enterocolitis*. Vol 75.; 1993.
187. Anderson WD, Greenhalgh AD, Takwale A, David S, Vadigepalli R. Novel influences of IL-10 on CNS inflammation revealed by integrated analyses of cytokine networks and microglial morphology. *Frontiers in Cellular Neuroscience*. 2017;11. doi:10.3389/fncel.2017.00233
188. Richwine AF, Sparkman NL, Dilger RN, Buchanan JB, Johnson RW. Cognitive deficits in interleukin-10-deficient mice after peripheral injection of lipopolysaccharide. *Brain, Behavior, and Immunity*. 2009;23(6):794-802. doi:10.1016/j.bbi.2009.02.020
189. Maschke M, Dietrich U, Prumbaum M, et al. *Opportunistic CNS Infection after Bone Marrow Transplantation*. Vol 23.; 1999. <http://www.stockton-press.co.uk/bmt>.
190. Jordão MJC, Sankowski R, Brendecke SM, et al. Neuroimmunology: Single-cell profiling identifies myeloid cell subsets with distinct fates during neuroinflammation. *Science*. 2019;363(6425). doi:10.1126/science.aat7554
191. Mundt S, Mrdjen D, Utz SG, Greter M, Schreiner B, Becher B. *Conventional DCs Sample and Present Myelin Antigens in the Healthy CNS and Allow Parenchymal T Cell Entry to Initiate Neuroinflammation*. Vol 4.; 2019. <http://immunology.sciencemag.org/>.
192. Pils MC, Pisano F, Fasnacht N, et al. Monocytes/macrophages and/or neutrophils are the target of IL-10 in the LPS endotoxemia model. *European Journal of Immunology*. 2010;40(2):443-448. doi:10.1002/eji.200939592
193. Lara-Astiaso D, et al. Immunogenetics. Chromatin state dynamics during blood formation. *Science*. 2014;345(6199):943-949.

194. Maggio N, Segal M. Striking variations in corticosteroid modulation of long-term potentiation along the septotemporal axis of the hippocampus. *Journal of Neuroscience*. 2007;27(21):5757-5765. doi:10.1523/JNEUROSCI.0155-07.2007